



Load balancing via inter-frequency handovers in LTE networks

Gonçalo Ourique Fernandes

Thesis to obtain the Master of Science Degree in
Electrical and Computer Engineering

Examination Committee

Chairperson: Prof. José Eduardo Charters Ribeiro da Cunha Sanguino

Supervisor: Prof. Luís Manuel de Jesus Sousa Correia

Member of Committee: Prof. António José Castelo Branco Rodrigues

Member of Committee: Eng. Marco Serrazina

February 2015

To my loved ones

Acknowledgements

First of all, I would like to thank Prof. Luís M. Correia for the opportunity to develop this thesis under his supervision. His support and advices will never be forgotten throughout my life, as well as his professionalism, attitude and work ethics. I also want to thank him for providing me the chance to develop this work in collaboration with a network operator, which allowed me to work on real life issues and even analyse better solutions for this situation. My acknowledgements are also extended to the remaining members of the Group for Research on Wireless (GROW), not only for their active participation in the group's meetings, but also because being a part of it was an outstanding experience that allowed me to improve my presentation skills and expand my knowledge on the world of wireless telecommunications.

Special acknowledgements are also dedicated to Eng. Marco Serrazina, Eng. Pedro Lourenço and Eng. Diogo Almeida, who followed my work from Vodafone's point of view and helped me with their advices and support during the development of this thesis.

I would also like to thank the other GROW's Msc. students Bruno Pires, David Doutor, Marco Castanho, Pedro Ganço, Pedro Ferreira, Pedro Venâncio, Rodrigo Santos and Vasco Simões for their friendship, mutual sharing of information and advices.

To my Father, Mother, Sisters, Brother, Nieces and Nephew, a very special thanks for always being supportive and for caring for me the way they do.

My gratitude is also dedicated to my dearest friends Pedro Nobre, Pedro Ponces, Gonçalo Tomé, Nuno Sousa and Raquel Bettencourt, who were always by my side in the best and in the hardest times and followed my journey from really close, never letting me down and being a very important part of my life.

To my housemates Pedro Martins, Ricardo Santana, Sofia Teles, José Rego and João Arnaud, who shared the same life as I did, under the same roofs. Also, to Diogo Martins, Emanuel Reis, Miguel Pimentel and Ricardo Raposo, whose friendship I could never forget for the twenty years we have been together.

Last, but not least, all of my remaining beloved friends and family, specially Sofia Rodrigues, André Alberto, Tiago Pereirinha, Pompeu Santos, Ana Gomes, Cláudia Pinto and all members of the electrical and computer engineering students commission.

Abstract

The main objective of this thesis was to develop and evaluate the performance of a load balancing mechanism using inter-frequency handovers in LTE networks considering multiple co-located frequency bands being deployed. The analyses were made regarding the 800, 1800 and 2600 MHz frequency bands, in urban scenarios. The addressed parameters were mainly network load, number of active users and their respective received power, number of allocated resources and throughput. Three different situations were studied using the three frequency bands by combining two carrier frequencies and prioritising the higher frequency bands for users to camp. Users requesting either typical data or Voice over LTE (VoLTE) services and their association to the serving sector was based on received power in order to better represent a real network. Studies were made in a high and a low load scenario and measurements over the city of Lisbon were performed and analysed. It is found that the implemented algorithm is more efficient in high user density scenarios, as it is capable of serving an average of 520 users using the combination of the 1800 MHz band with the 2600 or the 800 MHz bands, achieving throughputs of 2.5 Mbps and 1.5 Mbps respectively and stabilising network load on 90%.

Keywords

LTE, load balancing, inter-frequency handovers, co-located frequency band, Lisbon

Resumo

O objectivo principal desta dissertação foi desenvolver e avaliar o desempenho de um mecanismo de balanceamento de carga através do uso de handovers inter-frequência numa rede LTE de pequenas dimensões, considerando a implementação de várias bandas de frequência co-localizadas. As análises consideraram as bandas dos 800, 1800 e dos 2600 MHz em cenários urbanos. A carga da rede e o número de utilizadores activos, caracterizados pela potência recebida, número de recursos alocados e débito, foram os principais parâmetros estudados. Estudaram-se três situações contemplando a combinação de duas bandas de frequência, priorizando-se aquelas de maior valor para a alocação dos utilizadores. Os utilizadores solicitavam serviços de dados típicos ou de voz sobre LTE, sendo a sua associação a um sector feita com base na potência recebida de modo a melhor se assemelhar à realidade. Foram realizados estudos em ambientes de alta e de baixa carga e foram feitas e analisadas medições ao longo da cidade de Lisboa. Conclui-se que o algoritmo implementado obtém melhores resultados em cenários de alta densidade de utilizadores, tendo em conta que, em média, 520 utilizadores foram servidos utilizando as combinações da banda dos 1800 MHz com a dos 2600 MHz ou com a dos 800 MHz, atingindo débitos na ordem dos 2.5 Mbps e dos 1.5 Mbps, respectivamente, e mantendo a carga da rede estabilizada em 90%.

Palavras-chave

LTE, balanceamento de carga, *handovers* inter-frequência, bandas de frequência co-localizadas, Lisboa

Table of Contents

Acknowledgements	v
Abstract.....	vii
Resumo	viii
Table of Contents.....	ix
List of Figures	xi
List of Tables.....	xiii
List of Acronyms	xiv
List of Symbols.....	xvii
List of Software	xix
1 Introduction	1
1.1 Overview.....	2
1.2 Motivation and Contents	6
2 Fundamental Concepts and State of the Art.....	9
2.1 Network Architecture.....	10
2.2 Radio interface.....	11
2.3 Services and applications	14
2.4 Inter-frequency Handovers	17
2.5 State of the Art.....	19
3 Algorithms and Simulator Description	23
3.1 Initial Considerations.....	24
3.2 Algorithm Description.....	28
3.3 Simulator Description.....	30
3.4 Model Assessment	35
4 Results Analysis.....	41

4.1	Scenarios Description	42
4.2	High Load Analysis	45
4.3	Low Load Analysis	53
4.4	Walk-Tests Results	62
5	Conclusions	69
Annex A	Radio Link Budget.....	75
Annex B	COST 231 Walfisch-Ikegami Propagation Model	79
Annex C	SINR and Throughput	83
Annex D	User's Manual	85
References	89

List of Figures

Figure 1.1. Global traffic in mobile networks, 2010-2014 (extracted from [Eric14]).	2
Figure 1.2. Schedule of 3GPP standard and their commercial deployment (extracted from [HoTo11]).	4
Figure 1.3. Evolution of the peak data rates of 3GPP technologies (extracted from [HoTo11]).	4
Figure 1.4. Evolution of the network solutions from GSM to LTE (extracted from [3GPP13a]).	5
Figure 1.5. Global mobile traffic forecast, 2013-2018 (extracted from [Cisc14]).	5
Figure 2.1. System architecture for E-UTRAN only network (extracted from [HoTo11]).	10
Figure 2.2. Example of different carrier frequencies and respective coverage area.	12
Figure 2.3. Frame Structure Type 1 (extracted from [3GPP13b]).	12
Figure 2.4. OFDMA resource allocation in LTE (extracted from [Corr13]).	13
Figure 2.5. Resource mapping in SC-FDMA (extracted from [HoTo11]).	14
Figure 2.6. Inter-eNB HO procedure (extracted from [HoTo11]).	18
Figure 2.7. Handover delay and interruption time (extracted from [HoTo11]).	19
Figure 2.8. Assumed CC management policies (extracted from [YNII11]).	21
Figure 3.1. Ideal scenario for multiple carrier deployment and respective overlapping areas.	24
Figure 3.2. New call admission process.	28
Figure 3.3. Static analysis process.	29
Figure 3.4. Load restore process.	29
Figure 3.5. Dynamic analysis process.	30
Figure 3.6. Modules that compose the simulator and respective output files (simulator workflow).	31
Figure 3.7. Standard deviation over the average of the number of active users, for high and low load, for the 2600 MHz and 1800 MHz carriers combination.	36
Figure 3.8. Standard deviation over the average of the number of active users, for high and low load, for the 2600 MHz and 800 MHz carriers combination.	37
Figure 3.9. Standard deviation over the average of the number of active users, for high and low load, for the 1800 MHz and 800 MHz carriers combination.	37
Figure 3.10. Number of served users along the covered users in the network.	38
Figure 3.11. Network load behaviour during one hour, considering only the 2600 MHz and the 1800 MHz carriers (scenario 1).	38
Figure 4.1. Throughput versus received power according to different modulation and coding schemes.	44
Figure 4.2. Load distribution in each frequency band, for the three defined carrier combinations.	46
Figure 4.3. Load distribution for each type of service, for the three defined carrier combinations.	47
Figure 4.4. Load distribution for the three defined carrier combinations, for FTP users.	47
Figure 4.5. Load distribution for the three defined carrier combinations, for VoLTE users.	47
Figure 4.6. Number of active users by type of service, for the three defined carrier combinations.	48
Figure 4.7. Number of active users by frequency band, for the three defined carrier combinations.	48
Figure 4.8. Average received power for FTP users, for the three defined carrier combinations.	49
Figure 4.9. Average received power for VoLTE users, for the three defined carrier combinations.	49
Figure 4.10. Received power by frequency band, for the three defined carrier combinations.	50
Figure 4.11. Average SINR by frequency band, for the three defined carrier combinations.	50

Figure 4.12. Average SINR for FTP users, for the three defined carrier combinations.	51
Figure 4.13. Average SINR for VoLTE users, for the three defined carrier combinations.	51
Figure 4.14. Average throughput for FTP users, for the three defined carrier combinations.	52
Figure 4.15. Average number of allocated RBs for FTP users in each frequency band, for the three defined carrier combinations.	52
Figure 4.16. Average number of allocated RBs in a sector per type of service, for the three defined carrier combinations.	53
Figure 4.17. Load distribution in each frequency band, for the three defined carrier combinations.	54
Figure 4.18. Load distribution for each type of service, for the three defined carrier combinations.	55
Figure 4.19. Load distribution for the three defined carrier combinations, for FTP users.	55
Figure 4.20. Load distribution for the three defined carrier combinations, for VoLTE users.	56
Figure 4.21. Number of active users by type of service, for the three defined carrier combinations.	56
Figure 4.22. Number of active users by frequency band, for the three defined carrier combinations.	57
Figure 4.23. Average received power for FTP users, for the three defined carrier combinations.	57
Figure 4.24. Average received power for VoLTE users, for the three defined carrier combinations.	58
Figure 4.25. Received power by frequency band, for the three defined carrier combinations.	59
Figure 4.26. Average SINR by frequency band, for the three defined carrier combinations.	59
Figure 4.27. Average SINR for FTP users, for the three defined carrier combinations.	60
Figure 4.28. Average SINR for VoLTE users, for the three defined carrier combinations.	60
Figure 4.29. Average throughput for FTP users, for the three defined carrier combinations.	61
Figure 4.30. Average number of allocated RBs for FTP users in each frequency band, for the three defined carrier combinations.	61
Figure 4.31. Average number of allocated RBs in a sector per type of service, for the three defined carrier combinations.	62
Figure 4.32. Frequency bands for the walk-tests.	63
Figure 4.33. Measurement of the RSRP in the area of Baixa.	64
Figure 4.34. Measurement of the RSRP in the area of Moscavide.	64
Figure 4.35. Measurement of the SNR in the area of Baixa.	64
Figure 4.36. Measurement of the SNR in the area of Moscavide.	65
Figure 4.37. Measurement of the number of allocated RBs in the area of Baixa.	65
Figure 4.38. Measurement of the number of allocated RBs in the area of Moscavide.	66
Figure 4.39. Measurement of the throughput for the area of Baixa.	66
Figure 4.40. Measurement of the throughput for the area of Moscavide.	67
Figure B.1. COST 231 Walfisch-Ikegami Propagation Model, side view (extracted from [Corr13]).	80
Figure B.2. COST 231 Walfisch-Ikegami Propagation Model, view from above (extracted from [Mart13]).	80
Figure D.1. Propagation model parameters.	86
Figure D.2. Traffic properties.	86
Figure D.3. Network settings.	87

List of Tables

Table 2.1. Relationship between bandwidth, number of sub-carriers and of RBs (adapted from [Corr13]).....	13
Table 2.2. QoS traffic classes summary, according to 3GPP (adapted from [3GPP12b]).....	16
Table 2.3. QoS parameters for QCI (adapted from [3GPP13c]).	16
Table 4.1. Configuration of parameters for the COST 231 Walfisch-Ikegami model.	42
Table 4.2. Simulation parameters.	43

List of Acronyms

2G	Second Generation
3G	Third Generation
3GPP	Third Generation Partnership Project
4G	Fourth Generation
AMBR	Aggregated Maximum Bit Rate
AMC	Adaptive Modulation and Coding
AN	Access Network
ARP	Allocation and Retention Priority
BS	Base Station
CA	Carrier Aggregation
CAC	Call Admission Control
CAGR	Compound Annual Growth Rate
CC	Component Carrier
CCCH	Common Control Channel
CP	Cyclic Prefix
CQI	Channel Quality Indicator
DCCH	Dedicated Control Channel
DL	Down Link
E-UTRAN	Evolved Universal Terrestrial Radio Access Network
EDGE	Enhanced Data Rates for GSM Evolution
EIRP	Effective Isotropic Radiated Power
eNB	Evolved NodeB
EPA	Extended Pedestrian A
EPC	Evolved Packet Core
EPS	Evolved Packet System
ETSI	European Telecommunications Standards Institute
FDD	Frequency Division Duplex
FST1	Frame Structure Type 1
FST2	Frame Structure Type 2
FTP	File Transfer Protocol
GBR	Guaranteed Bit Rate
GERAN	GSM/EDGE Radio Access Network
GPRS	General Packet Radio Service
GSM	Global System for Mobile Communications

GTP	GPRS Tunnelling Protocol
HO	Handover
HSDPA	High Speed Down Link Packet data Access
HSPA	High Speed Packet data Access
HSS	Home Subscription Server
HSUPA	High Speed Up Link Packet data Access
IMT-A	International Mobile Telecommunications Advanced
IP	Internet Protocol
ISI	Inter-Symbol Interference
LB	Load Balancing
LoS	Line-of-Sight
LTE	Long Term Evolution
LTE-A	Long Term Evolution Advanced
MAC	Medium Access Control
MBR	Maximum Bit Rate
MIMO	Multiple Input Multiple Output
MM	Mobility Management
MME	Mobility Management Entity
NLoS	Non Line-of-Sight
OFDMA	Orthogonal Frequency Division Multiple Access
P-GW	Packet Data Network Gateway
PAR	Peak-to-Average Ratio
PBCH	Physical Broadcast Channel
PCC	Primary Component Carrier
PCEF	Policy and Charging Enforcement Function
PCell	Primary Cell
PCI	Physical Cell Identity
PCRF	Policy and Charging Resource Function
PDN	Packet Data Network
PDSCH	Physical Downlink Shared Channel
PDU	Protocol Data Unit
PF	Proportionally Fair
PLMN	Public Land Mobile Network
PMCH	Physical Multicast Channel
PRACH	Physical Random Access Channel
PS	Packet Scheduling
PUSCH	Physical Uplink Shared Channel
QAM	Quadrature Amplitude Modulation
QCI	Quality of Service Class Identifier
QoS	Quality of Service

QPSK	Quadrature Phase Shift Keying
RACH	Random Access Channel
RAT	Radio Access Technology
RB	Resource Block
RE	Resource Element
RRC	Radio Resource Control
RRM	Radio Resource Management
RS	Reference Signal
RSRP	Reference Symbol Received Power
RSRQ	Reference Symbol Received Quality
S-GW	Serving Gateway
SAE	System Architecture Evolution
SC-FDMA	Single Carrier Frequency Division Multiple Access
SCC	Secondary Component Carrier
SCell	Secondary Cell
SCTP	Stream Control Transmission Protocol
SINR	Signal-to-Interference-plus-Noise Ratio
SMS	Short Message Service
SNR	Signal-to-Noise Ratio
TDD	Time Division Duplex
TDMA	Time Division Multiple Access
TTI	Transmission Time Interval
UDP	User Datagram Protocol
UE	User Equipment
UL	Up Link
UMTS	Universal Mobile Telecommunication System
UP	User Plane
UTRAN	Universal Terrestrial Radio Access Network
USB	Universal Serial Bus
VoIP	Voice over IP
VoLTE	Voice over LTE

List of Symbols

α_B	Angle of incidence of the signal in the buildings
ε_r	Relative error
ρ_{IN}	SINR
ρ_N	SNR
φ	Street orientation angle
B_{RB}	RB bandwidth
C_{cell}	Cell load
C_{user}	User load
d	Distance between eNB and UE
f	Carrier frequency of the signal
F_N	Noise figure
G_r	Gain of the receiving antenna
G_t	Gain of the transmitting antenna
h_b	Height of the eNB antenna from ground
H_b	Buildings height
h_m	UE height
I	Interfering Power
L_0	Free space propagation path loss
L_c	Losses in the cable between the transmitter and the antenna
L_p	Path loss
$L_{p,total}$	Path loss from the COST 231 Walfisch-Ikegami model
L_p	Attenuation due to diffraction from the last rooftop to the UE
L_{rm}	Attenuation due to propagation from the BS to the last rooftop
L_{rt}	Losses due to the user
L_u	Fast fading margin
M_{FF}	Slow fading margin
M_{SF}	Noise power
N	Number of bits per symbol
$N_{b/sym}$	Number of cells in the network
N_{cells}	Number of interfering signals reaching the receiver
N_I	MIMO order
N_{MIMO}	Total number of RBs in a cell
$N_{RB,cell}$	Total number of scheduled RBs in a cell
$N_{RB,scheduled}$	Number of RBs allocated to a user
$N_{RB,user}$	

N_{RB}	Number of RBs to be considered
$N_{sub/RB}$	Number of sub-carriers per RB
$N_{sym/sub}$	Number of symbols per sub-carrier
P_{EIRP}	Effective Isotropic Radiated Power
P_r	Power available at the receiving antenna
P_{Rx}	Power at the input of the receiver
P_{Tx}	Transmitter output power
R_b	Throughput
T_{RB}	Time duration of an RB
$V_{measurement}$	Value obtained from the measurements
$V_{simulation}$	Value obtained from the simulator
w_B	Building separation
w_s	Street width

List of Software

Borland C++ Builder 6

FileZilla

Google Earth

MapInfo 11.5

Microsoft Excel 2010

Microsoft Powerpoint 2010

Microsoft Word 2010

TEMS Discovery 3.0.2

TEMS Investigation 13.1.33

C++ App Development Environment

FTP client

Geographical information program

Geographical information system software

Spreadsheet application

Presentation and slide program

Word processor

Drive-test analysis software

Software for verification of wireless networks

Chapter 1

Introduction

This chapter contains the main background and motivational framework for this study. Moreover, it presents the scope of the thesis and describes the structure of the work.

1.1 Overview

Humans have always felt the need for communication, be it within themselves, with another person or within groups. This need, together with the concern for nowadays users' mobility, has led to a rapid development of mobile voice communication over the last decade. Not only did the number of subscribers grow from one to five billions between 2002 and 2010, [HoTo11], but so did the requested traffic in the last years. This is where the most noteworthy change took place in terms of user demands, as one can see in Figure 1.1, showing that, in a period of four years, global traffic evolved from a situation where the request for both types of traffic was balanced to an overwhelming dominance of requested data traffic.

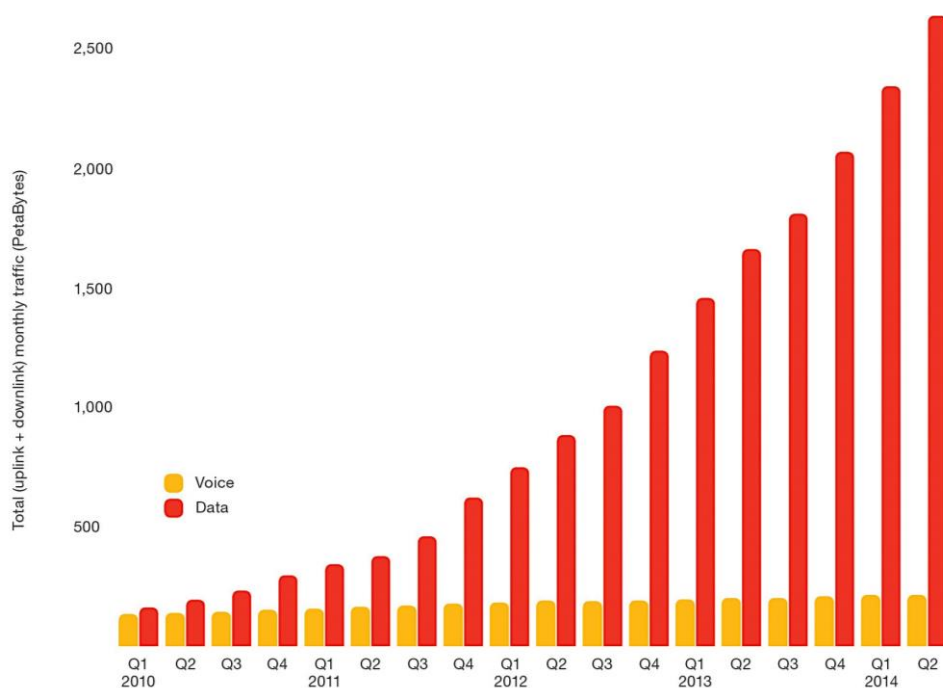


Figure 1.1. Global traffic in mobile networks, 2010-2014 (extracted from [Eric14]).

Although wireline networks are still capable of delivering the highest data rates, [HoTo11], wireless networks have continuously evolved in order to keep pace of the fixed services achieved data rates, since users expect to obtain a similar performance from their mobile network. Be that as it may, wireless technologies possess the capability to provide personal broadband access, independent of the user's location, this being its main asset. Also, they can work as a low-cost solution for broadband coverage comparing with new wireline installations, should there be no existing infrastructure for the latter technology.

In early stages, the main concern was to have a mobile network that would carry voice traffic. The Global System for Mobile Communications (GSM), as a second-generation (2G) mobile network developed by the European Telecommunications Standards Institute (ETSI), was designed for this

goal, with later improvements dealing with data traffic: the Enhanced Data Rates for GSM Evolution (EDGE) and the General Packet Radio Service (GPRS). This last one was the first step for having an Internet Protocol (IP) based packet switched solution for mobile systems and uses the same air access method, Time Division Multiple Access (TDMA).

In order to bridge the continuous development of cellular communications networks technologies, the Third Generation Partnership Project (3GPP) was created, comprising six telecommunications standards development organisations, known as Organisational Partners. The main focus of this group's Releases is both backward and forward compatibility where ever possible, and also to provide their members a stable environment to work on the reports and specifications that define 3GPP technologies, [3GPP14e]. This project includes the study of the radio access, the core transport network and the service capabilities, therefore being able to deliver full system specifications. Milestones achieved in particular Releases serve as progress measurement for this group.

The attractiveness of Internet and the improvements on image and video quality gave rise to a demand for larger data volumes and higher bit-rate services, which justified the need for a more capable mobile system. Thus, third-generation (3G) mobile networks were developed, such as Universal Mobile Telecommunication System (UMTS) in 3GPP's Release 99. This release was completed at the end of 1999 and contemplated a new access technology using Wideband Code Division Multiple Access (WCDMA). The IP address is only allocated after a service is requested by the user, and is released when the service ends.

The unceasing request for higher bit-rates and the need for better data download/upload services led to the upgrade of the packet data system. 3GPP introduced Release 5 High Speed Downlink (DL) Packet data Access (HSDPA) in 2002, and in 2004 Release 6 High Speed Uplink (UL) Packet data Access (HSUPA). These two improvements together are also referred to as High Speed Packed data Access (HSPA), and it was enhanced for even higher bit-rates (HSPA+) in 2007 with Release 7.

In the subsequent year, Long Term Evolution (LTE) was first specified with Release 8, where Orthogonal Frequency Division Multiple Access (OFDMA) is used for DL and Single Carrier Frequency Division Multiple Access (SC-FDMA) for UL. Some features were only added to this purely IP-based network in Release 9, such as backwards compatibility with UMTS and overall architecture improvements.

In order to achieve a better performance than the one offered by the existing 3GPP networks based on UMTS/HSPA, multiple requirements were defined for LTE, such as peak user throughputs reaching 100 Mbps in DL and 50 Mbps in UL, which is ten times more than that of HSPA Release 6. Latency also needs to be improved, so that user experience is enhanced and the terminal power consumption must be minimised, thus allowing a higher usage of multimedia applications without the need to constantly recharge the battery of the equipment. Regarding bandwidth allocation, LTE is supposed to be flexible to the point of allowing the use of less than 1.5 MHz and up to 20 MHz.

Figure 1.2 illustrates the time schedules of the 3GPP specifications together with their respective commercial deployment, where each date refers to the approval of the specification.

3GPP schedule

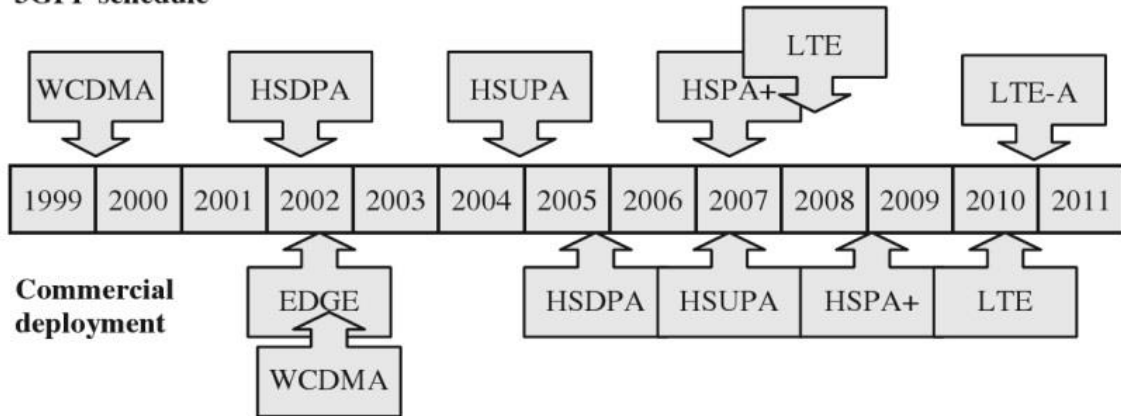


Figure 1.2. Schedule of 3GPP standard and their commercial deployment (extracted from [HoTo11]).

Further enrichments in LTE capabilities were presented in Release 10 Long Term Evolution Advanced (LTE-A) in December 2010, namely the use of Carrier Aggregation (CA) and enhanced Multiple Input Multiple Output (MIMO) with the purpose of fulfilling the requirements issued by the International Mobile Telecommunications Advanced (IMT-A) for a fourth Generation (4G) mobile network.

With the development and implementation of each new generation of technologies also comes an enhancement in the peak throughputs, as shown in Figure 1.3. Moreover, every new 3GPP technology is conceived to be deployed in coexistence with older ones, so seamless interworking between the different technologies is required. For instance, handovers are allowed from and to LTE even if the user is connected or wants to connect to the GSM or UMTS network. Besides, these three generations of technologies may share some network elements, e.g., those of the core network. In addition, some of the 3G network elements can be upgraded to support LTE, thus enabling the existence of a platform comprising both UMTS/HSPA and LTE.

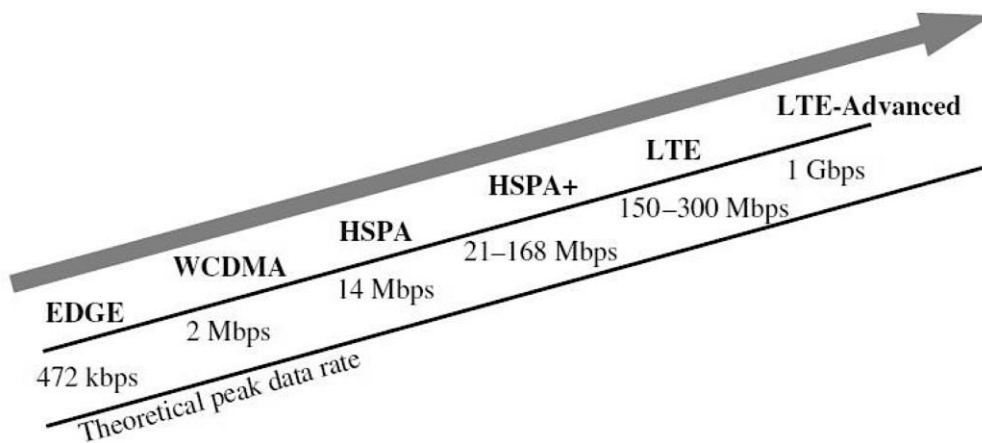


Figure 1.3. Evolution of the peak data rates of 3GPP technologies (extracted from [HoTo11]).

In Figure 1.4, one presents the network solutions from GSM to LTE. In the first two systems, the GSM/EDGE Radio Access Network (GERAN) and the Universal Terrestrial Radio Access Network (UTRAN) are the radio access networks for GSM and UMTS systems respectively. The Evolved Universal Terrestrial Radio Access Network (E-UTRAN) is the radio access network while the Evolved

Packet Core (EPC) is, as the name suggests, the core network and together they make the Evolved Packet System (EPS), which is responsible for providing IP based connectivity. The eNodeB (eNB) is, simply put, a Base Station (BS) that is responsible for all radio related functions. It is possible to find a more detailed description about the LTE network architecture and radio interface on Chapter 2.

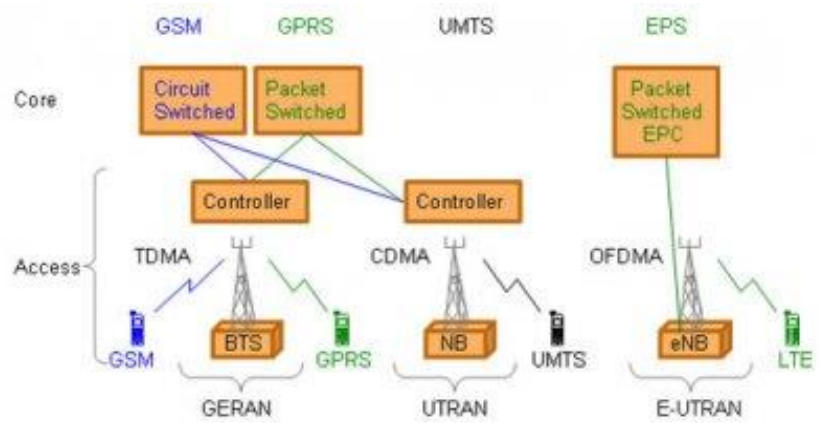


Figure 1.4. Evolution of the network solutions from GSM to LTE (extracted from [3GPP13a]).

It is expected that the overall mobile data traffic will continue its growth over the next years. According to [Cisc14], global mobile data traffic grew 81% in 2013, and it is estimated that it will grow at a Compound Annual Growth Rate (CAGR) of 61% from that date to 2018, as shown in Figure 1.5. Smartphones popularity nowadays strongly contributes to these expectations, mainly due to the growth in subscriptions and to the need for more demanding services in terms of throughput and latency. These devices accounted for 88% of the global mobile data traffic in 2013, even though they represented 21% of the total mobile devices and connections. By 2018, it is expected that smartphones will represent 54% of the total mobile devices, generating 96% of the global mobile traffic.

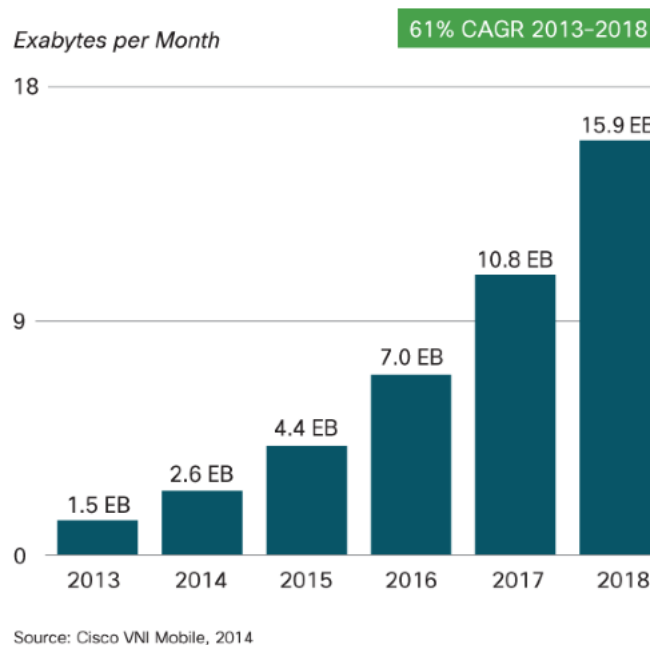


Figure 1.5. Global mobile traffic forecast, 2013-2018 (extracted from [Cisc14]).

1.2 Motivation and Contents

The attractiveness of LTE is an important factor in the growth of the number of subscribers of telecommunication services. Users are able to achieve higher data-rates and a wider variety of services with ensured quality levels, consequently demanding a better overall performance of the network. This increase in the number of users in the network incites operators to be concerned about the capacity of the system to accommodate such quantity of traffic, while maintaining the network load balanced. An interesting feature of E-UTRAN, which can be of assistance in this issue, is the deployment of multiple carrier frequencies over the same coverage area, bringing up and encouraging further study on inter-frequency Handovers (HOs). 3GPP provides the necessary procedures and requirements related to the use of inter-frequency HOs, in order to guarantee the efficient use of the multiple carrier frequencies.

The main goal of this thesis was to evaluate the performance of LTE in urban scenarios, regarding network load distribution, by studying different scenarios where users connect to the network detecting different carriers and experiencing variable throughputs. The purpose is then to optimise these throughputs, while maintaining the network load within suitable values. It is known for a fact that for each carrier frequency, different coverage areas and throughputs are obtained, resulting in a trade-off between both that deeply affects user experience.

This thesis was developed in collaboration with Vodafone, and the conclusions drawn throughout the developed work may be of interest, mainly on how to take advantage of the use of different frequency bands for distributing load and retaining signal quality. The measurements performed under the scope of this work were made using the equipment supplied by Vodafone and using its own network. Vodafone also provided support in examining the measured results, and the analysis performed in this thesis are based on the three frequency bands used in Vodafone's network to provide coverage.

The output of this work is the model developed for LTE networks in urban scenarios based on the city of Lisbon, but considering only a set of six eNBs in a region, where users require services from the network in given instances and in a given position, and are associated with a given throughput. Users then compete for the available network resources according to the priority of the service they are requesting and their signal quality.

Regarding the structure of this thesis, five different chapters are presented, providing a description of the developed work, the methods used and the obtained results. The present chapter is a guideline to explain the constant need to develop and improve mobile communications systems by briefly describing the existing systems and their adoption throughout the world.

Chapter 2 mainly introduces LTE, by initially providing a general understanding of the network architecture and radio interface. The main elements that constitute the network are described as well as the aspects of the modulations schemes, frame structures and spectrum organisation, followed by the description of the services and applications requirements and priorities. Afterwards, inter-frequency HOs in LTE networks are described, clarifying the messages that are traded between the

user and the network and characterising the different events and parameters that have to be taken into account, such as measured values and measurement periods, regarding HO preparation and execution. The final part of this chapter addresses the state of the art, presenting some previously developed works on the thesis subject.

Chapter 3 is dedicated to the description of the models used throughout this thesis, starting by explaining the various considerations that are of relevance for the development of the present work, such as coverage, capacity and throughput calculations, and the relationship between them. The implemented algorithm is then analysed so one can further understand how the network is able to achieve a balanced load distribution and how the different parameters can influence network performance. The description of the implemented simulator is also presented in this chapter, where an illustration shows the simulator workflow followed by a textual description to facilitate the comprehension of the different elements that compose it. At the end of this chapter, the developed models are assessed, ensuring that the obtained results are indeed relevant for this study.

Results obtained from the simulations are addressed in Chapter 4, together with the results obtained from the measurements made in the city of Lisbon, allowing the comparison between both, and thus providing one more way to assess the implemented models. The study of these results is made resorting to two distinct analyses, each one defined by the network load being considered. The low load analysis takes into account the simulated results obtained under a low load scenario, while the high load one considers a scenario where the existing load originates a situation of overload. The results in both analyses enable the study of the different parameters that are of interest for this work, such as network load distribution, signal quality and ratio of satisfied users. Afterwards, relevant results and figures obtained from the measurements performed in the city of Lisbon are presented.

Chapter 5 summarises the developed work in order to provide a superficial description of the main aspects of this thesis. Moreover, this chapter presents the conclusions that were drawn based on the results obtained in the previous chapter and it also contains some suggestions for future work.

The final content of this thesis consists of a group of annexes containing additional information. Annex A provides information on how to calculate the link budget, making use of the path loss that the signal suffers when travelling between the user and the eNB. This path loss is modelled by the COST 231 Walfisch-Ikegami model, which is addressed in Annex B. The models for Signal-to-Interference-plus-Noise-Ratio (SINR) and data rates are presented in Annex C. Finally, Annex D presents the user's manual, intended to aid in the use of the simulator.

Chapter 2

Fundamental Concepts and State of the Art

This chapter provides an overview of the LTE system, mainly focussing on inter-frequency HOs. The overall network architecture is presented in Section 2.1, followed by the main technical features of the radio interface in Section 2.2. The services and applications are examined in Section 2.3, while the study of the inter-frequency HO aspects that are more relevant for this thesis is presented in Section 2.4. Finally, some of the previously published work in this subject is presented in Section 2.5

2.1 Network Architecture

This section contains information on LTE and LTE-A network architecture, its contents being based on [3GPP13a] and [HoTo11].

The implementation of 3GPP System Architecture Evolution (SAE) was only possible after discussion of many aspects of the network. A flatter architecture would be required so that fewer nodes are involved and, therefore, lower latency and better performance.

Figure 2.1 represents the design for the E-UTRAN network, where the dotted line represents a connection in the Control Plane and the full one a connection in the User Plane (UP). The structure is divided into four main areas: User Equipment (UE), E-UTRAN, EPC and the Services domain.

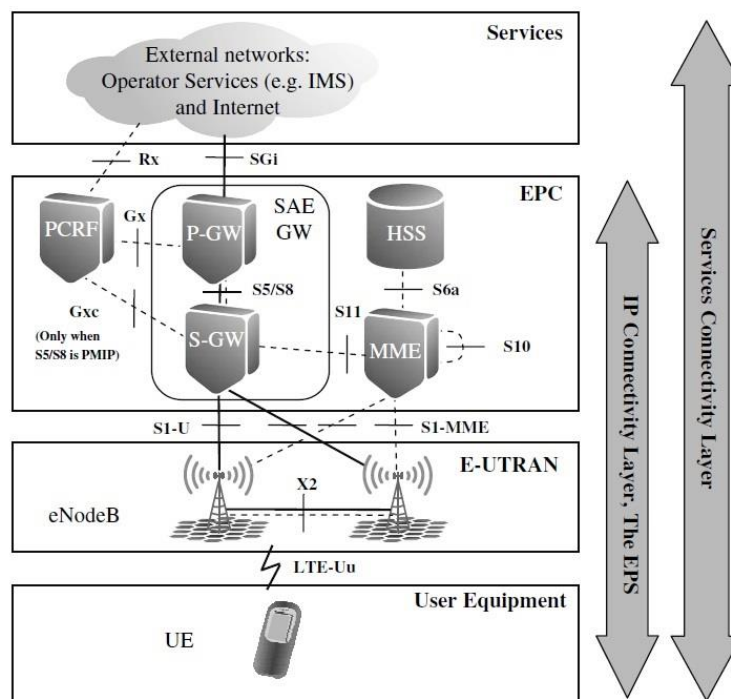


Figure 2.1. System architecture for E-UTRAN only network (extracted from [HoTo11]).

The EPC together with the E-UTRAN form the EPS. Functionally, the EPC is responsible for maintaining the communication between Access Networks (ANs), and its main components are:

- **Mobility Management Entity (MME).** This is the central control element, operating only in the Control Plane as the primary control channel between the UE and the network. It is responsible for the authentication and security of the UE in the network, it manages the subscription profile of the UE, and it deals with mobility issues, always regarding the Control Plane.
- **Serving Gateway (S-GW).** It acts as the mobility anchor in the UP in inter-eNB HOs and provides user data packet routing.

- Packet Data Network (PDN) Gateway (P-GW). It establishes the connection between the EPC and external IP networks. Also controls and delivers data over the UP tunnels for UL and DL.
- Policy and Charging Resource Function (PCRF). It provides policy control and flow based charging control decisions. It works together with the Policy and Charging Enforcement Function (PCEF), located in the P-GW, to ensure that the correct Quality of Service (QoS) is provided.
- Home Subscription Server (HSS). It records user subscription data including applicable services and allowable connections and stores the location of the UE within the visited network control node.

The E-UTRAN is a collection of eNBs interconnected via the X2 interface and connected to the EPC through the S1 one, Figure 2.1. Each eNB is the termination point for all radio related protocols, being responsible for Control Plane functions for monitoring radio resource usage, called Radio Resource Management (RRM).

Furthermore, it is in charge of the Mobility Management (MM), i.e., it evaluates radio signal level measurements performed by both the UE and the eNB itself for HO purposes. In addition, the eNB conducts data delivery in the UP while ensuring security and optimisation of the radio interface and performs IP header compression/decompression in order to avoid having repeated data transmissions.

2.2 Radio interface

This section addresses the radio interface for LTE and LTE-A, its contents being based on [3GPP13b], [3GPP14d] and [HoTo11].

According to 3GPP specifications, there are currently 25 frequency bands for Frequency Division Duplex (FDD) and 12 for Time Division Duplex (TDD) available for mobile operators, including the 800 MHz, 900 MHz, 1800 MHz, 2100 MHz and 2600 MHz bands. In Portugal, ANACOM (Portuguese Telecommunications Authority) decided to mainly use the 800 MHz, 1800 MHz and 2600 MHz bands for the operating frequency band licenses auction, [ANAC14]. It is pertinent to notice that different carrier frequencies originate different path losses, thus, different coverage areas. As shown in Annex B and better illustrated in

Figure 2.2, the radius of a cell grows inversely with frequency, when considering similar transmitting and receiving power and antenna gains. A more thorough study for the calculation of this radius is available in Section 3.1.

As discussed in Chapter 1, LTE uses OFDMA for DL and SC-FDMA for UL. The main reasons for this are due to the fact that using SC-FDMA allows better UL range and improved device battery life. Regarding the use of OFDMA, other properties are relevant (comparing with other access

technologies), namely:

- Good performance in frequency selective fading channels;
- Low complexity of base-band receiver;
- Good spectral properties;
- Handling multiple bandwidths;
- Link adaptation and frequency domain scheduling;
- Compatible with advanced receiver and antenna technologies (e.g., MIMO).

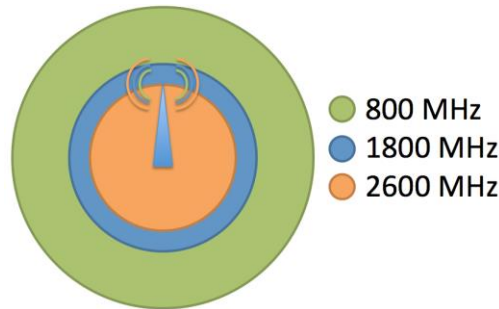


Figure 2.2. Example of different carrier frequencies and respective coverage area.

The orthogonality principle defines that the centre frequency for each of the sub-carriers corresponds to the one that matches the zero value of the neighbouring sub-carriers in the frequency domain. LTE specifies a constant 15 kHz spacing in between sub-carriers, which eases implementation error effects and Doppler Effect without much deterioration of sub-carriers orthogonality. In order to avoid Inter-Symbol Interference (ISI) a Cyclic Prefix (CP) is used, meaning that the last part of the symbol is copied to the beginning so that the symbol appears to be periodic. The prefix length can vary, so that it is large enough to exceed the delay spread.

Since LTE supports both FDD and TDD, two frame structures are used. Frame Structure Type 1 (FST1) is employed in FDD and Frame Structure Type 2 (FST2) in TDD. This thesis focuses on FST1, since FDD is the implemented duplexing method. The maximum frame length is 10 ms divided into 20 slots of 0.5 ms each, while two consecutive slots (1 ms) form one subframe, as illustrated in Figure 2.3, representing the Transmission Time Interval (TTI).

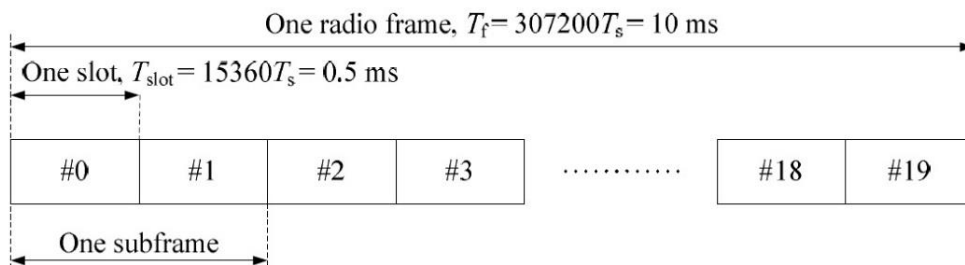


Figure 2.3. Frame Structure Type 1 (extracted from [3GPP13b]).

Frequency domain scheduling is another specification of LTE, allowing the dynamic allocation of resources in the frequency domain, based on Resource Blocks (RB), as illustrated in

Figure 2.4. Each RB consists of a group of 12 sub-carriers, using a total bandwidth of 180 kHz, and 7 or 6 OFDM symbols in the time domain, depending on if the used CP is short (5.21 μ s) or extended

(16.67 μ s). The minimum resource unit is the Resource Element (RE) consisting of one sub-carrier during one OFDM symbol, meaning that an RB can have 84 (12 sub-carriers \times 7 OFDM symbols) or 72 (12 sub-carriers \times 6 OFDM symbols) RE per slot in the time domain. LTE specifies channel bandwidths from 1.4 MHz to 20 MHz, corresponding to a total of 6 to 100 RB.

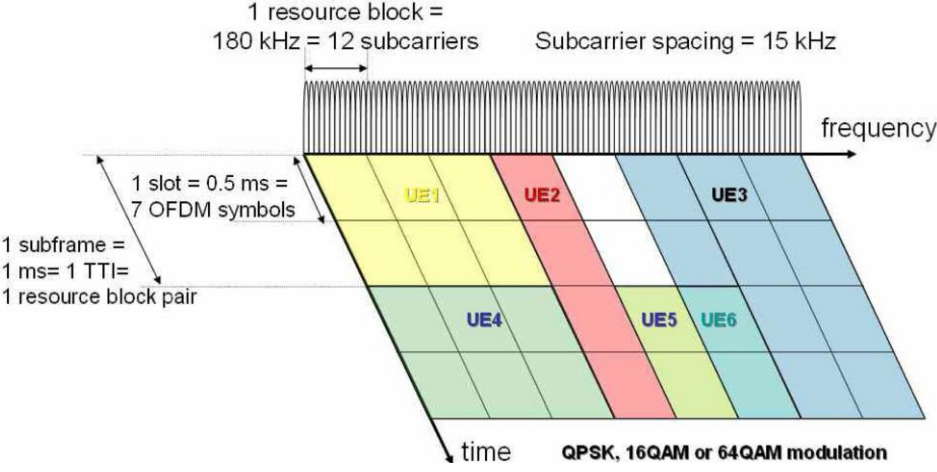


Figure 2.4. OFDMA resource allocation in LTE (extracted from [Corr13]).

Release 10 LTE-A enables the use of up to 100 MHz channel bandwidth by using CA in which up to five Release 8 carriers are grouped, each one with a maximum bandwidth of 20 MHz. CA can be used in both TDD and FDD systems and, besides providing a larger transmission bandwidth, it eases the efficient use of fragmented spectrum. FDD systems always have less UL component carriers than DL ones whereas in TDD each component carrier uses the same configuration in both DL and UL, allocating subframes in the same way. Table 2.1 depicts the relationship between available bandwidth, number of carriers and number of RBs.

Table 2.1. Relationship between bandwidth, number of sub-carriers and of RBs (adapted from [Corr13]).

Bandwidth [MHz]	1.4	3	5	10	15	20
Number of sub-carriers	72	180	300	600	900	1200
Number of RBs	6	15	25	50	75	100

On the other hand, the transmitted signal in OFDMA has a high Peak-to-Average Ratio (PAR), which requires high linearity in the transmitter. Linear amplifiers have low power conversion efficiency, hence, the use of SC-FDMA in UL enabling a better power amplifier efficiency.

When using SC-FDMA only one symbol is sent at a time like in TDMA, however, the signal is generated in the frequency domain so it maintains the good spectral properties of OFDMA. The CP is added periodically, but not in the end of each symbol due to the increase in symbol rate. Resource allocation is illustrated in Figure 2.5, being very similar to the OFDMA scheme, the difference being that RBs are allocated continuously to one user in the frequency domain. The maximum bandwidth to be allocated is 20 MHz, but this takes margins for the guard bands into account, reducing the useful bandwidth.

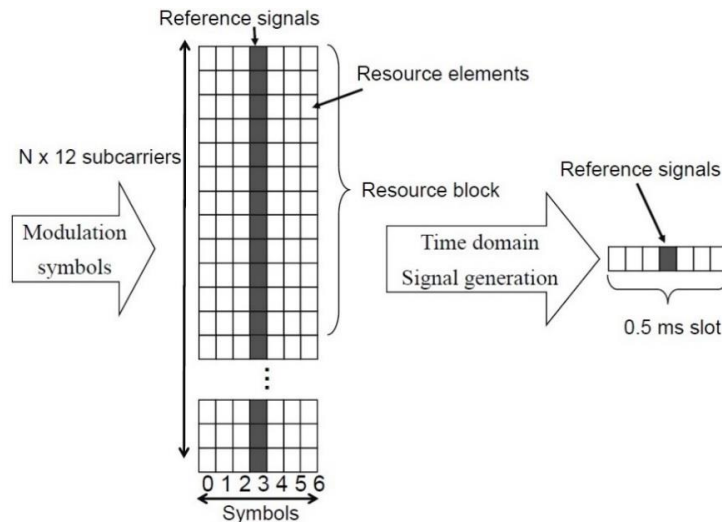


Figure 2.5. Resource mapping in SC-FDMA (extracted from [HoTo11]).

The introduction of MIMO is one of the fundamental improvements in LTE. Spatial multiplexing is one of the operations used and it increases peak data rate (by a factor of two or more) by sending signals from two or more different antennas with different data streams. Recent developments allow up to an 8×8 configuration for DL and 4×4 for UL. Pre-coding is another process used in which the signals transmitted from different antennas are weighed in order to maximise the received Signal-to-Noise Ratio (SNR). MIMO also relies on transmit diversity, where the same signal is sent from different antennas with some coding so that one may exploit the gains from independent fading between antennas.

The transport channels, acting as interfaces between the Medium Access Control (MAC) layer and the physical layer, are mapped onto physical channels. They can be:

- Physical Broadcast Channel (PBCH). Carries system parameters needed by the UE to access the system.
- Physical Downlink Shared Channel (PDSCH). Main downlink physical channel for user data, broadcast system information and paging messages.
- Physical Uplink Shared Channel (PUSCH). Equivalent to the PDSCH but for UL.
- Physical Multicast Channel (PMCH). Transfers multicast service content in DL to the UE.
- Physical Random Access Channel (PRACH). Used for random access.

2.3 Services and applications

In this section, there is information regarding the services and applications in LTE, the contents being based on [Corr13], [HoTo11], [3GPP12b] and [3GPP13d].

Mobile communication systems are mainly focused on offering wireless connection to its users, providing them with the services they request. Nowadays, services and applications may come in

many different forms and have various purposes, voice being the oldest and most popular among all. The voice service is particularly predictable, in the sense that it specifies a constant bit rate, so operators are primarily concerned with delay, which is the factor that can affect mostly the quality of a phone call. On the other hand, data services are becoming more popular, but they can also be very demanding in terms of bit rate, delay and duration while involving a tremendous traffic of data. Services such as Short Text Message (SMS), File Transfer Protocol (FTP), video streaming, email and web browsing can have different quality requirements according to their specific purpose. The main concern for mobile operators is to provide these services to their customers, anytime and anywhere, while guaranteeing a good QoS. 3GPP specifies the concept of UMTS and LTE QoS by defining four classes of services, also referred to as traffic classes, which can be used as a good approach for describing each type of service:

- Conversational services comprise telephony services, like voice and video calls, Voice over IP (VoIP) and conferencing tools. This class is mainly reliant on the transfer time (delay) and time relation (variation) between the information entities of the stream.
- Streaming services are strongly dependent on the time relation between both ends of the stream, as in audio-video streaming in mobile TV applications.
- Interactive services, where one end-user requests data from remote equipment, e.g. a server, are mostly characterised by the request response pattern from the end-user and also by the packet transfer transparency, with low bit error rate. Web browsing, social networking and automatic data base enquiries are some examples of this class.
- Background services consist of end-users sending and receiving data files in the background, where they are stored and can be later accessed. Email, SMS, MMS and Cloud applications serve as examples for this traffic class in which transparent payload transfer is also required, however the delivery time is less relevant.

In Table 2.2, there is information about the above mentioned QoS classes, namely real time requirements, data flows symmetry, guaranteed bit rate necessity, time delay restrictions, extended use of data buffers, traffic burstiness and switching type. However, since LTE is data oriented and regarding the astounding growth of mobile traffic, 3GPP re-specified the QoS standards to keep up with the requested service performance and, although there are less parameters to be defined, they were all optimised:

- QoS Class Identifier (QCI) indexes a set of locally configured values for Priority, Delay and Loss Rate. There are nine pre-configured classes as presented on Table 2.3.
- Allocation and Retention Priority (ARP) indicates the priority of the bearer compared to other bearers, providing information about admission control in bearer set-up and in congestion situations if bearers need to be dropped.
- Maximum Bit Rate (MBR) identifies the maximum bit rate for the bearer.
- Guaranteed Bit Rate (GBR) represents the bit rate that will be guaranteed to the bearer.
- Aggregated Maximum Bit Rate (AMBR) indicates the total maximum bit rate a UE may have for all bearers in the same PDN connection.

Table 2.2. QoS traffic classes summary, according to 3GPP (adapted from [3GPP12b]).

	Conversational	Streaming	Interactive	Background
Real Time	Yes	Yes	No	No
Symmetric	Yes	No	No	No
Bit Rate	Guaranteed	Guaranteed	Non-Guaranteed	Non-Guaranteed
Delay	Minimum fixed	Minimum variable	Moderate variable	High variable
Buffer	No	Yes	Yes	Yes
Bursty	No	No	Yes	Yes
Switching Type	Circuit	Circuit	Packet	Packet
Example	Voice/Video calls	Video streaming	Web browsing	SMS, MMS, Email

There are nine standardised QCI classes as shown on Table 2.3 and, together with their respective parameters, allow a better understanding of the main characteristics of the service. Resource type indicates which classes will have GBR, priority defines the priority for packet scheduling, delay budget helps the packet scheduler to maintain sufficient scheduling rate to meet the delay requirements for the bearer, and loss rate helps to use appropriate Radio Link Control (RLC) settings.

Table 2.3. QoS parameters for QCI (adapted from [3GPP13c]).

QCI	Resource Type	Priority	Packet Delay Budget [ms]	Packet Error Loss Ratio	Example Services
1	GBR	2	100	10^{-2}	Conversational Voice
2		4	150	10^{-3}	Conversational Video (Live Streaming)
3		3	50	10^{-3}	Real Time Gaming
4		5	300	10^{-6}	Non-Conversational Video (Buffered Streaming)
5	Non-GBR	1	100	10^{-6}	IMS Signalling
6		6	300	10^{-6}	Video (Buffered Streaming) TCP-based (e.g., www, e-mail, chat, ftp, p2p file sharing, progressive video, etc.)
7		7	100	10^{-3}	Voice, Video (Live Streaming) Interactive Gaming
8		8	300	10^{-6}	Video (Buffered Streaming) TCP-based (e.g., www, e-mail, chat, ftp, p2p file sharing, progressive video, etc.)
9		9			

2.4 Inter-frequency Handovers

This section addresses mobility related issues in LTE networks regarding inter-frequency HOs, its contents being based on [3GPP13e], [3GPP14b], [3GPP14c] and [HoTo11].

As discussed in Chapter 1, one of 3GPP's main goals is to maintain both backward and forward compatibility, therefore, when dealing with mobility issues one must always consider other generation access networks. HOs may be performed inside E-UTRAN, or from E-UTRAN to another RAT or to E-UTRAN from another RAT. This thesis focuses on inter-frequency intra-LTE HOs, where measurements are made at frequencies that differ from the DL carrier frequency of the serving cell, although all the other previously described situations may be of interest for other studies.

E-UTRAN allows the UE to be in one of two states whether its Radio Resource Control (RRC) connection is established (RRC_CONNECTED) or not (RRC_IDLE). In the RRC_IDLE state, the UE monitors a paging channel to detect received calls while acquiring system information and performing neighbouring cell measurements and cell selections or re-selections. In the RRC_CONNECTED, the UE communicates with the network by sending or receiving data. It also becomes responsible for monitoring control channels, which are associated with the shared data channel to determine if data are scheduled for it and it provides channel quality and feedback information to the eNB. Furthermore, the UE executes neighbouring cell measurements and measurement reporting, as the configuration provided by the eNB requires.

When the UE requests the RRC connection (e.g. when there is a new incoming call) it communicates with the eNB through the Common Control Channel (CCCH) by sending an RRC Connection Request message. The eNB uses this channel to send an RRC Connection Setup message back to the UE allowing it to establish a Dedicated Control Channel (DCCH) by sending an RRC Connection Setup Complete message again to the serving eNB.

As mentioned before, the UE is continuously performing measurements and reporting them according to the parameters established by the network. While in the RRC_IDLE state, the purpose of the UE is to find a cell from the Public Land Mobile Network (PLMN) that is suitable for initial cell selection or is believed to be a better candidate for cell reselection. In case the UE is in the RRC_CONNECTED state, measurements are made to decide whether a HO should take place or not. If needed, the UE may use measurement gaps, i.e. periods where measurements are performed, for inter-frequency measurements.

In order to control the way a UE prioritises camping on different RATs or frequencies of E-UTRAN (referred to as layers from now on), a new method for reselection decision was implemented, called absolute priority based reselection. Each layer is given a priority and, based on this value, the UE tries to camp on the highest priority frequency/RAT if it can provide proper service.

Measurement reporting can be periodic, as in measurements for automatic neighbour cell search, or event-triggered, in which the UE reports if one of the following five events occurs (only for E-UTRAN measurements):

- Event A1: Serving cell becomes better than absolute threshold;
- Event A2: Serving cell becomes worse than absolute threshold;
- Event A3: Neighbour cell becomes amount of offset better than serving cell;
- Event A4: Neighbour cell becomes better than absolute threshold;
- Event A5: Serving cell becomes worse than absolute threshold 1 and neighbour cell becomes better than absolute threshold 2.

The absolute thresholds mentioned above are some of the parameters specified by the network, being of use when compared to measured signal levels and quality, as explained in more detail in Chapter 3.

The eNB has a relevant role in MM, since it is responsible for controlling and evaluating radio signal level measurements made by the UE. It also carries out similar measurements itself and, based on both results, makes decisions to HO UEs between cells, including exchanging HO signalling between other eNBs and the MME.

In the case of an intra-LTE HO, a Handover Request message is sent from the source eNB to the target eNB to prepare the target cell. The latter builds an RRC Connection reconfiguration message and sends a Handover Request Acknowledge message to the source eNB. This message exchange is made through the X2 interface on the eNB, Figure 2.6.

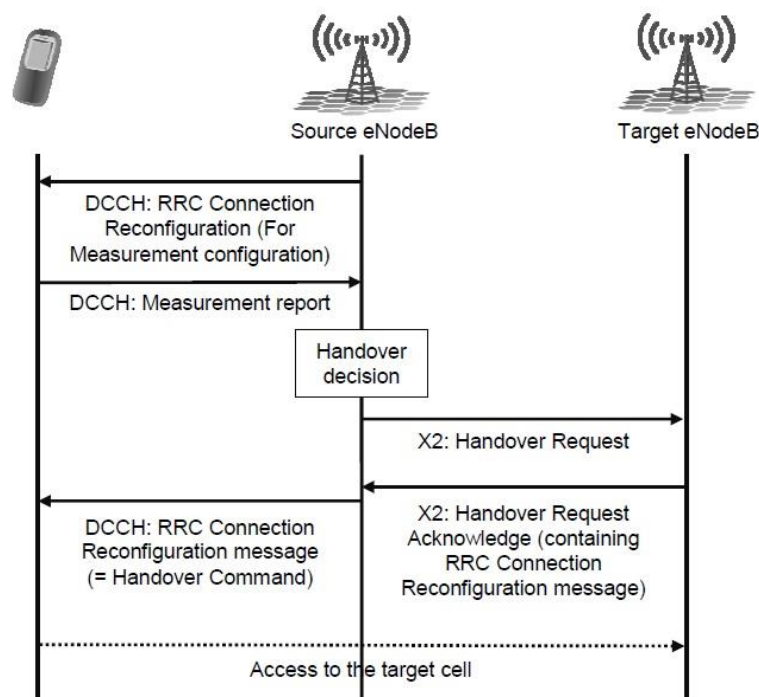


Figure 2.6. Inter-eNB HO procedure (extracted from [HoTo11]).

This interface normally transmits only Control Plane information but in connection with the HO, as it is temporary, used for user data forwarding. The main difference between the X2 Control Plane and UP protocol stacks is the use of Stream Control Transmission Protocol (SCTP) for the Control Plane, allowing reliable delivery of control information between eNBs, and the use of User Datagram Protocol (UDP) for data forwarding.

The Handover Request message contains different information elements, such as requested SAE bearers to be handed over, HO restrictions list (which may restrict a given HO for the UE) and last visited cells the UE has been connected to (considered to be beneficial in avoiding back and forth HOs between two cells, although this capability is only available if the UE historical information collection functionality is enabled). When this message is sent, the eNB starts a timer that, in case of no feedback, cancels the HO preparation and informs the target eNB that the timer expired. It is also possible to cancel an ongoing HO with the use of the Handover Cancel message.

The Handover Request Acknowledge message contains not only the information that the target eNB can accommodate all (or at least part) of the SAE bearers to be handed over, but also carries information on the GPRS Tunnelling Protocol (GTP) tunnel for each SAE bearer to allow the delivery of UL and DL Protocol Data Units (PDUs). Information about not admitted SAE bearers and the actual RRC Connection Reconfiguration message that the source eNB sends to the UE is also included in this message.

HO performance is mainly characterised by two delays, as shown in Figure 2.7. $D_{handover}$ is the total time since the end of transmission of the HO command on the source cell to the beginning of the UE transmissions towards the target cell. It includes RRC procedure delay or activation time, depending on the RRC connection state, and $T_{interrupt}$, which considers the maximum time that the UE uses to stop communicating with the source cell and start transmitting to the new cell, the target cell search time and interruption uncertainty for random access.

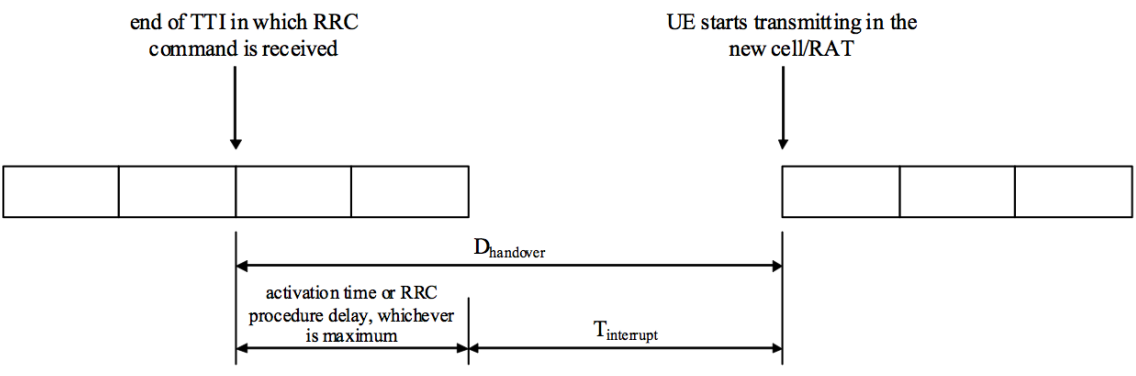


Figure 2.7. Handover delay and interruption time (extracted from [HoTo11]).

2.5 State of the Art

This section presents previous work developed by a variety of authors on LB via inter-frequency HOs, by briefly examining LTE network performance, and showing the main conclusions and results obtained through simulations and algorithm analysis.

Regarding performance assessment, one should mainly address capacity, QoS and interference aspects of LTE. 3GPP makes use of these and other performance-related concepts, such as spectrum efficiency, data rates and coverage, for the specification of E-UTRAN requirements and

enhancements, highlighting their relevance in the performance evaluation and deployment of LTE networks. This information and other useful data is available in [3GPP12a] while the remaining contents on LTE performance in this section are based on [HoTo11], [CCox12], [Mart13] and [Falc13].

In LTE, as well as in other cellular networks, capacity can be seen as the maximum aggregated data rate that one cell can handle at a given time. The aggregated data rate in this case corresponds to the sum of the data rates from all active users served by the cell, which in turn, are directly related to the number of allocated RBs per user proving a correlation between the number of available RBs and the number of users that can be assigned to them. Another possible approach for capacity evaluation is in terms of a specific service or QoS requirements for determining the number of users served in equal conditions, simultaneously. Available bandwidth and its efficient use would be the main limitation but, due to the variety of service requirements, other system performance parameters prove to be more limiting, such as throughput, latency and SINR.

Throughput is also limited by the available bandwidth and the number of allocated RBs, nevertheless, other factors are of relevance, such as subcarrier spacing, modulation scheme, number of symbols in each subframe, CP size, channel encoding rate, antenna configuration and control/signalling overhead. According to [3GPP12a] the targeted maximum data rate to be supported from a system requirement viewpoint, i.e. the peak data rate regardless of some of the parameters described above should be 1 Gpbs for DL and 500 Mbps for UL. 3GPP also defined that the target peak spectrum efficiency (highest data rate normalised by overall cell bandwidth, assuming error free conditions, when all available radio resources for the corresponding link direction are assigned to only one single UE) of the system should be of 30 bps/Hz for DL with an 8×8 antenna configuration and of 15 bps/Hz for UL with a 4×4 one. The average spectrum efficiency is defined as the number of bits correctly received over a certain time interval normalised by the overall cell bandwidth and divided by the number of cells. The system should target a total of 3.7 bps/Hz/cell for DL with a 4×4 antenna configuration and 2 bps/Hz/cell for UL with a 2×4 one. The target throughput for users at cell edges is also stated in [3GPP12a] and should be, at most, 0.12 bps/Hz/cell/user for DL and 0.07 bps/Hz/cell/user for UL (using the same antenna configurations as in the average spectrum efficiency).

Regarding mobility performance, the system should be able to support a UE moving up to 350 km/h (or up to 500 km/h, depending on the frequency band). 3GPP states that system performance should be enhanced when the mobile moving between 0 km/h and 10 km/h, and it should never be worse than its performance when dealing with higher movement speed of the UE.

Regarding Component Carrier (CC) management, [YNII11] introduces three management policies that offer various RRC signalling overheads and different SINR curves for CA scenarios where the cells have different coverage areas. The loose management policy aims at minimising the number of RRC reconfigurations by fixing the Primary CC (PCC) while configuring a UE with a Secondary Cell (SCell) whenever possible, regardless of any existing differences in the radio conditions between the Primary Cell (PCell) and the SCell. On the other hand, a tight management policy is also presented in the paper, where the goal is to improve dynamically and persistently the CCs used by the UE by

consistently changing the PCC and adding or removing Secondary CCs (SCCs) according to the experienced radio conditions. The third management policy is a compromise between the former two, i.e. the PCC is changed dynamically according to the radio conditions but an SCell is always assigned to the UE as long as it is possible. Figure 2.8 sums the three proposed management policies.

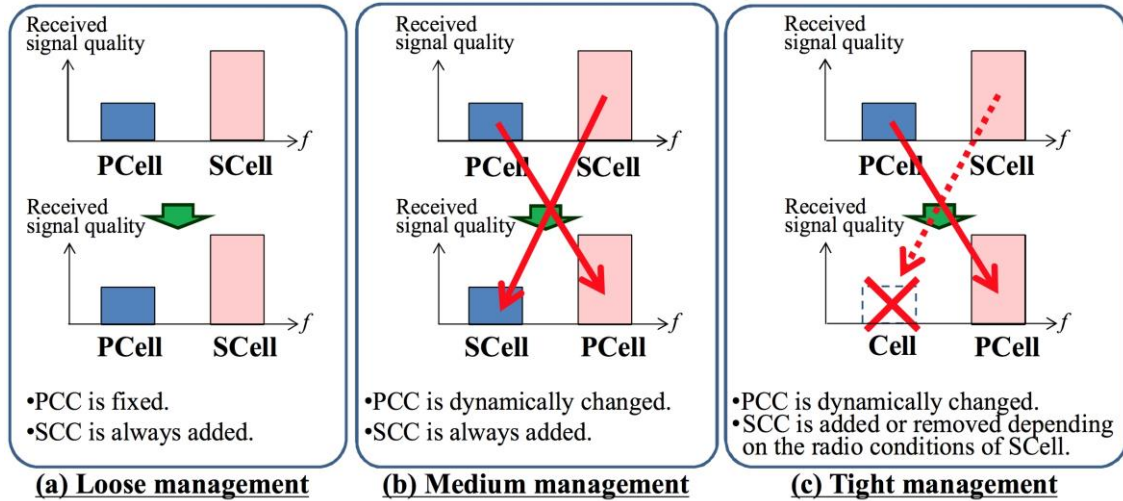


Figure 2.8. Assumed CC management policies (extracted from [YNI11]).

Simulation results show that the SINR curves of the PCell in the medium and tight management policies are enhanced compared to the curves obtained in the loose one, at the sacrifice of having a larger RRC signalling overhead.

[WPSM10] addresses CC management and packet scheduling methods, by evaluating two load balancing (LB) techniques and by comparing a suggested cross-CC Packet Scheduling (PS) algorithm with the one used in LTE systems. The Round Robin (RR) algorithm assigns a newly arrived user to the carrier with less active users while the Mobile Hashing (MH) algorithm makes use of the output of the UE's hashing algorithm, being mapped afterwards directly onto the CC indexes and providing balanced load conditions across CCs in the long term. This paper concludes that the former algorithm achieves better performance with low number of users and low percentage of LTE-A users. For PS, this study selects the existing Proportionally Fair (PF) scheduler and suggests a simple extension to it, where scheduling metric on each CC takes into account the past user throughput over all aggregated CCs instead of considering each CC independently in terms of throughput. Simulation results show that coverage gains can go up to 90%, or up to 40% depending on the user arrival rate, when comparing both algorithms.

The authors of [LHPL11] use a different approach by considering LB and network load minimisation simultaneously as a multi-objective optimisation problem and converting it later into a single aggregated objective function optimisation problem. The proposed algorithm consists of a HO decision and Call Admission Control (CAC), both constrained by resource availability in target cell, user's SINR and by a defined LB gain, expressed in terms of the objective function previously mentioned. The first two simulation results evaluate the efficiency of the algorithm, in terms of LB and new call blocking rates, when the optimisation problem focuses only on LB, only on network load minimisation or in other eight configurations where the influence of both these parameters is weighted using the single

aggregated objective function, in search of an optimal value regarding this trade-off. The remaining simulations assess the variation of user arrival rates on LB, new call blocking rates, network average load and network bandwidth efficiency, comparing the LB optimised algorithm with the network average load optimised algorithm and with the weighted algorithm, using the optimal value chosen on the first simulations. The presented conclusions show that the weighted algorithm can decrease the new call blocking rate while reducing network resource occupation and increasing the network bandwidth efficiency.

Another approach that allows improvements on the overall performance of the network is through load estimation, as suggested by the authors of [LSJB10]. The proposed algorithm relies on UE measurements and eNB data to estimate load on the target cell before handing over a user due to LB HO. This method aims at finding the optimum HO offset value, between the overloaded cell and a potential target cell, which assures that users being handed over do not return to the source cell, therefore reducing its load. Simulation results compare the virtual load existent on the cells through time and the number of unsatisfied users (i.e., the part of the users that cannot be served with the required service quality) when using the 3GPP LTE reference system or the proposed algorithm. The final remarks show that this solution may improve load distribution among network cells, therefore enhancing network performance. However, no considerations are made on the complexity of this algorithm and its effects on the network, by increasing the signalling overhead and the eNB processing time.

As expected, the analysis of RSRP and RSRQ measurements is quite relevant when studying HOs. [KuHK08] contains simulation results on number of accomplished, unnecessary and missed HOs in different network load situations and considering different levels of interference, when using only the RSRQ measurement value. This method proved to be of little or no benefit comparing with the use of only RSRP measurements. The final remarks on the paper suggest that the use of both measurement values for HO should be studied. This work was developed in [KSMW09], where the authors evaluate inter-frequency HO criteria when RSRP, RSRQ or a combination of these two values is used. Furthermore, five criteria are defined, according to inter-frequency measurement gap triggering and HO decision criteria, and assessed through packet loss rate and number of HOs observed in the simulations. The network is simulated in both high and low system load scenarios and the frame timing of the simulated cells may be synchronous or set independently. First results show that the RSRQ variation is very sensitive to the system load whereas the RSRP reveals high stability, in both synchronous and asynchronous deployments. Afterwards, the authors emphasise on the criterion that considers either RSRP or RSRQ thresholds for inter-frequency measurement gap triggering, and makes use of both measurement values for inter-frequency HO decision, since this criterion leads to a mean packet loss rate lower than 1%, while achieving a mean number of handovers close to 50% of the reference case, which only considers RSRP measurement for inter-frequency HOs. The other criteria may achieve better results in one of the parameters, but the overall performance of the mentioned criterion is better, regarding the trade-off between packet loss rate and number of HOs.

Chapter 3

Algorithms and Simulator Description

This chapter contains an explanation on the models and considerations taken into account and used in the simulator. Section 3.1 describes the main considerations used for the development of the implemented algorithm, which, in its turn, is presented in detail in Section 3.2. In Section 3.3 is the description of the simulator and, finally, Section 3.4 provides a brief assessment of the models used, in order to verify that the results obtained are within expected realistic values.

3.1 Initial Considerations

When considering various BSs that use multiple carriers, an ideal scenario was chosen in order to assess the different parameters that are of interest for the scope of the thesis. A hierarchical coverage scenario is implemented, consisting of three carriers, operating in the 2600 MHz, 1800 MHz and 800 MHz bands, each one with a designated maximum number of RBs, according to the system bandwidth. The 2600 MHz carrier has a maximum number of 100 RBs, while the 1800 MHz one has 75 RBs and the 800 MHz has 50 RBs, meaning that each carrier has a bandwidth of 20 MHz, 15 MHz and 10 MHz respectively. The hierarchical coverage concept refers to the fact that the most centred carrier is able to offer higher throughputs and, therefore, is considered to be a better solution for a given UE. The BSs are considered to be close enough in order to allow continuous coverage by overlapping part of the 1800 MHz and the 800 MHz coverage areas, as depicted in Figure 3.1.

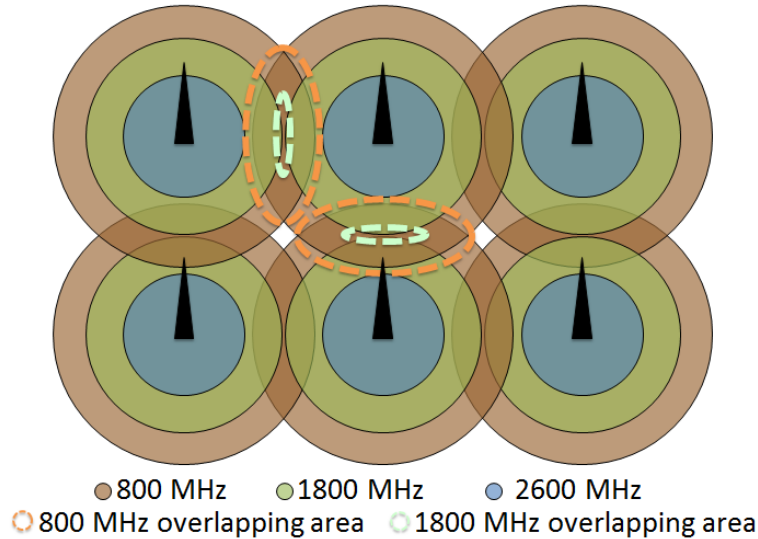


Figure 3.1. Ideal scenario for multiple carrier deployment and respective overlapping areas.

For the initial steps of the simulation no interference power is considered, therefore, the SNR can be used to determine the radio channel conditions for a given UE:

$$\rho_{N[\text{dB}]} = P_{Rx[\text{dBm}]} - N_{[\text{dBm}]} \quad (3.1)$$

where:

- P_{Rx} : Power at the input of the receiver;
- N : Noise power at the receiver.

The power at the input of the receiver is given by (A.4), making use of the link budget presented in Annex A and considering the COST 231 Walfisch-Ikegami propagation model presented in Annex B for path loss. The noise power is obtained using (A.6).

Afterwards, when the information on RB distribution among users and their respective SNRs is

accessible, the available SINR can be calculated so that interference is considered on system performance using:

$$\rho_{IN[\text{dB}]} = 10 \times \log\left(\frac{P_{Rx[\text{mW}]}}{N_{[\text{mW}]} + I_{[\text{mW}]}}\right) \quad (3.2)$$

where:

- I : Interference power at the receiver, given by

$$I_{[\text{mW}]} = \sum_{i=1}^{N_I} I_{i[\text{mW}]} \quad (3.3)$$

where:

- I_i : Interference power coming from transmitter i ;
- N_i : Number of interfering signals reaching the receiver.

The power of each interfering signal is also given by (A.4), considering the same propagation model and path loss expressions. Only the signals that have a power equal or greater than the noise power are considered, for only these may have a negative impact on system performance.

The SINR disparity between cell-centre and cell-edge users is usually very high in cellular systems, as aforementioned, especially if they suffer from coverage limitations. This leads to lower throughput values for cell-edge users relative to cell-centre ones, originating a large QoS inconsistency in terms of geographical coverage, as well as in terms of available data throughput within the coverage area.

As for throughput calculation, one can obtain theoretical bit rates in DL using, [Alme13]:

$$R_{b[\text{Mbit/s}]} = \frac{N_{sub/RB[\text{sub-carrier/RB}]} \times N_{sym/sub[\text{symbol/sub-carrier}]} \times N_{b/sym[\text{bit/symbol}]} \times N_{RB} \times N_{MIMO}}{T_{RB[\mu\text{s}]}} \quad (3.4)$$

where:

- $N_{sub/RB}$: Number of sub-carriers per RB (12 when considering a 15 kHz sub-carrier spacing, which fulfil the 180 kHz bandwidth of an RB);
- $N_{sym/sub}$: Number of symbols per sub-carrier (7 when the normal CP is used);
- $N_{b/sym}$: Number of bits per symbol, which depends on the modulation scheme and coding rate used;
- N_{RB} : Number of RBs;
- N_{MIMO} : MIMO order (2, for 2x2);
- T_{RB} : Time duration of an RB, which is 500 μs .

According to [SeTB11] and using (3.2), the achievable throughput when considering interference is given by:

$$R_{b[\text{Mbit/s}]} = N_{RB} \times B_{RB[\text{MHz}]} \times \log_2(1 + \rho_{IN}) \quad (3.5)$$

where:

- B_{RB} : Bandwidth of an RB.

For an initial approach, the sector antenna's range is calculated by considering an NLoS scenario, since that as the distance to the BS increases, the probability of LoS decreases. Therefore, it is more probable that UEs farther from their serving sector are in NLoS conditions. A UE is considered to be served if it reaches a defined minimum throughput for their service demands. Afterwards, the sector antenna's range is calculated as the distance of the UE that is farther away from its serving sector:

$$R_{sector [m]} = d_{max [m]} \quad (3.6)$$

where:

- d_{max} : Distance of the UE farther away from its serving sector antenna.

In order to achieve a more accurate evaluation of both system and link performances, a realistic modelling of propagation conditions is done by using the channel models presented in [SeTB11]. LTE channel models follow the ones previously defined by the International Telecommunication Union (ITU) and 3GPP for GSM and UMTS, being associated with low, medium and large delay spreads. The Extended Pedestrian A (EPA) model provides a low delay spread (with a root mean square delay spread of 43 ns), being employed in an urban environment with fairly small cell sizes, while the Extended Vehicular A (EVA) and Extended Typical Urban (ETU) models are associated with medium (with a root mean square value of 357 ns) and large (with a root mean square value of 991 ns) delay spreads, respectively. These models take into account low (5 Hz), medium (70 Hz) and high (300 Hz) Doppler shifts, which enable the common combinations EPA 5 Hz, EVA 5 Hz, EVA 70 Hz and ETU 70 Hz.

The quality of the signal received by the UE is affected by the channel quality of the serving sector, the interference levels from other sectors and also by the experienced noise level. In order to solve this and improve capacity and coverage for a given transmission power, the transmitter tries to match the data rate for each user to the fluctuations in received signal quality, referred to as link adaptation, which is typically based on Adaptive Modulation and Coding (AMC), enabling the adaption of the modulation scheme and coding rate according to the channel conditions.

When regarding modulation schemes one takes into account that lower-order modulations are more robust and, therefore, a better choice for situations in which higher levels of interference are experienced. Nevertheless, lower transmission bit rates are achieved with these modulations schemes, such as Quadrature Phase Shift Keying (QPSK), so high-order modulations are also considered in LTE. Quadrature Amplitude Modulation (QAM) offers better bit rates, although it is more susceptible to errors due to its sensitivity to noise, interference and channel estimation errors. This means that if the SINR is sufficiently high, a high-order modulation is usually chosen. The code rate used also depends on the channel conditions. If a high SINR is detected, a high code rate can be used while lower code rates are used when experiencing poor channel conditions. Code rate adaptation is implemented by applying puncturing or repetition to the output of a mother code, to increase or reduce the code rate, respectively.

The above stated concepts are of use when applied to the modelling of system behaviour and respective simulator using the expressions provided in Annex C, which establish a good approximation for the relationship between throughput and SINR using the following general expression, where A, B and C are constants defined according to the modulation and coding scheme used:

$$R_{b[\text{Mbit/s}]} = \frac{A}{B + e^{-C \times \rho_{IN[\text{dB}]}}} \quad (3.7)$$

Regarding the definition of load, one can use a generic formulation, by dividing the quantity of required resources by the total available resources in a cell. Specifically, since LTE resources consist of OFDM symbols in the time-domain and sub-carriers in the frequency-domain, the DL data symbol rate is given by the number of DL OFDM symbols times the number of data sub-carriers over the frame duration. Moreover, the total number of RBs in an LTE cell is fixed, therefore, one can use (3.8) to determine the respective cell load:

$$C_{cell} = \frac{N_{RB,scheduled}}{N_{RB,cell}} \quad (3.8)$$

where:

- $N_{RB,scheduled}$: Total number of scheduled RBs in the respective cell;
- $N_{RB,cell}$: Total number of RBs in the respective cell.

This value ranges from 0 to 1 and, when close to 1, it indicates that a given cell is congested and therefore has a higher probability of service outage to some users, therefore, LB is to be considered when C_{cell} exceeds 90%. The same notation can be used for representing the load of a given user in a certain cell, being:

$$C_{user} = \frac{N_{RB,user}}{N_{RB,cell}} \quad (3.9)$$

where:

- $N_{RB,user}$: Total number of scheduled RBs to a certain user in the respective serving cell;

The parameters presented in this section enable the study of system performance relevant to the goal of this thesis. The load distribution is still one of the main objects of study along the considered network, while other important parameters, such as the number of RBs allocated in each carrier frequency and in each type of service, are also analysed so that it is possible to optimise the throughput and the distribution of the users along the network.

3.2 Algorithm Description

The proposed algorithm is focused on granting the best throughput possible to users by taking their position relatively to the transmitting antenna into account, as well as the priority of the services being used. As mentioned before, the load of each user in a sector and the load of each sector are other parameters that are also of great importance for the algorithm to progress, as they serve as decision-making parameters.

Whenever a user tries to connect to the network, he/she is subject to the new call admission process, in which the UE tries to connect to the first eNB that guarantees the minimum required throughput for the desired service, while constrained by its SINR and by the available resources of the sector, Figure 3.2. Users that end up not being served are stored in a delayed users list for later analysis.

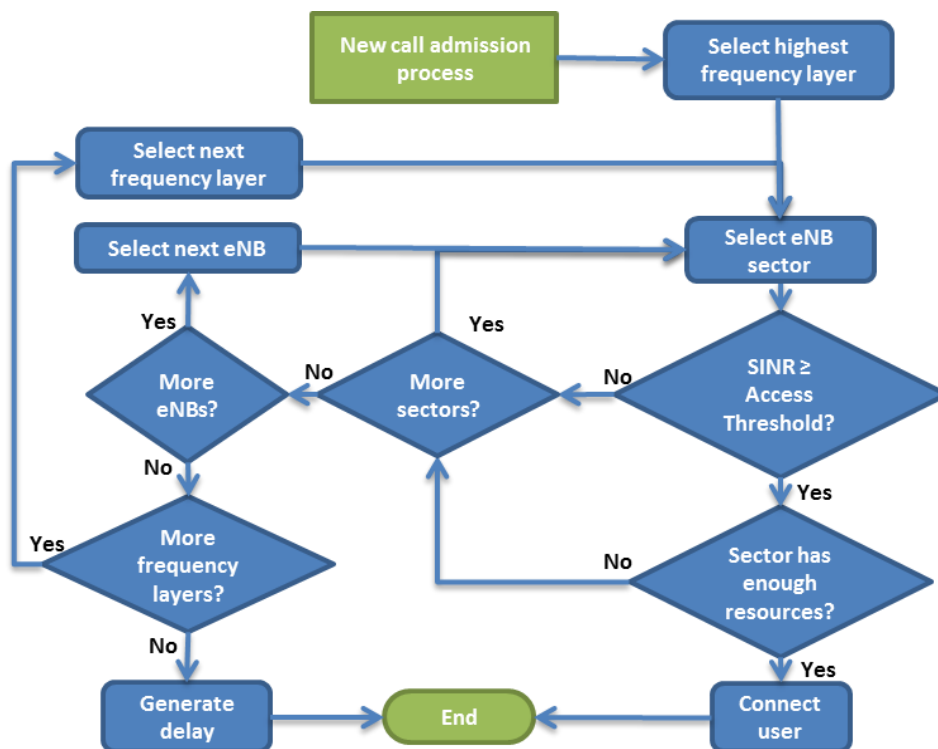


Figure 3.2. New call admission process.

In a first step, a static analysis is made to study the influence of the existence of different combinations of carrier frequencies in terms of served users, network load and user SIN throughput. Each sector capacity is evaluated and, in case the load condition of the sector is above 90%, users are selected to be added to the delayed users list also for later analysis. The algorithm searches for the user with the lowest priority service using a number of RBs enough to be able to unload the sector all by himself. Should there be two or more users in this situation, the algorithm selects the one that occupies the less resources and, afterwards, the user whose throughput is the lowest, Figure 3.3.

Afterwards, the algorithm attempts to reconnect the users in the delayed users list back in the network. The load restore process is very similar to the new call admission process, the difference being that it takes a targeted sector load of 90% into account, as shown in Figure 3.4. Users that end up not connected after this step are delayed and stored for the dynamic analysis process.

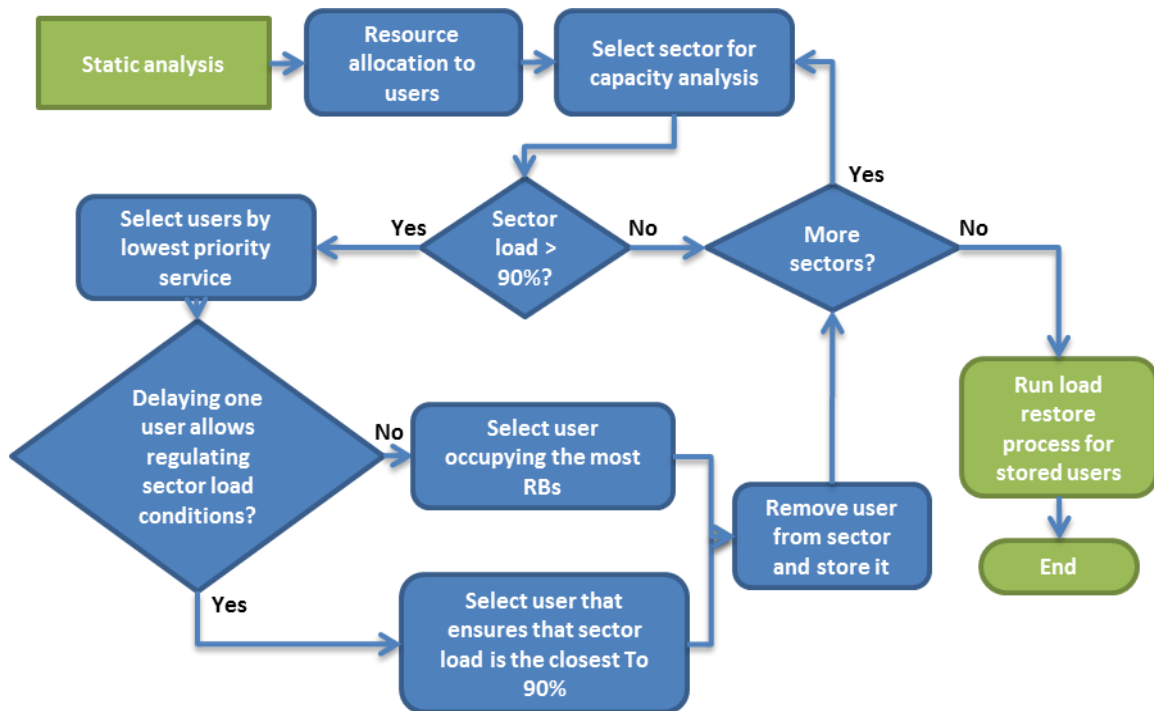


Figure 3.3. Static analysis process.

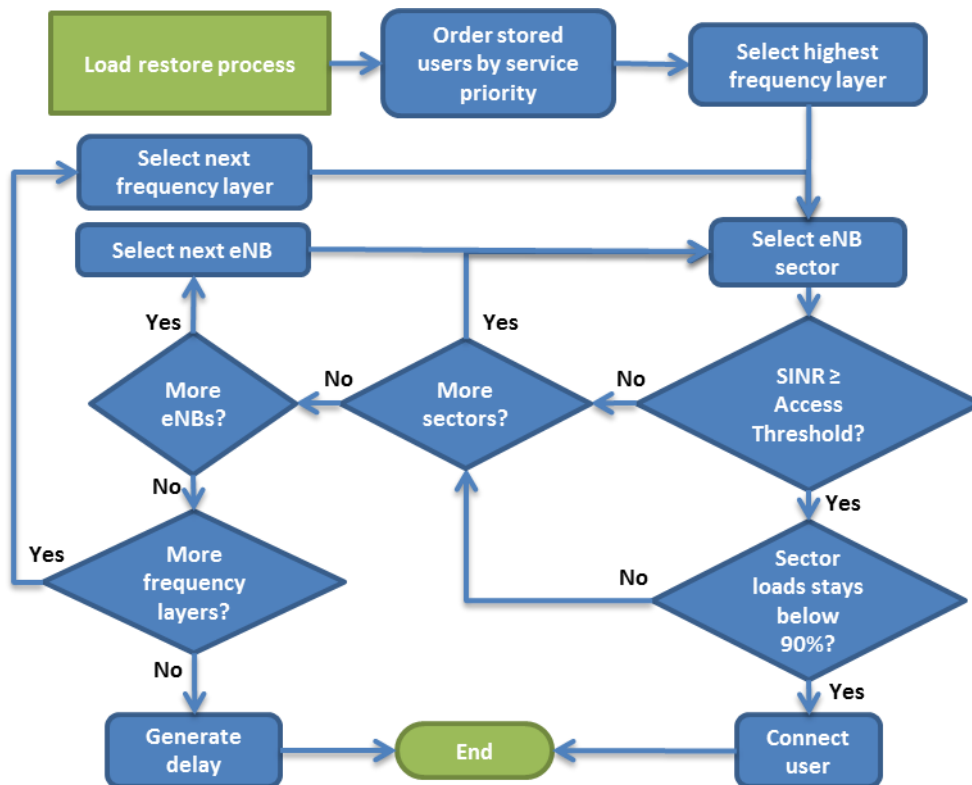


Figure 3.4. Load restore process.

When all sectors have their load under or equal to 90%, a file size or a call duration is allocated to each user according to their service, as explained in the next section, and the dynamic network analysis begins, Figure 3.5. At each time step, users have their files sizes or their call durations decreased until they finish their download or phone call. The user is then removed from the sector, the RBs allocated to him are freed, and he/she is stored in a list of users that will be attempting to connect

to the network at a later stage.

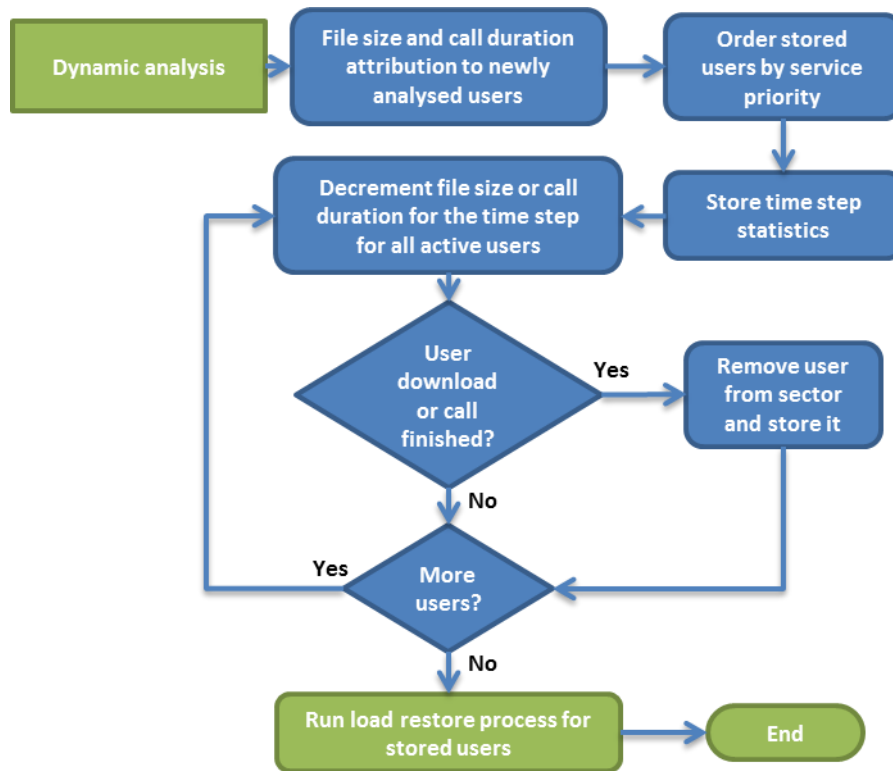


Figure 3.5. Dynamic analysis process.

3.3 Simulator Description

The developed simulator is a tool that aims at analysing the performance of LTE in DL, deployed over a dense urban UMTS cellular network. It is composed by several modules, resulting from previous studies, especially [Alme13] but also [Falc13] and [Pire12], plus the modified modules developed in this thesis. In Figure 3.6, one presents the main structure of the simulator, where the green modules correspond to the modified parts that allow the implementation of the performance models described earlier in this chapter. The work previously developed in this simulator considers only LTE, using a snapshot approach, where results refer to the behaviour of the network at a given instant. Some input data has to be directly provided to the simulator, regarding information about the environment and the BSs' location:

- DADOS_Lisboa.tab, which contains information about the city of Lisbon, namely its districts;
- ZONAS_Lisboa.tab, which characterises the areas of Lisbon;
- BS.tab, which has information on the BSs' location;
- Users.txt, which contains information on the users to be considered during the simulations.

The file names are just suggestive, as the BS.tab and the Users.txt files can have different names according to the eNB distribution along the considered area and the quantity and type of users being considered on the simulation, respectively.

There are files that work as both output and input for different modules of the simulator, such as:

- Data.dat and Data2.dat, which provide information on the location of the BSs, their respective number of sectors and also potential users being covered, including their location, requested service and distance to the eNB;
- Definitions.dat, which provides information about propagation model parameters, frequency band, bandwidth, minimum and maximum throughputs for each service, antennas' parameters, type of environment, LoS probability method and whether the allocation of resources is considered localised or distributed.

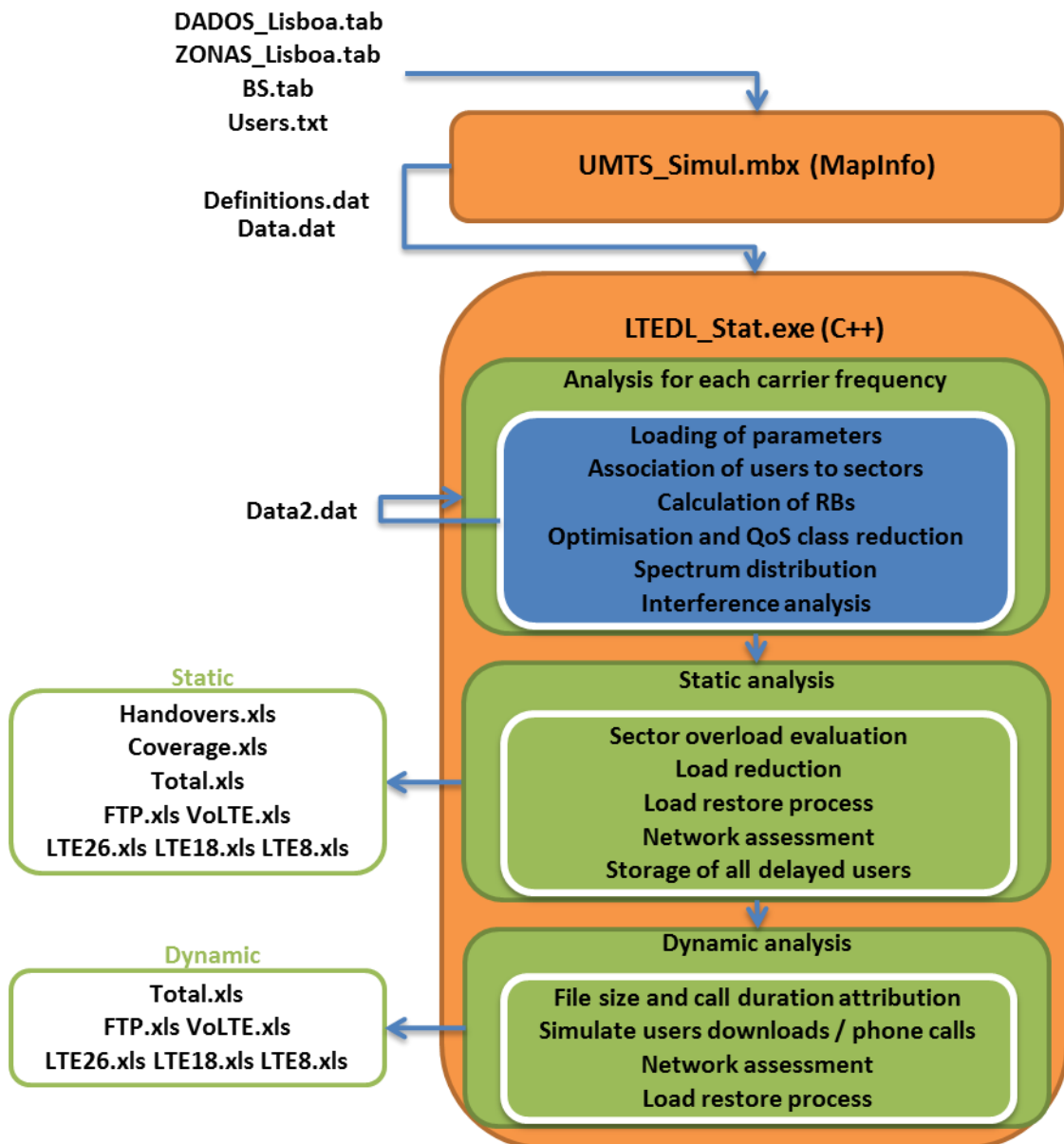


Figure 3.6 Modules that compose the simulator and respective output files (simulator workflow).

The output files provided by the simulator contain the data required to produce the network statistics. These are generated in different folders according to the type of analysis being executed, meaning that, in the static analysis the files have the exact names presented in Figure 3.6 and each row contains information regarding each simulation, while in the dynamic analysis each row has

information regarding a time instant of the simulation and each of the files mentioned before is created with an index in the end of its name indicating the respective simulation number. The created files are:

- FTP.xls, it contains, in each row, information about number of RBs in usage, average throughput, number of users, load regarding only FTP traffic in the whole network and also the same load existing in each existing carrier frequency, and average received power and average SINR for FTP traffic in the whole network and in each considered frequency band;
- VoLTE.xls, similar to FTP.xls but regarding only VoLTE users;
- LTE26.xls, LTE18.xls and LTE8.xls, which provide information about the number of RBs in usage, average throughput, number of users, total load and load of FTP and VoLTE traffic for the 2600 MHz, 1800 MHz and 800 MHz carriers respectively and average received power and average SINR also for each type of traffic, regarding the respective carrier frequency;
- Total.xls, in which each row includes information on number of RBs in usage, average throughput, number of users, average received power, average SINR, total load and load discriminated by type of traffic (FTP or VoLTE) and by carrier frequency (2600 MHz, 1800 MHz and 800 MHz);
- Coverage.xls, which contains information on the number of users covered and on the number of users that end up being served at the beginning of the simulations;
- Handovers.xls, which contains information regarding the users that are removed from a given sector when evaluating its load situation. This file is only produced to verify the correctness of the implemented algorithm.

The desired scenario is defined from a set of defined input parameters, and, to ensure that no inconsistencies occur during the simulations, some of these parameters are pre-processed automatically.

The first module that needs to be executed is UMTS_Simul.mbx. Although this program has UMTS in its name, UMTS is not considered in this thesis and the reason is that the previous works, in which this simulator is based, dealt with 3G systems. It is responsible for the creation of a file containing information about the users' positioning along the entire city of Lisbon and their requested services according to the percentage introduced as input. Real population density is taken into account along the city, but occurs in a square containing the whole city and some areas that are not a part of it, resulting in the non-consideration of about 10% of the users as the simulator only performs an analysis over the city of Lisbon. The MapBasic programming environment allows the user to manually introduce the parameters with the help of a straightforward interface, shown in Annex D. Those parameters are pre-processed by MapInfo before being written in Definitions.dat to be read by LTEDL_Stat.exe.

After that, a preliminary coverage study is done, based on a reference minimum throughput, which is translated into a minimum SNR via (C.4), considering that at the cell-edge QPSK is the modulation scheme used, as it is the most robust one, enabling realistic throughputs at a relatively low SNR. By taking noise into account, the minimum received power is obtained from the minimum SNR so that the maximum distance that ensures the aforementioned minimum received power can be calculated. The

method for computing the coverage areas is not very realistic, in the sense that it only considers the horizontal radiation pattern of the antennas, originating in areas much larger than the ones in a real network, therefore, a more detailed analysis of coverage is done afterwards in LTEDL_Stat.exe. The primary coverage analysis also processes geographical information so that the previously filtered users are associated with sectors based on whether they are located inside or outside the coverage area. Since overlapping of coverage areas happens quite often, users can be often associated with more than one sector.

After the input parameters are introduced in UMTS_Simul.mbx, they are processed by LTEDL_Stat.exe, which reads Definitions.dat and data.dat and saves this information in internal data structures. Users being covered by more than one sector are assigned to the one from which they receive the highest power, taking into account that in this stage all users are considered to be under NLoS conditions. When the received power from two or more sectors is equal (situation in which the user is covered by more than one sector and the antenna's gain is equal, which happens near the frontier between sectors) the user is associated with the one that guarantees the lowest azimuth, according to the work developed in [Alme13].

The number of RBs in each sector is determined by the considered bandwidth, according to Table 2.1. Initially, users are given all the RBs they need in order to receive the maximum throughput associated with the service they are demanding, if the radio channel conditions support it. System capacity is not taken into account at this step.

In order to be able to calculate the number of RBs that a user requires to fulfil its desired data rate, single RB throughput is calculated based on the SNR given by (3.4) and using the expressions provided in Annex C. Resource allocation is done on an RB basis instead of on a sub-frame one, since the simulator is snapshot based. All RBs are assumed to have the highest frequency in the frequency band under study at this step in order to ensure that the allocations respect the user's requirements in terms of throughput, seeing that higher frequencies induce higher path losses. More realistic SNRs and SINRs are obtained later in the simulation, after all allocations take place. By dividing the user's desired throughput by the throughput of a single RB one obtains, in a first approach, the number of RBs requested by each user.

When computing SNR, the received power is calculated using the expressions in Annex A and Annex B together with the antenna's gain in the user's direction. The latter was developed in [Alme13] and allows a more realistic assessment of the received power by taking the classification of users as either LoS or NLoS into account.

After the allocation process is finished, system capacity is taken into account and in case the users in a given sector are requesting more resources than the ones it has can allocate, reductions have to occur. Regarding the distribution of RBs, an adapted version of the Proportional Fair algorithm was implemented in previous works, such as [Pire12] and [Alme13]. The fairness concept is applied in the sense that resources are supposed to be assigned to all users. Nevertheless, this assignment takes the type of service the user is requesting and their location inside the cell into account, not considering system capacity. For the same service, cell-centre users usually request fewer resources than cell-

edge ones due to channel conditions. Then, system capacity is taken into account by decreasing the requested throughput of the users until a minimum throughput is reached or system capacity is not exceeded. This reduction takes place in case system capacity is not respected and it takes into consideration the priority of the service being requested by reducing in first place the lowest priority services. Reductions can be considered fair, since lowest priority service users are assigned a half of the RBs they previously had, then the second lowest priority service users are assigned a half of the RBs they previously had, and so on and so forth, until system capacity is not exceeded. In the first round of reductions, if after each resource reduction users still have RBs assigned, but are not able to reach a minimum throughput, they are guaranteed minimum throughput. From the second round onwards, if that continues to happen, they are delayed (i.e., they are not served at the instant of the simulation). In case these reductions are necessary, optimisation occurs: users that end up being served with a throughput slightly higher than the one they wanted are reduced one RB.

When system capacity is coherent after the RB distribution, all RBs are assigned a position in the available spectrum using localised Resource Allocation Type 2 (explained in detail in [Alme13]), which allows the possibility to allocate one or the maximum available RBs to a single UE.

Each RB has an associated frequency, taken as the frequency of the RB's sub-carrier, which is centred in the highest frequency. Since a uniform distribution of RBs along the available bandwidth and the consideration of only 10, 15 and 20 MHz bandwidths in this thesis is considered, one can take a uniform 200 kHz spacing to fulfil the entire spectrum, respecting the number of RBs corresponding to each bandwidth presented in Table 2.1.

Afterwards, the inter-cell interference analysis is done by verifying, for each user, if there are other sector antennas sending RBs that use the same sub-carriers as the ones used to serve the UE in its sector but are used to serve other users. An RB is considered to be an interfering RB if it represents a received power higher than noise. Then, SINR is computed so that interference is considered, and a new throughput is calculated for each RB using the expressions in Annex C (modulation is determined per RB and not per user, as in a real network). In case the new throughput is below the minimum throughput for the service, the UE is delayed, meaning it will not be served at the instant of simulation.

At this point, the users that ended up not being served are stored in Data2.dat, which will now serve as input for re-processing these users on the second and third considered carrier frequencies, meaning that the allocation of RBs to each user is made firstly for the 2600 MHz carrier, then for the 1800 MHz one and finally for the 800 MHz carrier.

Then, a final load analysis takes place, by setting a threshold of 90% for the maximum number of RBs that can be allocated in each sector. In this process, if a given sector does not respect this limit, lower priority service users are removed from it and stored temporarily in internal data structures. If one single user has allocated to him a number of resources enough to lower the load under the threshold, it is removed and the next sector (or eNB, or carrier frequency) is analysed. Also, if two or more users respect this condition, the one with lowest number of RBs and then with the lowest throughput is removed. Otherwise, in case no single user is enough to lower the load enough, the one with the highest number of RBs is removed and the sector is re-analysed. Should there be two or more users

in this situation with the same number of RBs, the one with the lowest throughput is the one being removed in this step. The information of these users is then written in the Handovers.xls file so that an appropriate assessment can be made towards the number of active users on the network.

Afterwards, an attempt to reconnect back the users that were removed is made, by making use of the remaining resources existing all along the network, but now taking into account the same previously mentioned 90% load threshold. The static analysis module then generates the remaining output files so that one can assess the initial stage of the network.

Next, a file is assigned to each active FTP user (with sizes randomly distributed between 1 byte and 50000 bytes) and a call duration is attributed to each active VoLTE user (with an exponential distribution between 60 and 1800 seconds), and the simulator is ready to start executing the dynamic analysis. In every time step, each active user decrements its file size by its throughput or its call duration by a second, and the dynamic output files are updated, allowing the assessment of the network during each simulation. In case a user wishes to terminate its connection (meaning that it is no longer requesting RBs to the network since it has finished using its requested service), he/she is removed from its serving sector and a new user is stored in the queue of future users trying to connect to the network. This queue is then analysed so that new users may be added to the network in case they are requesting a connection, although only some of these users may be able to do it due to their location, service priority and also depending on the network load conditions.

Finally, the output files are analysed with the use of Microsoft Excel. As explained before, the Excel files contain the required information for results analysis, each one regarding a given carrier frequency or the service type mentioned in the file name. The file Total.xls allows the analysis to be made at a network level, since it contains data concerning the load distribution between different carriers and between different services, as well as the number of users being served and the number of RBs allocated all over the network.

3.4 Model Assessment

The results provided by the simulator are later computed using average and standard deviation metrics. These are essential elements that are of great importance, as they support subsequent analyses. Up to 30 simulations are considered for each analysis, thus ensuring statistical relevance. All of the three carrier frequencies are considered both simultaneously and separately, allowing one to assess the whole network or just a given carrier or pair of carriers as explained later in this work. The total average and standard deviation are computed in each scenario by taking into account the values obtained in each of the simulations, using (3.10) and (3.11) respectively.

$$\mu = \frac{1}{N} \times \sum_{n=1}^N \mu_n \tag{3.10}$$

where:

- N : Number of simulations;
- μ_n : Average obtained in simulation n .

$$\sigma = \sqrt{\frac{1}{N} \times \sum_{n=1}^N \sigma_n^2} \quad (3.11)$$

where:

- σ_n : Standard deviation obtained in simulation n .

In order to evaluate the results in terms of number of active users for each of the carriers, its value was obtained and analysed as aforementioned, so that one is able to produce Figure 3.7, Figure 3.8 and Figure 3.9. Each of the figures corresponds to information on a given pair of carrier frequencies and takes the different number of covered users into account. The considered pairs of carriers are combinations of two from the three available frequency bands for LTE, each combination being a defined scenario for study, as explained in further detail on Chapter 4. For each scenario, it is possible to see that the standard deviation over the average of the number of active users tends always to stabilise to a given value.

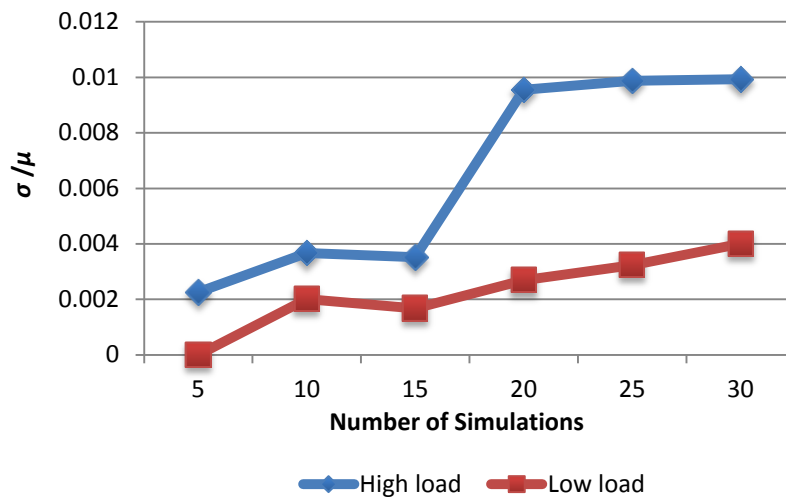


Figure 3.7. Standard deviation over the average of the number of active users, for high and low load, for the 2600 MHz and 1800 MHz carriers combination.

Since the simulation considers a set of six eNBs, users were generated from 100 to 1000 in steps of 100 and the number of served users grows until the network reaches its maximum capacity and, consequently, saturates. Afterwards, a larger number of users was generated in order to ensure that the load analysis is in its limit. The obtained values variation in consecutive simulations over the same scenario occur due to the fact that some analysis performed by the simulator are stochastic, such as the probability of LoS occurrence for a certain user, the spectrum distribution and the distribution of users along the different areas of Lisbon, i.e. centre or off-centre. In Figure 3.10, one presents the previously described behaviour in terms of active users towards covered users.

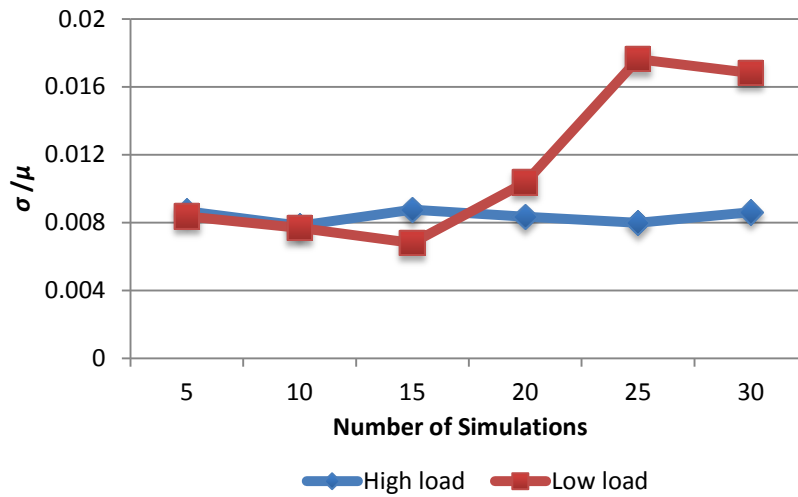


Figure 3.8. Standard deviation over the average of the number of active users, for high and low load, for the 2600 MHz and 800 MHz carriers combination.

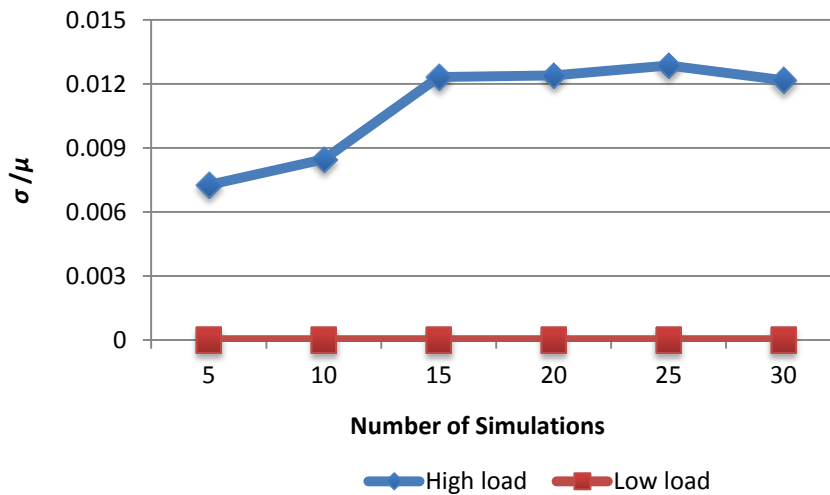


Figure 3.9. Standard deviation over the average of the number of active users, for high and low load, for the 1800 MHz and 800 MHz carriers combination.

In order to confirm that the network is able to provide maximum throughput some simulations, considering only a single UE in the network, were done. The user was very close to the eNB serving it, and was able to reach 99.44 Mbps and 101.11 Mbps using 84 RBs, which are very close to the theoretical throughput values for a Category 3 terminal (which has a maximum theoretical throughput of 100 Mbps). If one considered a Category 4 terminal, the maximum theoretical throughput would be 150 Mbps, but it is not reached since the simulator does not consider the maximum coding rate for the 64QAM modulation scheme (check Annex C), in order to have a good approximation of the behaviour of a real network. Therefore, the maximum throughput achieved by the simulator corresponds to about 120 Mbps.

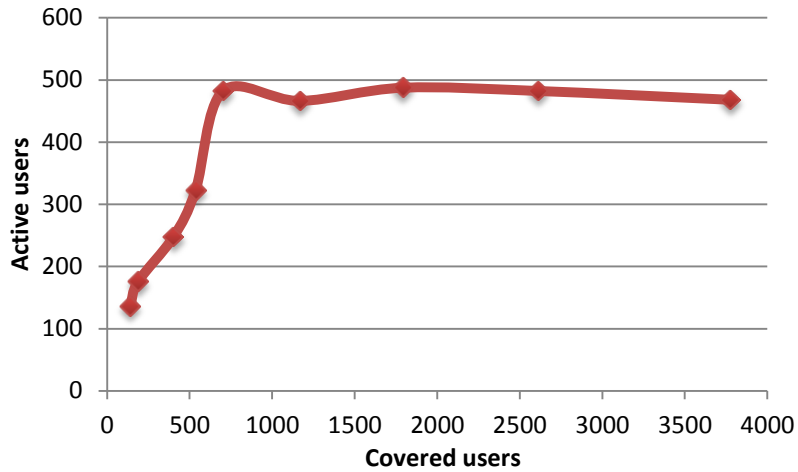


Figure 3.10. Number of served users along the covered users in the network.

Regarding the dynamic behaviour of the network, Figure 3.11 shows the analysis of the total load for one hour of simulation time after a period of another hour has passed, so that the presented results show the network load stability over time. Since in all scenarios the observed behaviour was very similar, Figure 3.11 presents this assessment only for one scenario, in which the existent carriers are the 2600 MHz and the 1800 MHz ones. The points represented in Figure 3.11 do not correspond to one second because otherwise the information would not be decipherable due to the overlap of the standard deviation bars, therefore one took 25 seconds as a time step between samples.

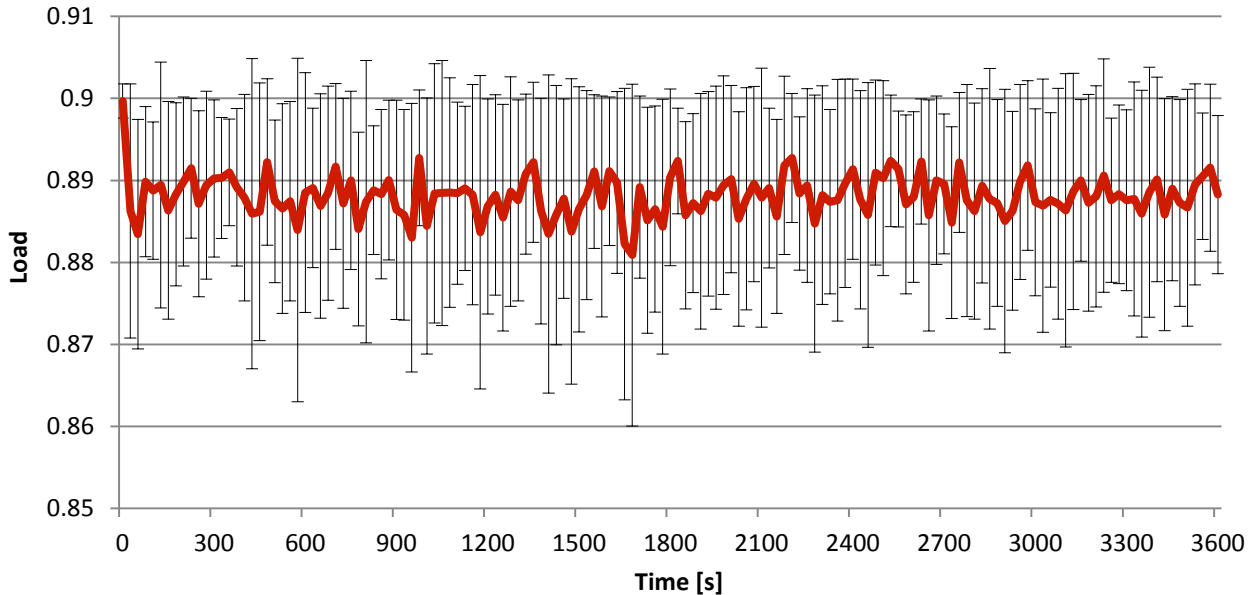


Figure 3.11. Network load behaviour during one hour, considering only the 2600 MHz and the 1800 MHz carriers (scenario 1).

The assessment of the model is also made with the help of comparisons between the results obtained in the simulations and the collected measurements during the walk-tests. In order to do this, one defines the following relative error, taking the measurement results as the reference:

$$\varepsilon_r = \frac{V_{simulation} - V_{measurement}}{V_{measurement}} \times 100\% \quad (3.12)$$

where:

- $V_{simulation}$: Value obtained from the simulator;
- $V_{measurement}$: Value obtained from the measurements.

Chapter 4

Results Analysis

This chapter contains information on the results obtained from the simulations and from the walk-tests performed over the city of Lisbon. The first section describes the scenarios that are considered throughout this work. Section 4.2 contains an analysis of a low load scenario, followed by the study of the network under a high load situation, presented in Section 4.3. The final section of this chapter addresses the results obtained from the measurements made in the areas of Baixa and Moscavide.

4.1 Scenarios Description

The city of Lisbon is defined as the default scenario, since it represents an urban environment with a vast variety of distribution of users and services and where LTE is implemented in an area with a high density of users and eNBs, some with two operating carrier frequencies.

Path loss is calculated using the COST 231 Walfisch-Ikegami propagation model presented in Annex C and the parameters shown in Table 4.1. The values of the parameters are presented for dense urban scenarios, being based on the work developed in [Alme13] and observations of the city of Lisbon. The UE height is the one verified during the measurements performed in the city of Lisbon as it matches the average UE height among different people holding their equipment in a typical data usage position.

Table 4.1. Configuration of parameters for the COST 231 Walfisch-Ikegami model.

Parameter	Dense Urban
Transmitter antenna height [m]	25
Height of the buildings [m]	21
Street width [m]	30
Distance between buildings' centres [m]	50
Incidence angle [°]	90
UE height [m]	1.2

Three frequency bands are considered, each one associated with their maximum available bandwidth:

- 800 MHz band (with an associated bandwidth of 10 MHz), providing high coverage and, therefore, may suffer from high inter-cell interference;
- 1800 MHz band (with an associated bandwidth of 15 MHz), which provides high capacity in urban areas and compatibility with a wide range of devices;
- 2600 MHz band (with an associated bandwidth of 20 MHz), providing high capacity.

By combining two of these three frequency bands, three different scenarios are defined as deployments of co-located bands, these combinations being denominated as:

- Scenario 1, to refer to the combination of the 2600 MHz with the 1800 MHz frequency bands;
- Scenario 2, that considers the co-location of the 2600 MHz with the 800 MHz frequency bands;
- Scenario 3, which defines the deployment of the 1800 MHz and the 800 MHz frequency bands in a co-located site.

Other simulation parameters are shown in Table 4.2. Concerning the propagation characteristics, a fast fading margin is not taken into account and, although UMTS uses it due to fast power control, LTE does not. The considered slow fading margin is based on [HoTo11].

The considered traffic consists of VoLTE and common data users (referred to as FTP users), prioritising the first type, since these have more strict demands in terms of latency. The minimum and desired throughputs taken into account are of 12.2 kbps and 12.65 kbps respectively for VoLTE users whereas for FTP users the minimum throughput is set to 1.024 Mbps and the desired throughput to 100 Mbps. The chosen values are defined according to the information provided in [3GPP12c], [Alme13] and [PHHK12], considering the use of the Adaptive Multi-Rate (AMR) speech codec typical bitrate values that ensure voice quality over a call, for VoLTE users, and also achieve an approach similar to the one obtained in the walk-test measurements, for FTP users.

Table 4.2. Simulation parameters.

Parameter	DL		
Frequency Bands [MHz]	800	1800	2600
Maximum Bandwidth [MHz]	10	15	20
Transmitter output power [dBm]	44.7		
UE antenna gain [dBi]	1		
Modulations	QPSK, 16QAM, 64QAM		
Antenna configuration	2x2		
Electrical downtilt [°]	5		
Mechanical downtilt [°]	0		
User losses [dB]	1		
Cable losses [dB]	2		
Noise figure [dB]	7		
Slow fading margin [dB]	8.8		
Frequency reuse scheme	Universal Frequency Reuse		
Type of users	EPA5		

In order to study and estimate the relationship between achieved user throughput and received power, one must assess these values on different sets of implementations. Figure 4.1 illustrates an example of a good theoretical approximation of the expected curves for the three proposed carrier frequencies and three modulation and coding schemes, taking [Alme13] as suggested in Annex C. These curves were obtained considering a single user with all RBs scheduled to him/her.

Regarding cell coverage areas, as stated in Section 3.1, the ideal scenario consists of multiple BSs with three carrier frequencies in which the 1800 MHz and the 800 MHz carriers have overlapping areas between eNBs.

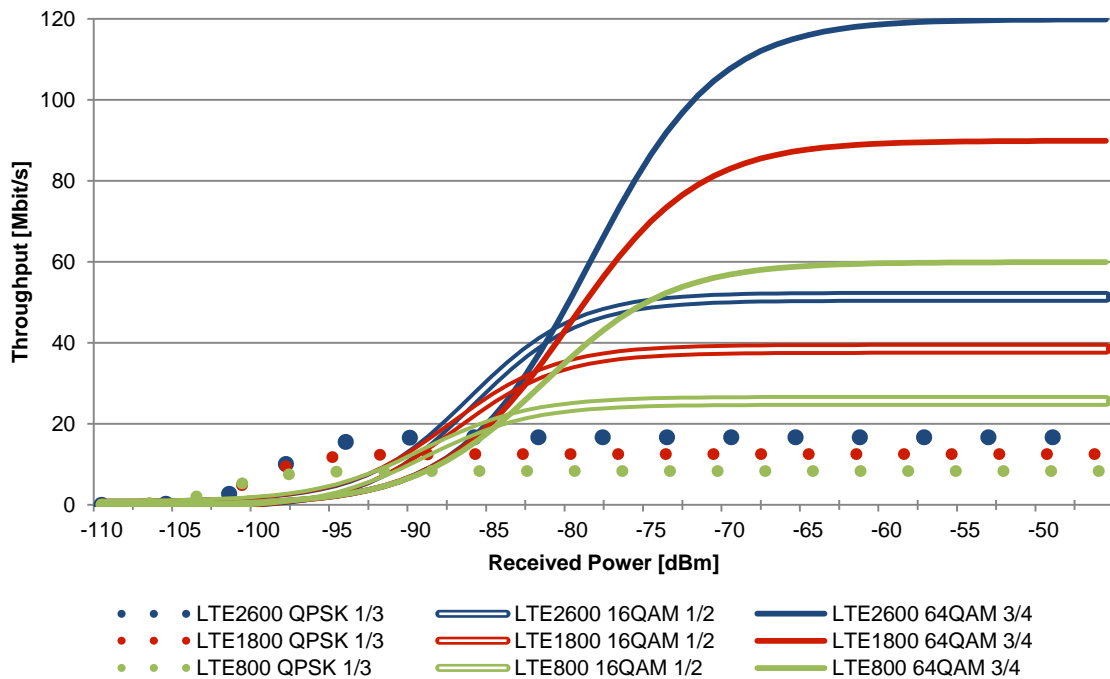


Figure 4.1. Throughput versus received power according to different modulation and coding schemes.

The measurements obtained from the walk-tests performed in two different areas of the city of Lisbon are intended to provide updated information on the existing network and thus allow one to compare the collected values with the results from the simulations. The areas where the tests are performed, together with the various parameters under study, are presented in Section 4.4. In both these regions there is a higher density of eNBs providing coverage with the use of two frequency bands than in other areas, justifying the selected routes for the walk-tests. Using a laptop connected to a Universal Serial Bus (USB) dongle (Vodafone Connect Pen K5150, manufactured by Huawei [Huaw15]) and with an incorporated GPS receiver, one was able to register the information on latitude and longitude, for each of the measured parameters. The UE used for the tests works with a 2×2 MIMO configuration and is theoretically capable of reaching a coding ratio of 0.95 when using the 64-QAM modulation scheme and when it is located very close to the eNB. Nevertheless, although the equipment is (theoretically) able to achieve a throughput of 150 Mbps, this value ended up never being registered, meaning that either the received signal quality was rather low or other UEs were already requesting resources from the network. The UE was performing an FTP file download from Vodafone's servers and the measured values were registered in a logfile, generated by the measurement software running in the laptop, the TEMS Investigation 13.1.33 [Asco15a]. Afterwards, the logfiles were processed with the use of TEMS Discovery 3.0.2 [Asco15b].

The average UE height during the walk-tests was approximately 1.20 m above ground, corresponding to a typical smartphone usage when a user requests a usual data connection.

Regarding the speed of the UE, one aimed at maintaining a regular speed between 3 and 4 km/h. This

was done so that the speed would stay as close as possible to the one that corresponds to an EPA5 scenario, which is the one considered in the simulations.

As mentioned before in this section, the areas where the walk-tests took place were selected due to the existence of eNBs in which two frequency bands were operable, enabling the study of some of the scenarios considered in the simulations and, therefore, allowing one to compare both of the obtained results for similar scenarios. Each of the considered areas is intended to represent different types of environment: Moscavide illustrates a typical urban scenario, while the area of Baixa is an example of a dense urban scenario. Although the measurements in Moscavide were projected to collect data on the combination of the 1800 MHz with the 800 MHz frequency band, the UE also connected to the 2600 MHz band for a part of the route. Nevertheless, the results obtained during this period are also analysed and taken for this thesis, as they can also be of relevance.

The collected measurements show that a considerable amount of resources was being used during the walk-tests, since the number of RBs allocated to the UE is rather low, most of the times, even in situations where radio conditions are favourable to establish connection. Efforts were then made to replicate this scenario in the simulator in the best way possible in order to have coherent comparisons between simulation results and collected measurements. In order to represent a suitable compromise between the number of users and the respective generated load, together with the combination of a sufficient number of users with a sufficient number of simulations to ensure statistical relevance, one placed 1300 and 200 users in the city of Lisbon for high and low load scenarios, respectively.

In order to further assess the models implemented in the simulator, one should consider the following sections not only as presentations of the obtained results but also as a means to compare the results acquired from measurements with the ones obtained in simulations, with the intention to help in validating the implemented models. As mentioned before, the choice of the simulation settings and environment corresponds to the one that is able to provide the best approximations to the walk-tests results. The compared parameters are basically received power, SNR/SINR and throughput. Each of these comparisons is made for the three frequency bands scenarios under study and for the two network load condition situations previously mentioned.

The relative errors between measurements and simulations are obtained using (3.12). Negative variations correspond to measurement values above the ones obtained via simulations, and positive values refer to the opposite case. Also, one must take into account that the comparisons are made only for typical data users since the walk-tests only considered FTP file downloads, so VoLTE users are not compared.

4.2 High Load Analysis

The results presented in this section refer to the analysis of the network when considering the insertion of 1300 users in the simulator. These outcomes concern mainly the distribution of the

generated load throughout the network, as well as the number of active users, average SINR, average received power, average number of allocated RBs and average throughput for each of the considered services and for each scenario defined in the previous section.

In Figure 4.2, one can observe the total load distribution among the different frequency bands. Taking into account that higher frequency bands comprise a higher number of available RBs, it is of no surprise that the 2600 MHz band contains more load than the 1800 MHz or the 800 MHz ones (for Scenarios 1 and 2, respectively) and that the 1800 MHz band follows the same behaviour regarding the 800 MHz, in Scenario 3. Also, users are connected preferably to the higher frequency bands, since these are capable of offering a better signal quality than of that offered by lower ones. Both these observations are in agreement with the presented load distribution. Moreover, the presented standard deviation bars show that this behaviour is verified for all simulations, proving that, although some simulated parameters are stochastic (explained in Section 4.1) the network is able to distribute the load among the different carriers in a consistent way. This is also confirmed by verifying the total existing network load, which is always very close to 0.9.

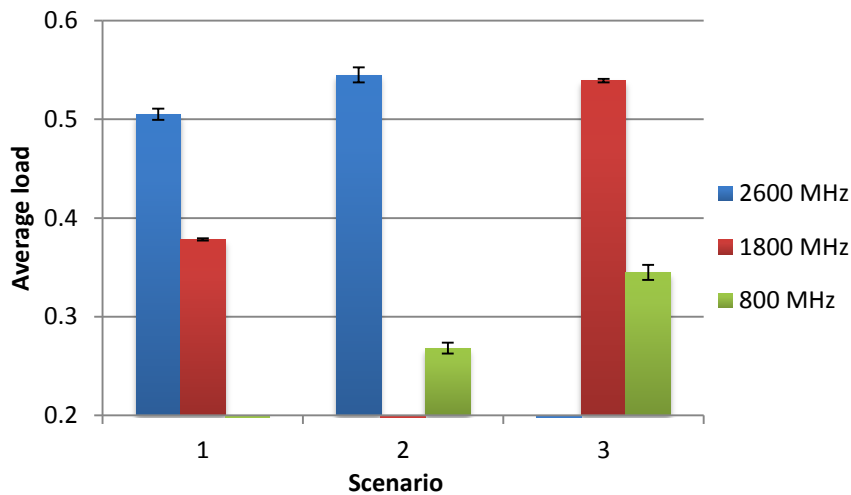


Figure 4.2. Load distribution in each frequency band, for the three defined carrier combinations.

Another relevant result to be observed is the load distribution by requested service on each scenario. Figure 4.3 shows the load associated with FTP and VoLTE users and, as expected, the first ones are responsible for most of the generated load, since the required resources to satisfy the demands for this type of service are much higher than the ones for the VoLTE service.

Figure 4.4 and Figure 4.5 show the distribution of the load for the FTP and the VoLTE services, respectively, but divided in each different considered scenario. Once again, one can observe that the higher frequency bands contain more load than the lower ones, as expected. The simulator takes into account that users should be connected to a frequency band capable of delivering a better data rate, thus, in Scenarios 1 and 2 the 2600 MHz band is responsible for handling more load than the 1800 MHz and the 800 MHz ones respectively, and in Scenario 3 the same behaviour is also verified, but for the 1800 MHz frequency band comparing to the 800 MHz one. The presented results are in agreement with the ones in the previous figure, since the FTP load reaches values much higher than the equivalents for VoLTE users.

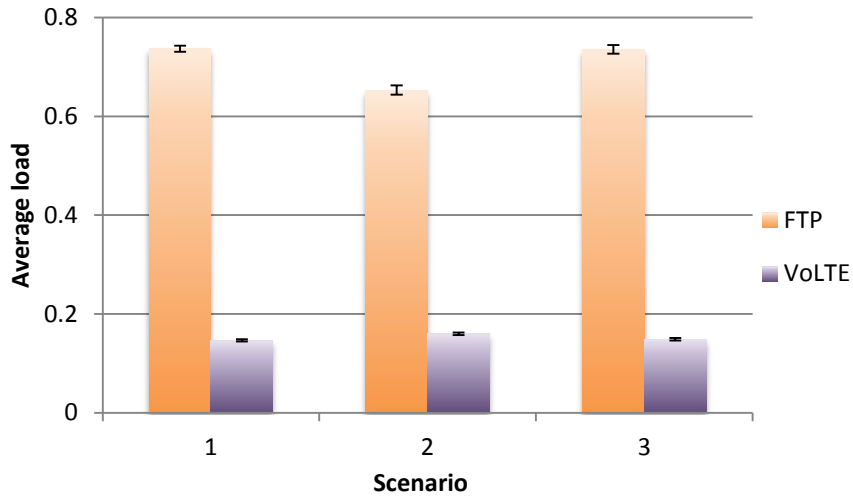


Figure 4.3. Load distribution for each type of service, for the three defined carrier combinations.

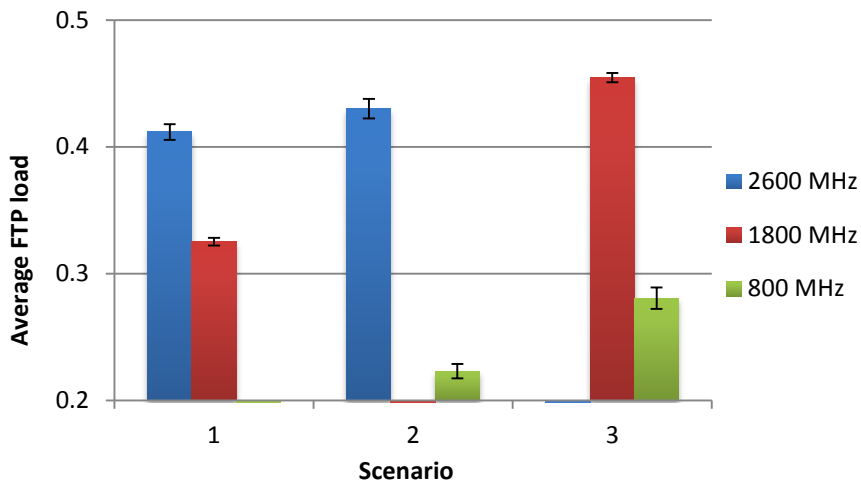


Figure 4.4. Load distribution for the three defined carrier combinations, for FTP users.

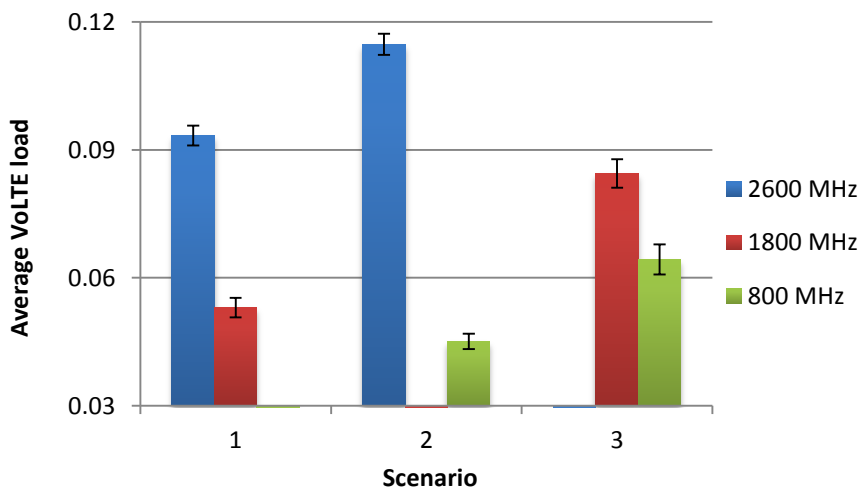


Figure 4.5. Load distribution for the three defined carrier combinations, for VoLTE users.

Nevertheless, one should keep in mind that the VoLTE service was defined as of higher priority, so it is expected that users requesting this type of service be firstly allocated to the higher frequency bands.

Figure 4.6 shows the number of active FTP and VoLTE users for each scenario, and the results allow one to confirm that a higher number of VoLTE users is served, mainly due to the low number of RBs they require to satisfy their desired throughput but also because of the priority of their service.

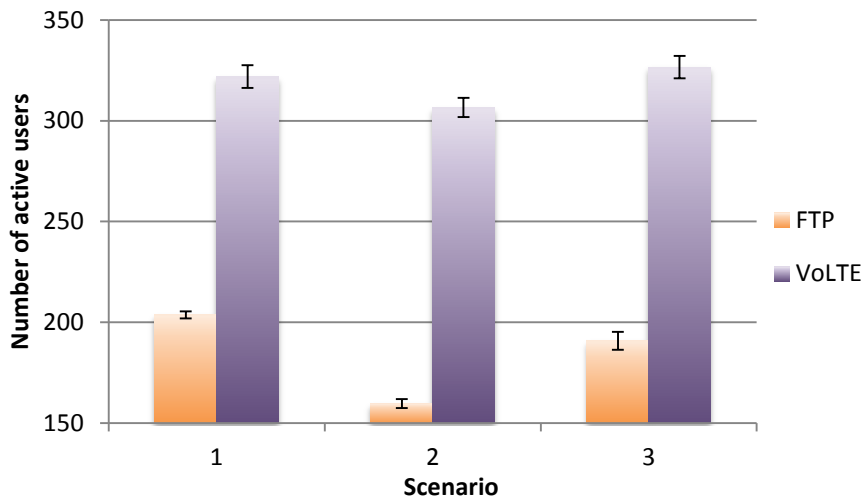


Figure 4.6. Number of active users by type of service, for the three defined carrier combinations.

Figure 4.7 also presents the number of active users among the different considered scenarios, however, it shows how the algorithm distributes them between the existing frequency bands. The first result to be noticed is that there are more users being allocated to the higher frequency bands than to the lower ones. This is a result of the implemented algorithm, which only considers that users camp on the frequency band that they are firstly connected to and, due to the prioritisation of the higher frequency bands, this may represent repercussions in terms of the achieved data rate, as it is presented further in this section. However, and as presented in the previous analysis of Figure 4.6, the majority of the users that establish their connection to the higher frequency bands are VoLTE users, since their service priority is the highest in order to better safeguard their QoS.

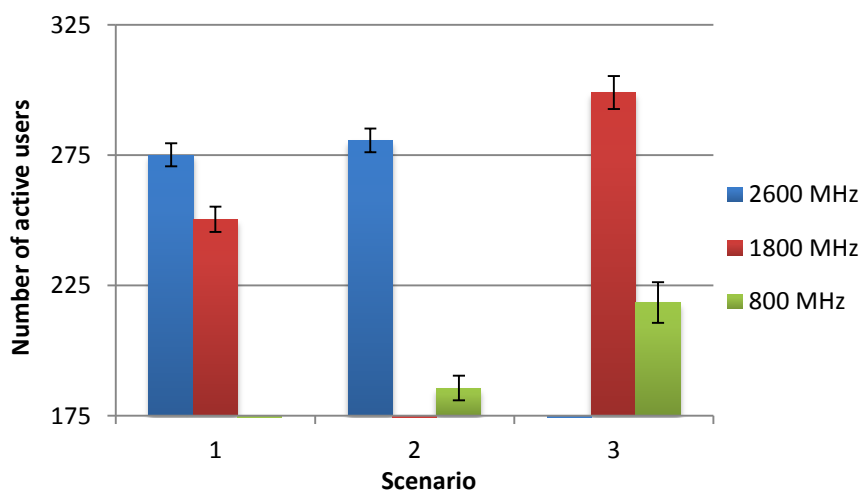


Figure 4.7. Number of active users by frequency band, for the three defined carrier combinations.

The study of the received power for each service is presented in Figure 4.8 and Figure 4.9, respectively. It shows that the received power is deeply related to the type of service being requested,

this being a consequence of the number of RBs allocated for each user: the more allocated resources to a user, the higher will be the received power. This means that the obtained results for VoLTE users are expected to be lower than for FTP users, since each RB is transmitted with a certain power. Other factors that influence these results are, e.g., the distance from the serving sector and the LoS situation of the UE.

Given the results obtained for FTP users, one should assume that the distance taken into account for the calculations of the received power for these users is rather low, since the network is only composed by a set of six eNBs, making it possible to have higher values for the received power due to the high probability that the user is positioned very close to the serving antenna. Also, this distribution of eNBs leads to a higher probability of LoS occurrence, which can also represent a boost in received power. On the other hand, the simulator does not consider all the terrain irregularities of the city, so the LoS occurrence probability should be higher than expected, reinforcing the previously mentioned influence on the received power.

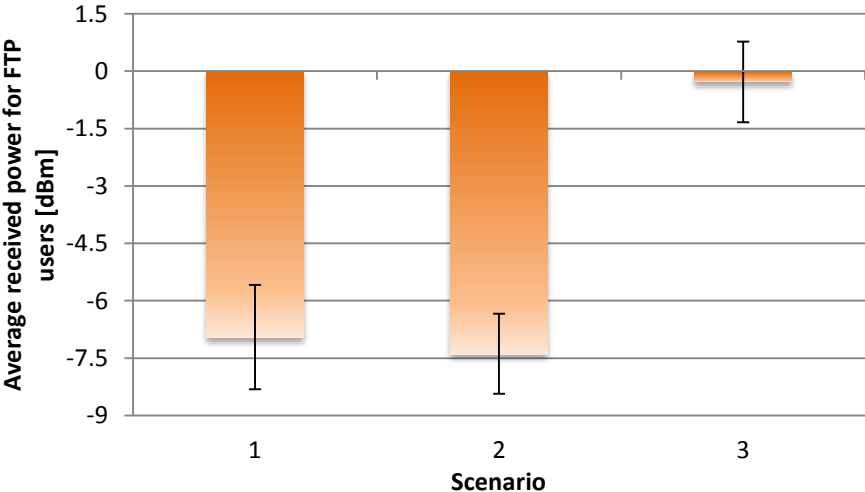


Figure 4.8. Average received power for FTP users, for the three defined carrier combinations.

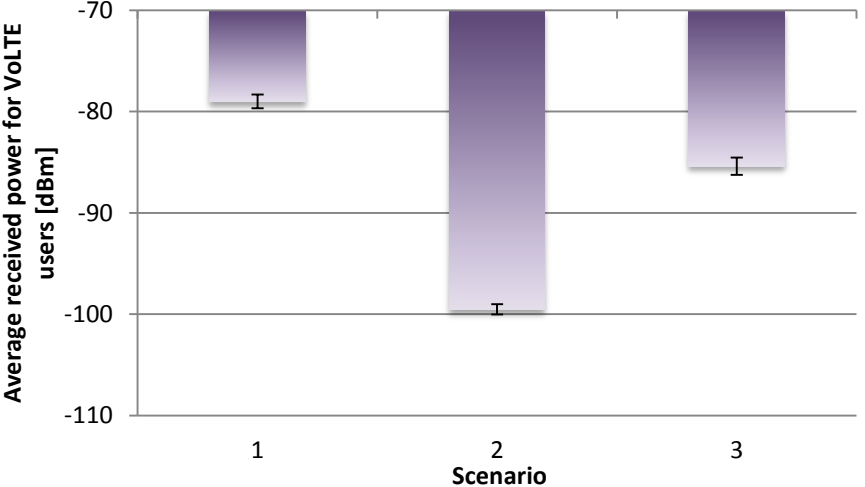


Figure 4.9. Average received power for VoLTE users, for the three defined carrier combinations.

Still regarding the analysis of the received power, Figure 4.10 enables the study of this parameter for

the different existing frequency bands. One can notice that in the 800 MHz is where the received power reaches the lowest values, which should be of no surprise since this frequency band is able to provide a wider area of coverage, meaning that some of the users connected to this carrier can be further away from the serving antenna. Regarding the low values associated with the received power in the 2600 MHz band one must again take into account that VoLTE traffic is more abundant and, therefore, is responsible for the obtained values, since the number of RBs associated with this service is very reduced, leading to lower results for the received power.

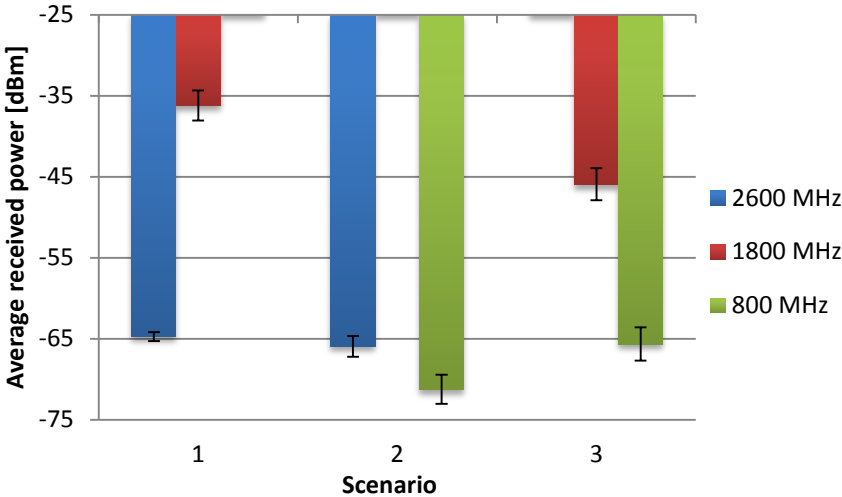


Figure 4.10. Received power by frequency band, for the three defined carrier combinations.

Another result to be analysed is the average SINR. As stated by (3.2), this parameter is linked to the received power, which means that the behaviour of both these parameters should be similar, as shown in Figure 4.11. Additionally, these results take interference into consideration, meaning that the signal quality suffers deterioration due to the presence of other users whose allocated RBs use the same frequency as those used by a given user. The quantity of users present in the network and the reduced size of it are then of great significance for the experienced SINR, leading it to reach low values such as those presented in the illustration below.

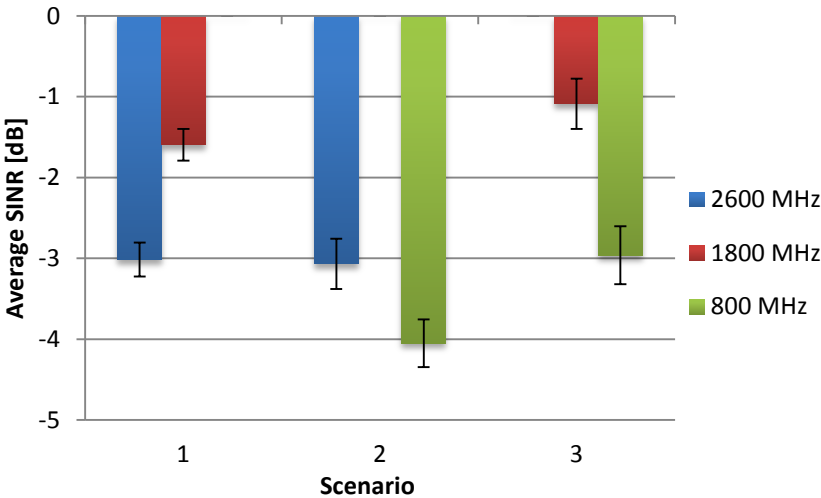


Figure 4.11. Average SINR by frequency band, for the three defined carrier combinations.

The SINR analysis is also made for each type of service in the different considered scenarios, as shown in Figure 4.12 and Figure 4.13. The presented results show that VoLTE users tend to reach lower values for this parameter in comparison to the users requesting the FTP service but, on the other hand, and recalling the enunciated concepts of SINR and received power, one should be expecting this difference between services. As FTP users require more RBs to satisfy their service demands, the higher will be the received power and, thus, the SINR.

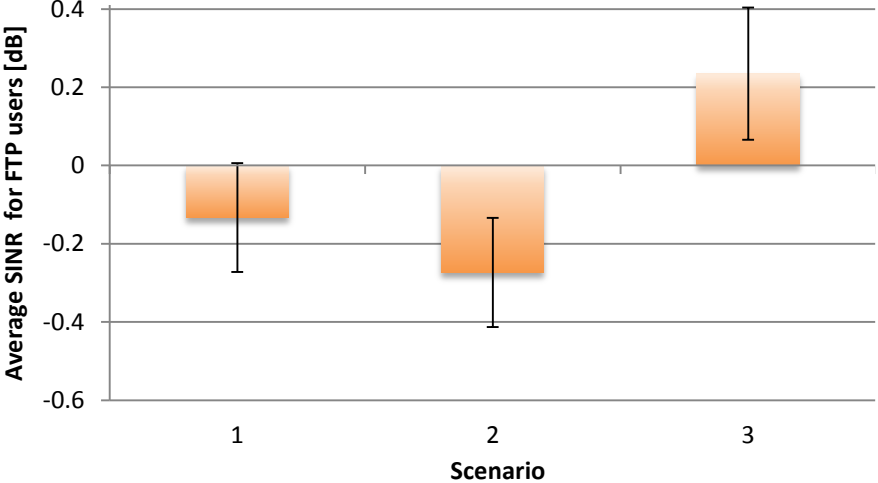


Figure 4.12. Average SINR for FTP users, for the three defined carrier combinations.

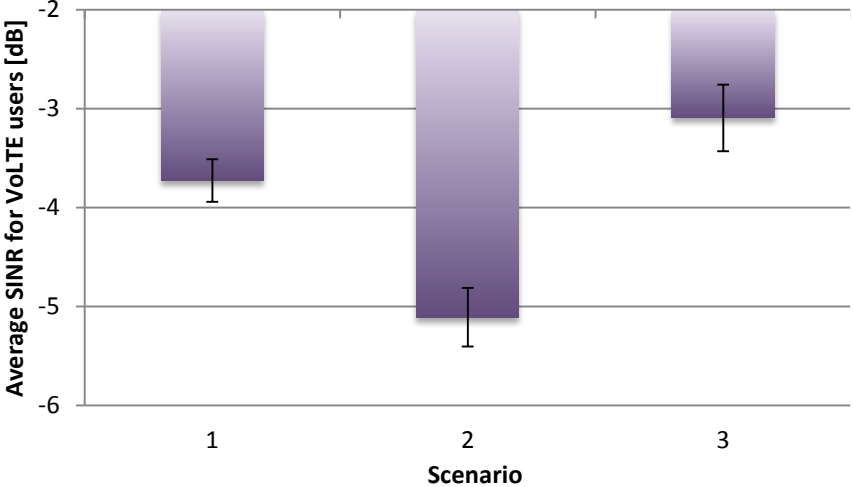


Figure 4.13. Average SINR for VoLTE users, for the three defined carrier combinations.

The following presented analysis refers to the average throughput, but only for the FTP users. The study of the same parameter for VoLTE users is not presented in a figure, due the fact that the demands for this type of service are defined by the voice codecs used to execute it, and they only require that the data rates stay between 12.2 and 12.65 kbps, as mentioned in Section 4.1. Nevertheless, these results were also scrutinised and one is able to confirm that the experienced throughput was indeed, on average, between the previously stated values.

The analysis of the average throughputs for FTP users is illustrated in Figure 4.14. As previously mentioned, the data rates for this type of service do not reach high values, mainly due to the number

of active users on the network and the required resource splitting associated with it. The implemented algorithm focuses on the prioritisation of the higher frequency bands so it is an expected result that the throughputs are indeed very low, when one takes into account the theoretically achievable ranges of this parameter. Another observable result is the fact that scenario 3 provides lower average data rates, since this frequency band combination is the one with the lowest number of available RBs due to the associated bandwidth of each of the existing frequency bands.

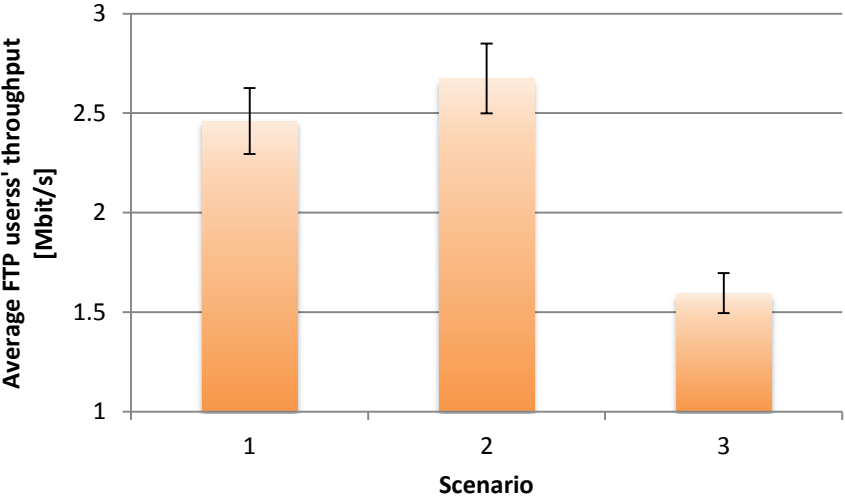


Figure 4.14. Average throughput for FTP users, for the three defined carrier combinations.

The next parameter being studied is the average number of allocated RBs to the FTP users, presented in Figure 4.15. A first glance at this analysis allows one to easily confirm the expected behaviour in terms of the distribution of the RBs in each frequency band. Moreover, this is also verified for all the scenarios in the sense that the higher frequency bands are capable of providing more RBs due to the associated bandwidth for each of them. From this figure it is also possible to notice the relationship between the FTP user RB allocation and the average throughput that it experiences, since the more RBs being allocated to a user represent an increase in its throughput, that behaviour being observable in the figure presented below as well as in Figure 4.14.

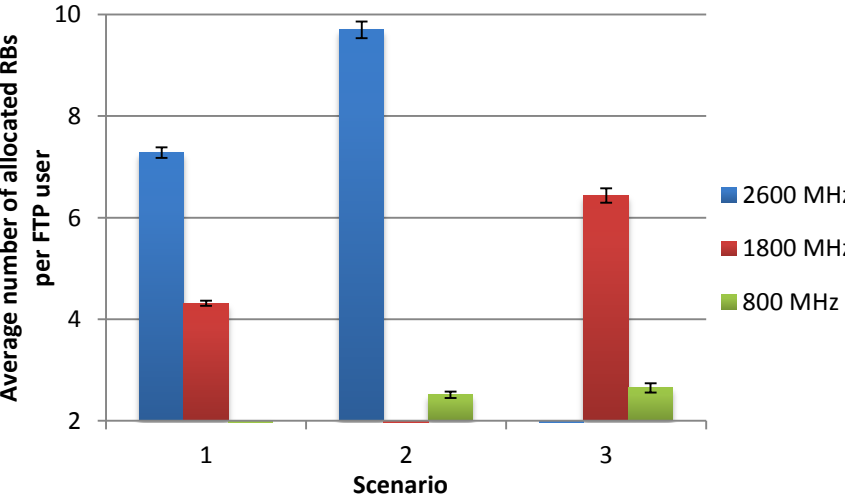


Figure 4.15. Average number of allocated RBs for FTP users in each frequency band, for the three defined carrier combinations.

The analysis of the average number of allocated RBs to VoLTE users is not illustrated in this work, for the same reason as the one presented for the average throughput analysis, which is the fact that this parameter is quite stable due to the low number of RBs required to satisfy the demanded throughput for this service. Therefore, the following analysis has solely the purpose to compare the difference between the number of allocated RBs to FTP and VoLTE users, by showing the average number of allocated RBs for each type of service per sector. Then, from Figure 4.16 it is possible to confirm once again that the total number of available resources decreases according to the frequency bands being considered for each scenario. One should keep in mind that, although there are more resources being allocated to FTP users than to VoLTE users, the latter is still of higher priority, which leads to a higher number of this type of user.

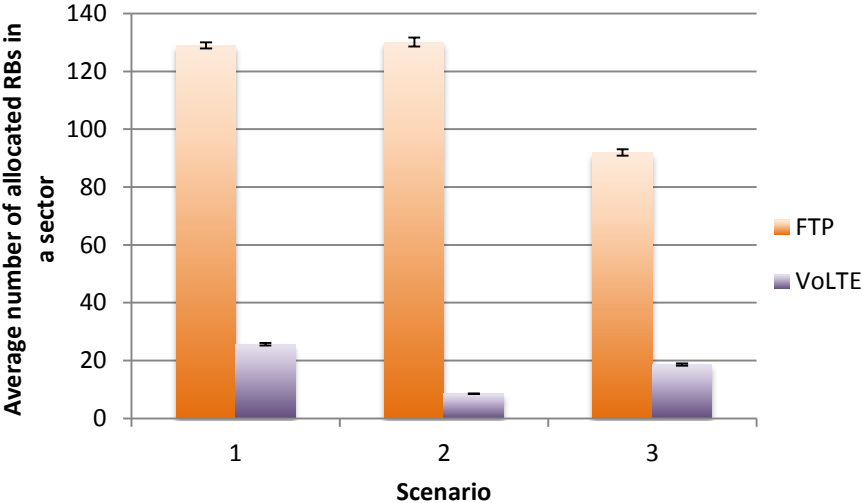


Figure 4.16. Average number of allocated RBs in a sector per type of service, for the three defined carrier combinations.

4.3 Low Load Analysis

In what follows, one presents the results obtained by the simulator regarding the analysis of the network considering that 200 users are inserted. The presented results mainly address the distribution of the generated load throughout the network, the average number of active users, average SINR, average received power, average number of allocated RBs and average throughput for the three scenarios defined in Section 4.1.

The first analysis concerns the load distribution among the different frequency bands, as shown in Figure 4.17. Once again, it is possible to see that the higher frequency bands end up containing more load than the lower ones. This is a consequence of the available resources for each carrier due to their associated bandwidth and due to the prioritisation of the higher frequency bands on the simulator. One can also notice that the standard deviations have increased, compared with the high load scenario, which is an expected result, since the number of existing users is much lower than in

the previous analysis, i.e., taking into account that some parameters for the radio conditions of the users are stochastic, it is more likely that different simulations end up generating different load values. Also, analysing the total generated load, one can perceive that it decreases as well, this being a consequence of the lower number of existing users in the network. Moreover, this total network load reaches the highest values in Scenario 1, followed by Scenario 2 and finally Scenario 3, as a result of the total number of available resources for each combination of carriers. Another observable outcome is that the 1800 MHz frequency band reaches higher load values, justified by the fact that this band has a higher coverage area than the 2600 MHz one and, therefore, is able to comprise users that are further away from the eNB, hence, originating the similar load values observed for Scenario 1. Besides, since the implemented algorithm is focused on allocating users to the higher frequency bands, scenario 3 shows that the 1800 MHz band load reaches almost the double of the 800 MHz one, meaning that most of the users are covered by the firstly mentioned frequency band and are, therefore, allocated to it.

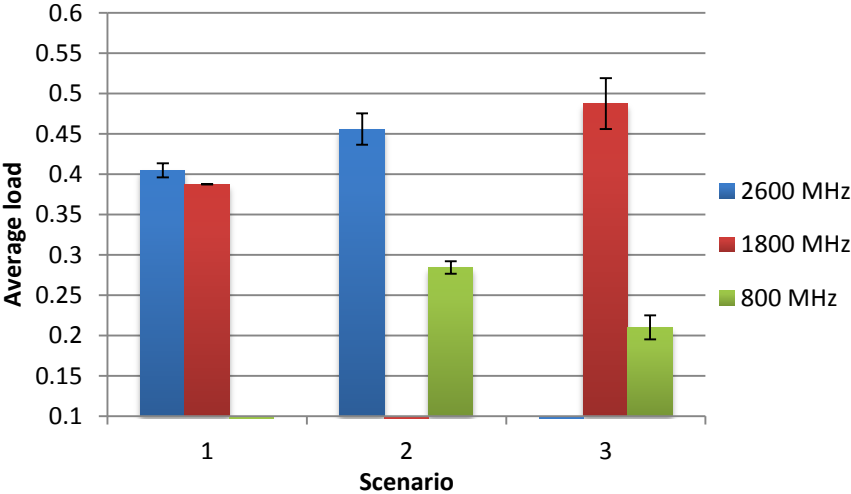


Figure 4.17. Load distribution in each frequency band, for the three defined carrier combinations.

It is also of interest to observe the load distribution between the different considered services. In Figure 4.18, one can see the FTP and VoLTE services respective loads and observe that the latter contributes with a small portion to the total load, once again since these users never require many RBs to satisfy their demands and recalling that the total number of considered users is only 200.

Regarding FTP users, three main observations can be made. The first one (enforcing the previously mentioned result) is that FTP users require more resources for their service, since their requested throughputs are the highest from both considered services. Next, one can confirm that the total network load is higher in Scenario 1, followed by Scenario 2 and then Scenario 3, this being a consequence of the existing available resources in each scenario, as analysed above in this section. Finally, it is possible to observe the increase of the standard deviation in each scenario, which is an expected result that is in agreement with the coverage areas of each scenario, meaning that more users can be served but their radio conditions suffer higher variations, leading to the presented differences in their associated load.

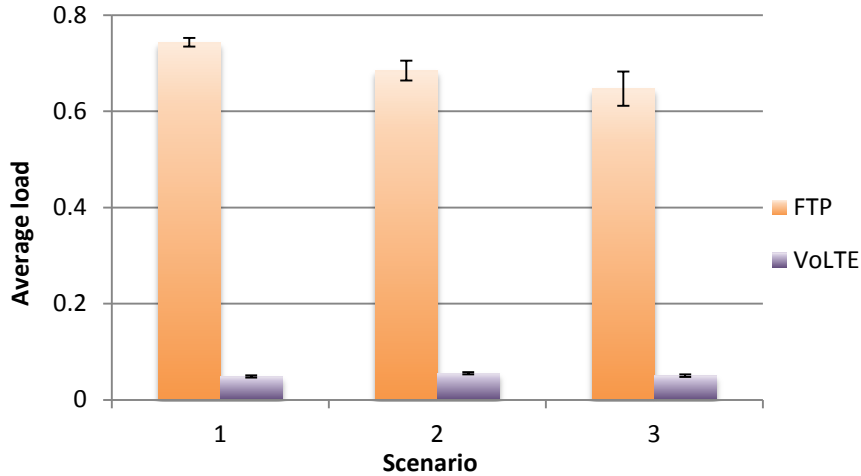


Figure 4.18. Load distribution for each type of service, for the three defined carrier combinations.

Next, a more detailed study on load distribution is presented for each of the considered services. The analysis regarding only FTP users is shown in Figure 4.19, where one can observe, once again, that these users are responsible for most of the load generated throughout the network. Comparing to the high load analysis previously made, it is possible to see an increase of the standard deviation, especially in Scenarios 2 and 3, as a result of the low number of users that is being considered. Besides, one should notice the increase in these variations throughout the different scenarios, this being a consequence of the coverage areas associated with the different frequency bands available in each one them. Another important result to look at is that the higher frequency bands always comprise more load than the remaining ones, as one should expect based on the way the algorithm is implemented. Only Scenario 1 presents similar loads for each carrier due to the fact that there is a reduced number of users and that the 1800 MHz frequency band turns out to be responsible for the users that are further away from the eNBs and, therefore, are not able to connect to the 2600 MHz band. This observation is not so clear for Scenarios 2 and 3 due to the fact that the 800 MHz band has the lowest number of RBs, consequence of the available bandwidth for this carrier.

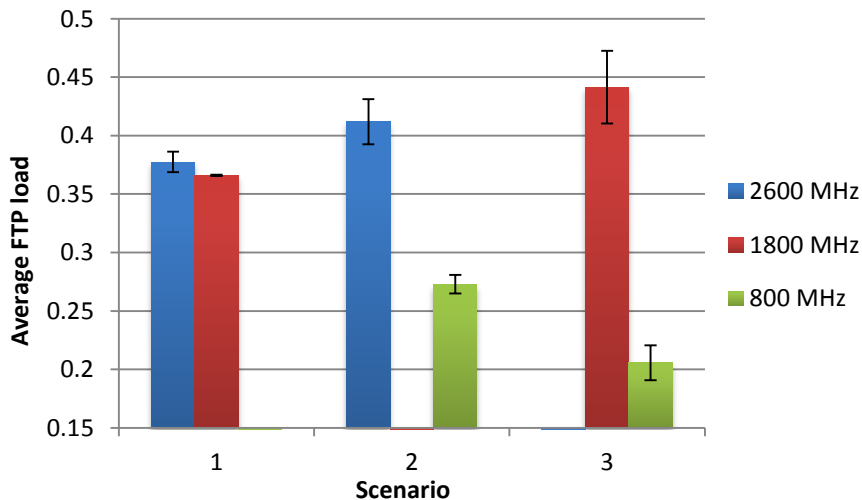


Figure 4.19. Load distribution for the three defined carrier combinations, for FTP users.

Average VoLTE users generated load throughout the network is presented in Figure 4.20, and from it

one can again observe that these users, although considered of more priority, and therefore assigned to higher frequency bands, do not occupy many of the network resources. This remark is aggravated with the low number of users being considered.

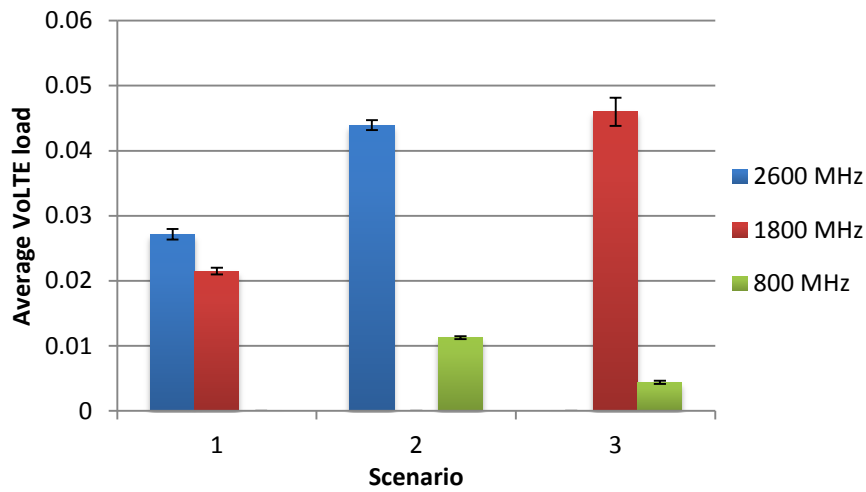


Figure 4.20. Load distribution for the three defined carrier combinations, for VoLTE users.

The number of active FTP and VoLTE users is presented in Figure 4.21, where one can rapidly observe that the number of VoLTE users remains unchanged for all scenarios besides exhibiting no standard deviation. This is a result of the number of generated users, i.e., 81 VoLTE users are being considered along the whole network in all simulations and, in all of them, they are able to end up being served. It is a result that meets the expected, due to the priority assigned to this service. Moreover, one can also see the number of active FTP reaching higher values from Scenario 1 to Scenario 2, and again from the latter towards Scenario 3. This behaviour is a consequence of the increasing coverage areas associated with the frequency bands in consideration for each scenario.

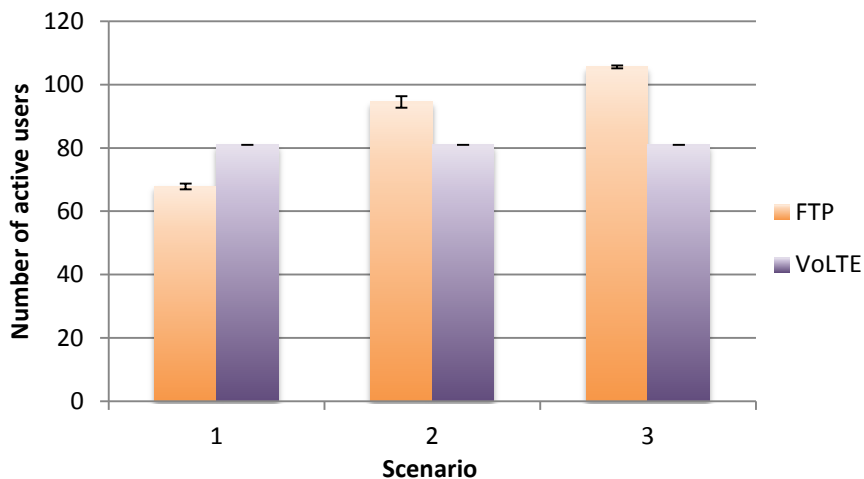


Figure 4.21. Number of active users by type of service, for the three defined carrier combinations.

The analysis of the number of active users in each frequency band in each scenario is also presented, however, the obtained results are much different from the ones presented in the previous section, as shown in Figure 4.22. The first observation to be made is that the total number of considered users

does not correspond to the number of active users for every defined scenario. In Scenario 1, it is possible to see that the number of users assigned to the 2600 MHz band is lower than expected, only explained by the fact that there are less users being considered throughout the network and also due to the impact that the stochastic processes, taken into account for the required calculations for the signal quality levels, may have in this value. This result leads to the assignment of a higher number of users to the 1800 MHz, besides the ones that are outside the coverage area of the firstly mentioned band. This situation is also replicated in Scenario 2, where the influence of the wider coverage area of the 800 MHz band is more noticeable. Nevertheless, Scenario 3 presents an expected behaviour in the sense that, given that the trade-off between cell coverage area and number of available RBs is less pronounced for the 1800 MHz band, it is possible to allocate most of the users to this band, as it is the one with highest priority for the referred scenario.

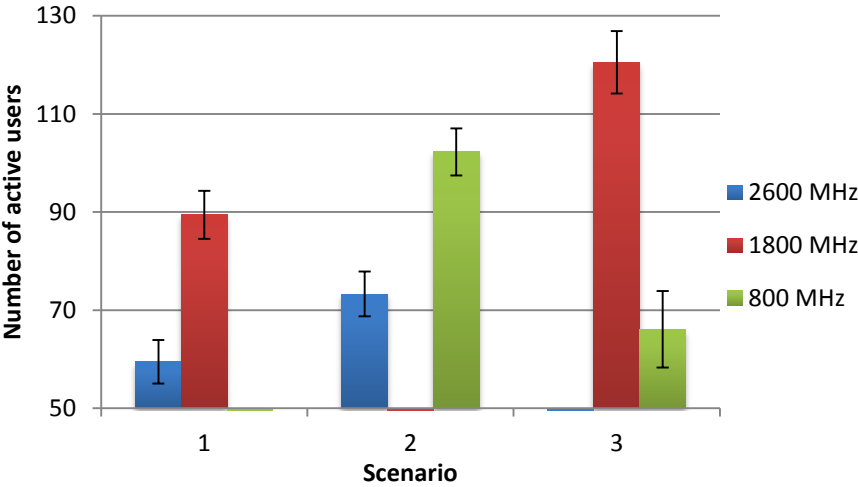


Figure 4.22. Number of active users by frequency band, for the three defined carrier combinations.

Next, Figure 4.23 and Figure 4.24 present the analysis of the received power for FTP and VoLTE services, respectively.

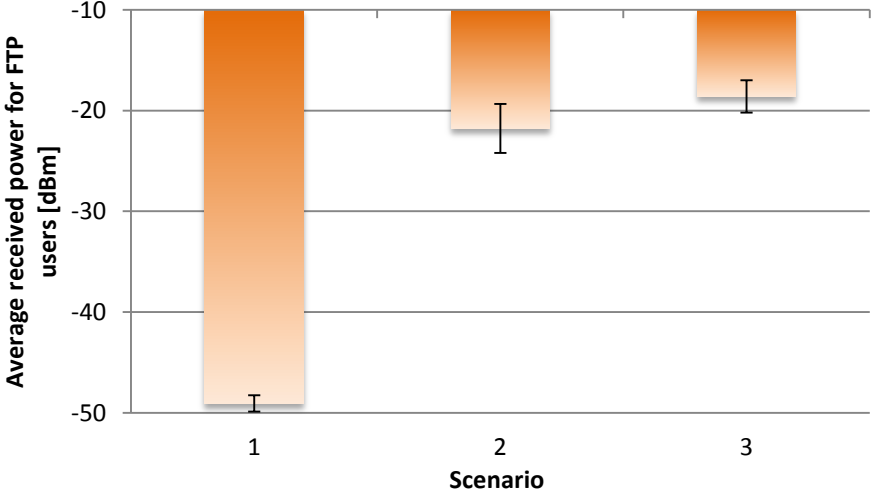


Figure 4.23. Average received power for FTP users, for the three defined carrier combinations.

As mentioned in the high load analysis, the type of service being used has a major influence on the

received power, due to the number of RBs required by each service, justifying the fact that this parameter assumes higher values for the FTP service, comparing to the VoLTE one. Nevertheless, the distance from the serving antenna and the LoS conditions of the UEs should be taken into account for the calculation of this parameter. Another result to be observed is the increase in the received power from Scenario 1 to Scenario 2, followed by an increase in Scenario 3, regarding the FTP service. This is a consequence of the increase in the number of active FTP users from each different scenario. Besides, given that the total number of considered users is rather low, the more RBs can be allocated to each active user.

Regarding the received power of the VoLTE users, one can observe that it reaches higher values than in the high load analysis as a result of the number of considered users throughout the network. However, Scenario 2 presents slightly lower results for this value, this being a consequence of the assignment of many VoLTE users to the 800 MHz band due to their distance from the serving antenna and, possibly, due to their radio conditions.

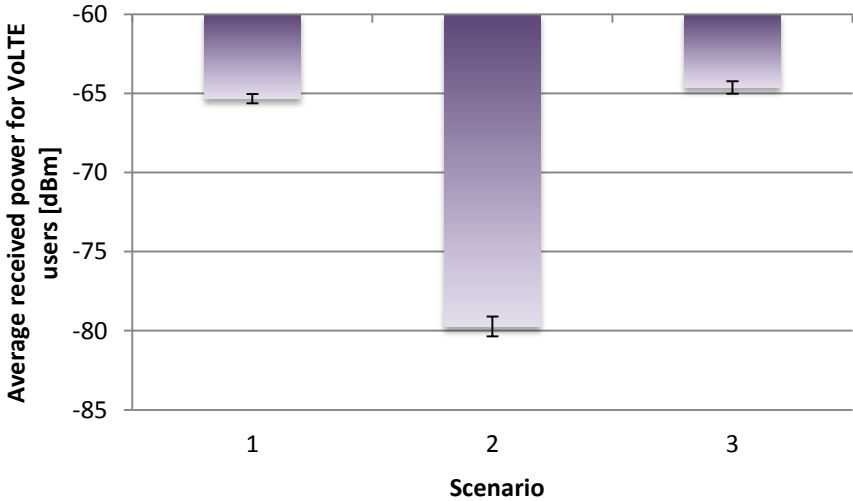


Figure 4.24. Average received power for VoLTE users, for the three defined carrier combinations.

The last analysis regarding the average received power is presented in Figure 4.25, allowing one to further study this parameter in terms of the different frequency bands. Since the number of users being considered in this analysis is of only 200, and recalling that all VoLTE users end up being served, one can expect that the average received power, in each highest priority frequency band, achieves very low values. Also, one can once again grasp that the received power grows from Scenario 1 towards Scenario 2, and even more for Scenario 3, as a result of the increase in the number of FTP users being served in each of the scenarios. Most of these users end up being served by the carriers of lower priority as a result of the implemented algorithm and, therefore, one can observe the increase in the average received power, especially in Scenario 3, where it is possible to see a larger difference between the average received powers in each of the considered carriers.

Next, an analysis of the average SINR is made and it is presented in Figure 4.26. The results are also in agreement with the direct connection existent between this parameter and the average received power, as they were for Section 4.2, the difference being that interference and noise are taken into

consideration. These two last factors would typically have a less pronounced influence in this low load analysis, since there are less users being considered. However, this is not verified as much as expected mainly due to the size of the network and due to the previously mentioned relationship with the received power, which in itself is very low as above mentioned.

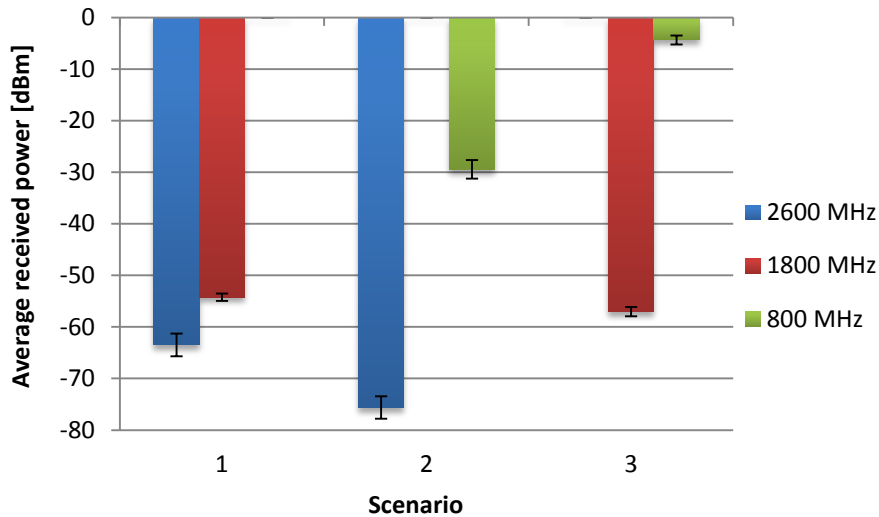


Figure 4.25. Received power by frequency band, for the three defined carrier combinations.

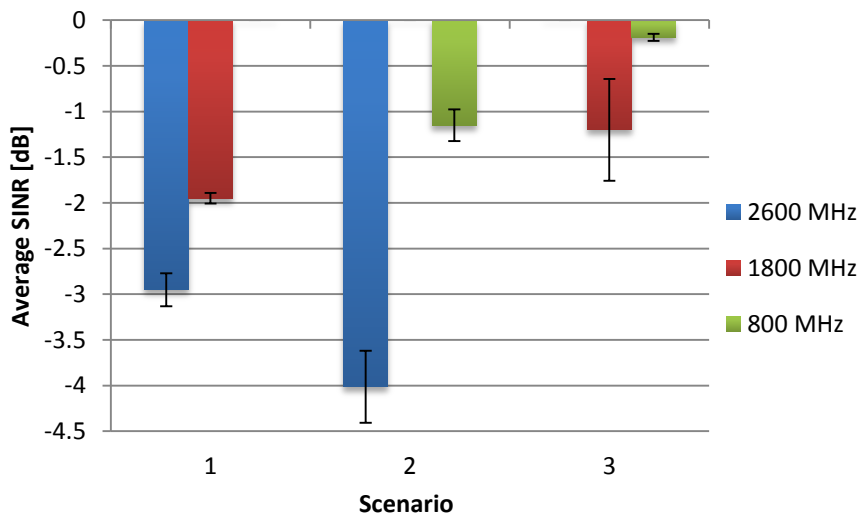


Figure 4.26. Average SINR by frequency band, for the three defined carrier combinations.

Figure 4.27 and Figure 4.28 also present the average SINR analysis, but regarding FTP and VoLTE services, respectively. Again, one can confirm the influence of the average received power in the obtained results, which leads to the presented low average SINR values. Also, comparing the outcomes between each service, it is possible to observe that FTP users once again have higher values for this parameter in comparison with the VoLTE users, as a consequence of the number of RBs required by each service to satisfy its requirements in terms of throughput. Another observation to be made is the confirmation of the increase of the average SINR for FTP users from Scenario 1 to Scenario 2, followed by Scenario 3, as an effect of the increase in the number of users for this type of service.

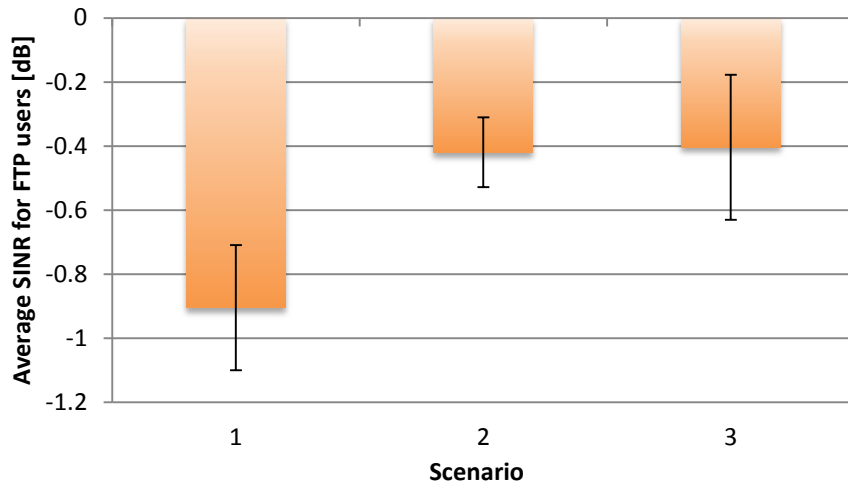


Figure 4.27. Average SINR for FTP users, for the three defined carrier combinations.

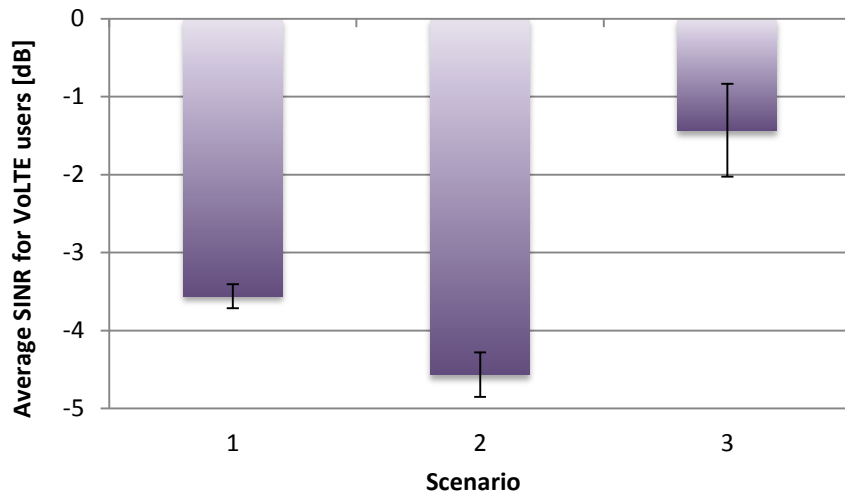


Figure 4.28. Average SINR for VoLTE users, for the three defined carrier combinations.

The next parameter to be analysed is the average achieved throughput. As it was done in the previous section, only the FTP users' throughput is presented in the form of a figure for the same reasons presented in the high load analysis. Furthermore, the average achieved throughputs for the VoLTE users were also studied in order to confirm that the data rates are indeed inside the range defined for this type of service.

As one can observe from Figure 4.29, the average throughput for FTP users achieves higher values than the ones in Section 4.2, as expected due to the fact that fewer users are requesting resources from the network. However, the achieved data rates are still below the theoretically achievable ones, this being a consequence of the implemented algorithm, which prioritises the higher frequency bands before allocating the available resources in the lower priority bands, leading to the need to divide the available RBs among the connected users. It is also perceptible that each combination of carriers leads to different achieved throughputs, given that the number of active FTP users grows and the number of available resources decreases. Scenario 1 comprises the least number of active FTP users and the most available RBs and therefore achieves higher throughputs but with a higher standard

deviation, followed by Scenario 2 and finally by Scenario 3. These results are in agreement with the expected if one takes into account the justifications previously presented.

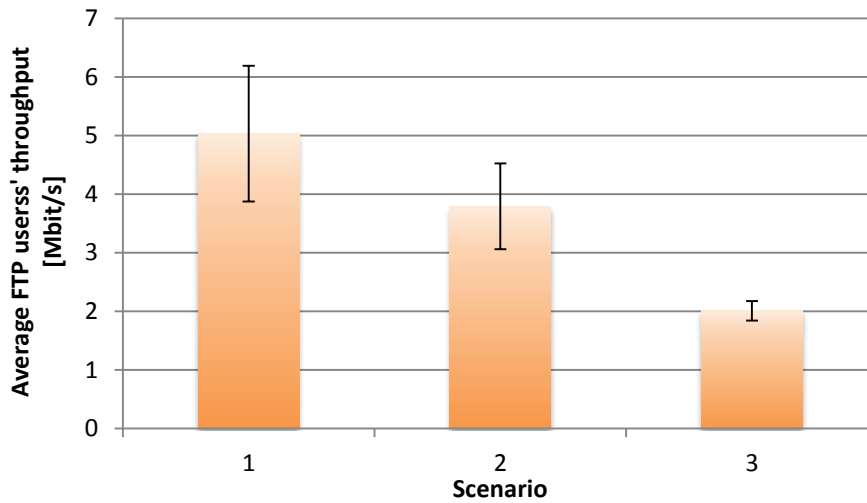


Figure 4.29. Average throughput for FTP users, for the three defined carrier combinations.

The following analysis regards the average number of allocated RBs to FTP users. From the study of the results presented in Figure 4.30, it is possible to observe the distribution of RBs to these users in each frequency band and one can also verify that higher frequency bands end up providing a higher average number of resources to its connected users, as expected. There is also a clear relationship between the experienced throughputs of these users with the average number of allocated RBs to them, as one can observe by comparing the figure below with the data presented in Figure 4.29.

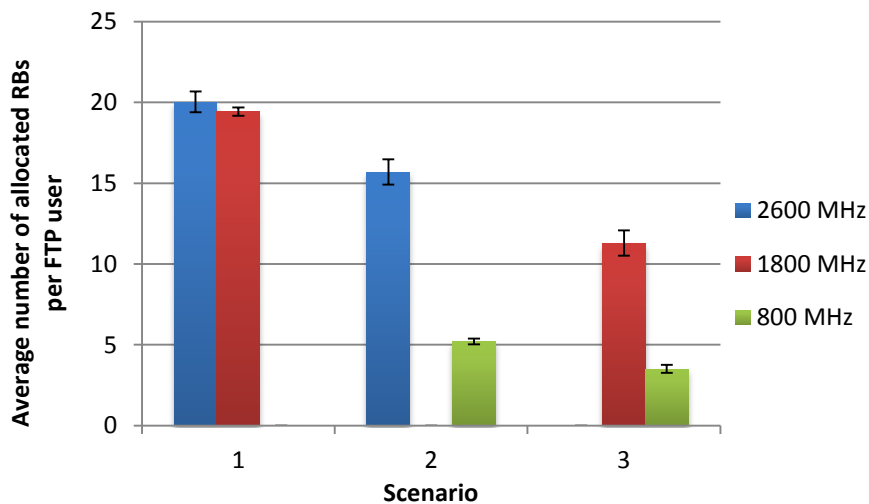


Figure 4.30. Average number of allocated RBs for FTP users in each frequency band, for the three defined carrier combinations.

As it was mentioned in the previous section, the study of the average number of allocated RBs to VoLTE users is not presented since the results obtained are as expected and do not represent a large added value to this work, since the number of resources required to satisfy the demands of this type of user is rather low, ranging from 1 to 2 RBs.

The final study in this section is then intended only to compare the average number of allocated RBs

for each type of service per sector, as it was done in Section 4.2. Figure 4.31 shows, once again, that VoLTE traffic requires a much lower number of RBs than the equivalent for FTP users, due to the throughput demands of each service. It is also possible to observe that the number of allocated RBs per sector decreases in agreement with the number of available resources associated with the bandwidth of the carriers, meaning that Scenario 1 is able to provide more RBs, followed by Scenario 2 and finally by Scenario 3, as expected from the definition of each of the scenarios.

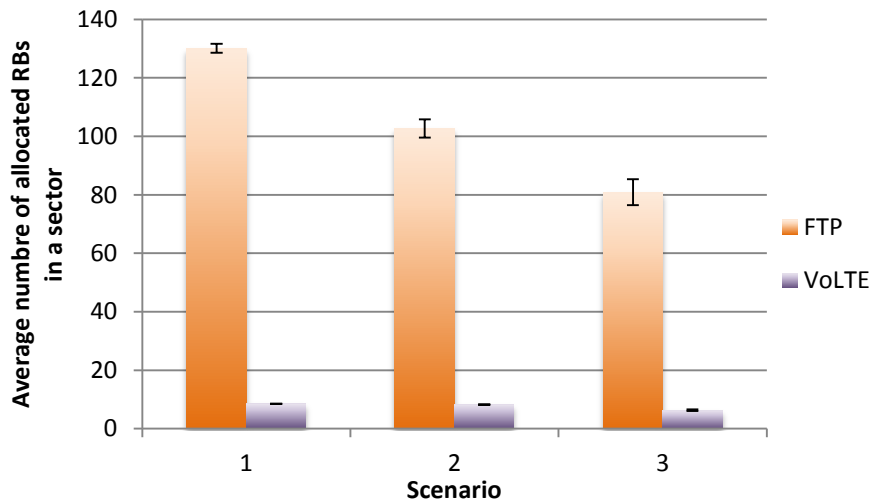


Figure 4.31. Average number of allocated RBs in a sector per type of service, for the three defined carrier combinations.

4.4 Walk-Tests Results

Since the ideal scenario does not exist in a network, two areas were tested in order to study different situations, both considering only two co-located carrier frequencies. The region of Moscavide was selected to represent a typical urban scenario, in which the walk-test would mainly assess the combination of the 800 MHz with the 1800 MHz carrier (although the 2600 MHz carrier is also used during a small duration of the test), while the central area of Baixa represents a dense urban environment used to assess the combination of the 800 MHz with the 2600 MHz carrier.

The results obtained from the simulations proved to be much different from the ones presented in this section. The best comparison that one was able to find was the usage of Scenario 2 to compare the measurements performed in the area of Moscavide with the simulation results for a low load scenario. The remaining walk-test results are also shown in this section, although their comparison would not provide any added value to the development of this thesis, since the relative errors that were obtained are large. The reasons for these large differences may be originated from many different factors. Many of the terrain irregularities of the city of Lisbon are not considered in the simulator, which can have a large influence in the propagation of the signal from the eNB to the UE. Moreover, the propagation model considers that all buildings are of the same height and all streets are of the same width, which

is not verified throughout the city. Another factor that may influence the obtained results is the difference in the number of users and their respective traffic in the sector from which the measurements were being acquired, meaning that the occupation of the serving sector is likely to differ from the one considered in the simulations. Also, the positioning of the eNBs and their number of sectors and respective antennas' orientation throughout the network does not correspond exactly to the one existing in Vodafone's network. Furthermore, the simulations do not take into account rapid signal variations associated with HO by poor radio conditions or triggered by the movement of the UE, since the simulator considers only users in the same geographic location.

In Figure 4.32, one presents the usage of the different frequency bands for each considered environment where, as stated in [Voda13a], the 1275 serving cell DL EARFCN corresponds to the 1800 MHz band, the 2950 refers to the 2600 MHz band, and the 6300 corresponds to the 800 MHz band.

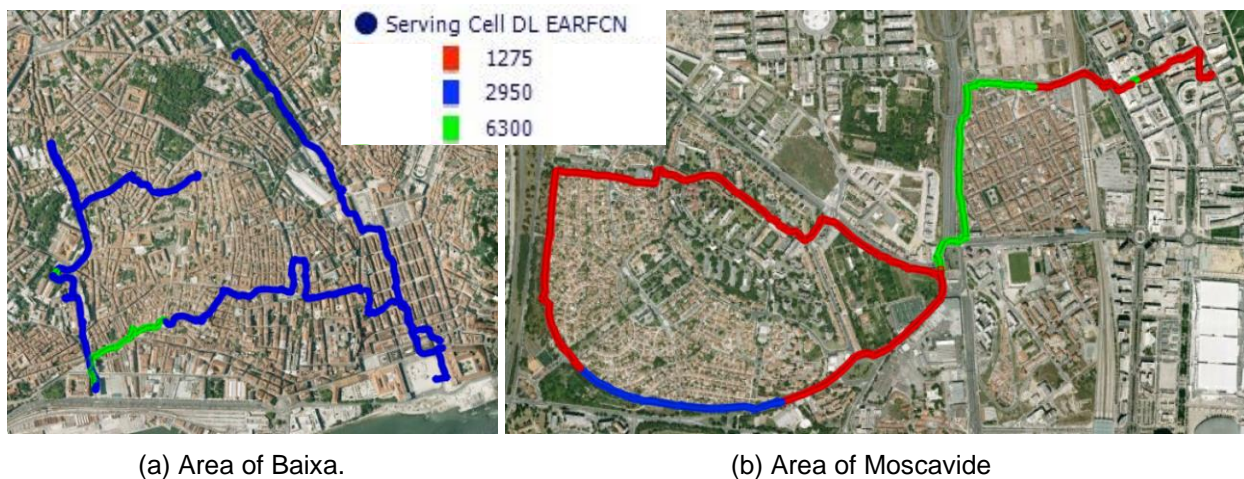


Figure 4.32. Frequency bands for the walk-tests.

The serving cell RSRP is the average of the measured power of the resource elements that contain cell-specific reference signals, according to [HoTo11], its value being also a result of the average between the various receiver branches. In Figure 4.33 and Figure 4.34, one shows the obtained RSRP during the walk-tests for each area of Lisbon. It is worth noticing that the measured values are higher whenever the equipment is in open areas and also when it is closer to the serving sector antenna, the latter being verified during the walk-tests, being both situations a result of the higher probability of LoS occurrence.

The relative error obtained for this parameter was of 41.90%, meaning that almost the double of the received power was obtained in the simulations comparing to the measurements. This can be a consequence of the size of the network taken into consideration in the simulator.

In Figure 4.35 and Figure 4.36, one presents the Reference Signal (RS) SNR measured during the walk-tests, being evident that there is indeed a relationship between it and the received power, i.e., areas in which the RSRP is higher share the same behaviour in terms of SNR, as expected. This relationship also reveals that interference has little effect on system performance, since the SNR always follows the growth of the RSRP, possibly meaning that there was a low number of UEs using

the same part of the spectrum at the time of the walk-tests. Also, it is possible to observe that no RS SNR values above 30 dB were detected in the area of Baixa, showing that the type of environment is also a relevant factor on the quality of the received signal.

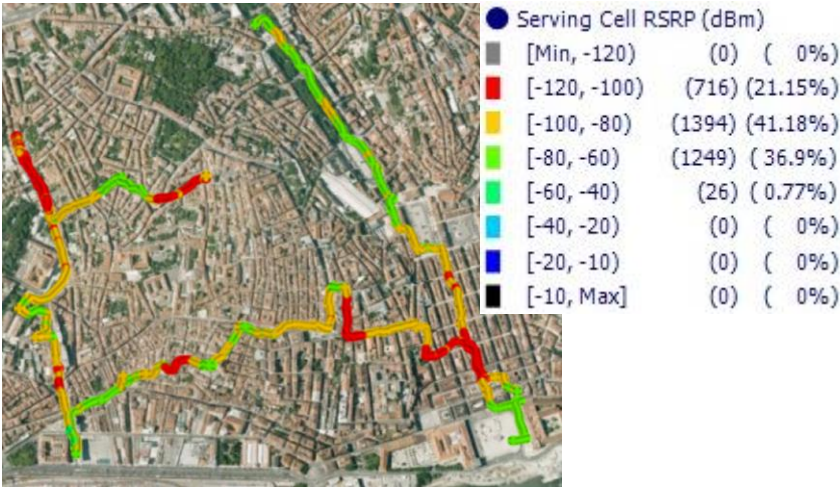


Figure 4.33. Measurement of the RSRP in the area of Baixa.



Figure 4.34. Measurement of the RSRP in the area of Moscavide.

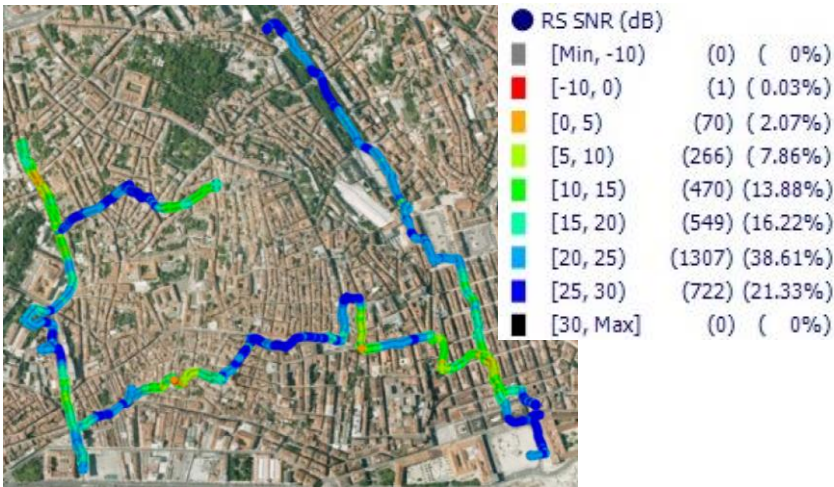


Figure 4.35. Measurement of the SNR in the area of Baixa.

The obtained relative error associated with the SNR is -104.35%, which is an unreasonably high value

for any possible comparison. This may also be a result of the small size of the network and the fact that, for the SNR, no interference is taken into account, while the simulator makes use of the SINR



Figure 4.36. Measurement of the SNR in the area of Moscavide.

The number of PDSCH RBs was also a measurement object for the walk-tests. Figure 4.37 and Figure 4.38 contain information regarding the number of allocated RBs during the tests and one can observe that different factors are of relevance for the presented values. It is possible to see that, on average, the higher the frequency band being used the more RBs end up being allocated. Besides that, the number of allocated RBs is greatly related to the experienced SNR, which is an expected result. Nevertheless, as shown, for example, in the area of Terreiro do Paço, the signal quality may reach high enough values but the number of allocated RBs ends up being rather low. This is possibly a consequence of the number of users being served by the same serving cell, meaning that the existing resources are already being used for other users. Taking this into account and comparing the obtained values with the measurements presented in [Alme13], one is able to say that the number of LTE users has undeniably increased. Also, the number of allocated RBs may sometimes decrease considerably in situations of cell reselection or when the connection is lost.

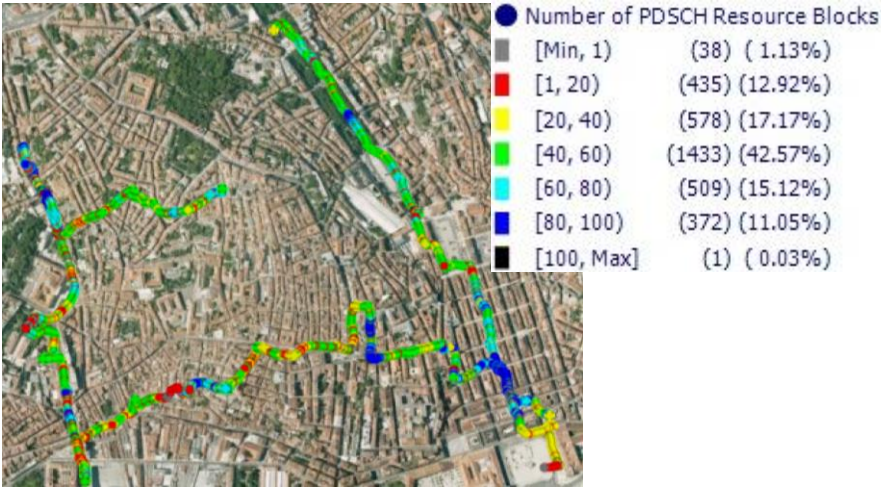


Figure 4.37. Measurement of the number of allocated RBs in the area of Baixa.

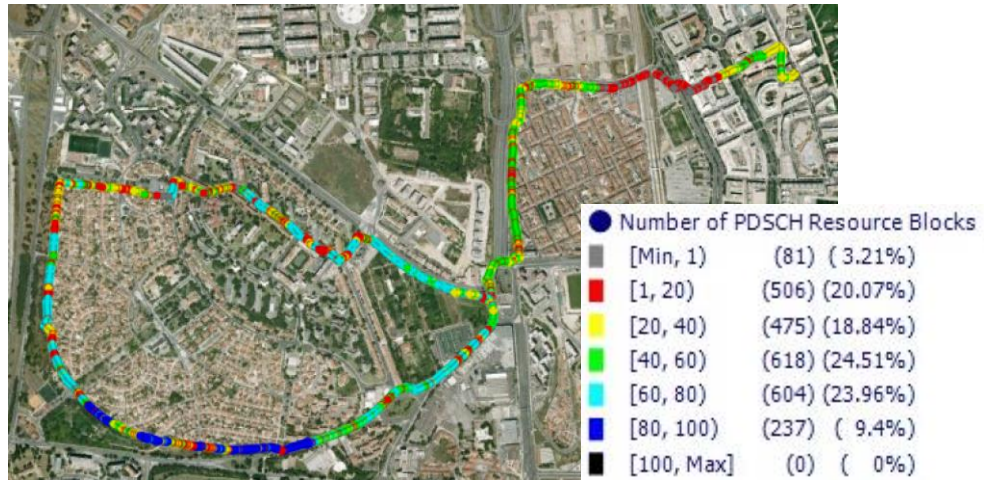


Figure 4.38. Measurement of the number of allocated RBs in the area of Moscavide.

Regarding the relative error between the performed measurements and the acquired results from the simulations, for the number of allocated RBs, one obtained a value of -26.93%, meaning that at the time the measurements were performed, there were less users requesting resources than the ones considered in the simulations. Nevertheless, this was the parameter that presented the lowest absolute value for the relative error between simulations and measurements.

Figure 4.39 and Figure 4.40 show the measured PDSCH Physical Layer Throughput for the two considered environments. It is of no surprise that the type of environment has a strong impact on the experienced throughput, as one can see in the measurements in the area of Baixa where the maximum achieved throughput was of 36.45 Mbps, when in the area of Moscavide reached 91.8 Mbps. Taking into account the frequency bands being used, one can notice, especially in the area of Moscavide, that the higher throughputs are achieved when the connection is established on higher frequency bands, which is also an expected result. Furthermore, considering the information on experienced SNR and on number of allocated RBs, one can observe that the achieved throughput behaves according to both previously mentioned factors, meaning that the throughput increases in areas where both signal quality and number of RBs being used reach the higher values, concluding that throughput is limited by system capacity and by radio conditions, as expected.

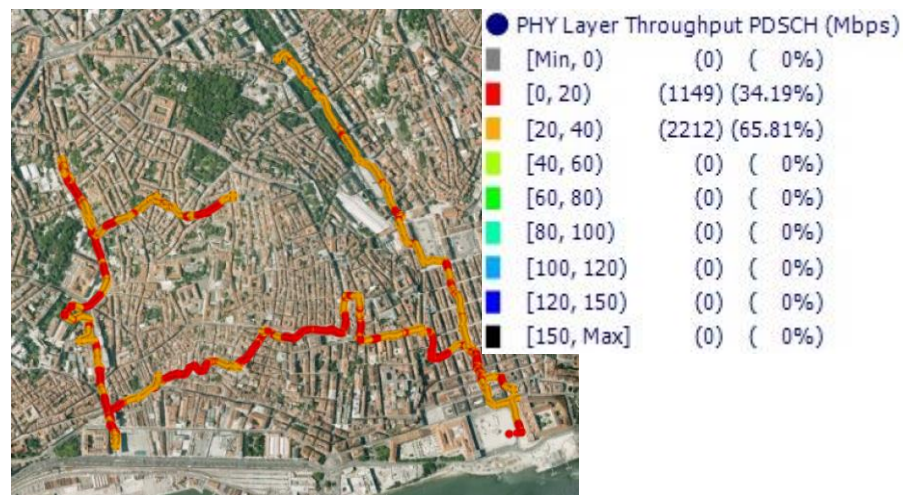


Figure 4.39. Measurement of the throughput for the area of Baixa.

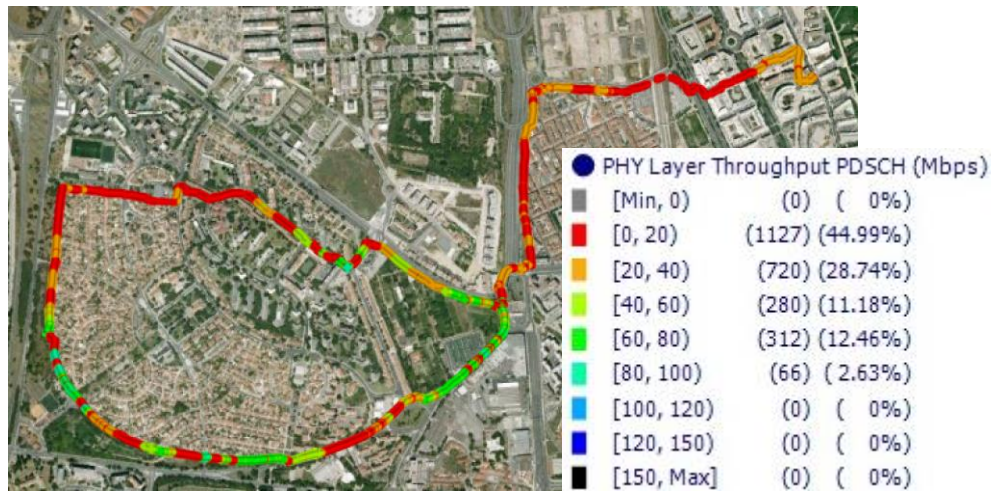


Figure 4.40. Measurement of the throughput for the area of Moscaide.

The relative error obtained for the throughput is -82.28%, which may be a consequence of the radio conditions experienced by the UEs in the simulations and can also be a result of the difference in the resource availability in the different situations.

Chapter 5

Conclusions

This chapter completes the present work, summarising the main conclusions obtained and as well as pointing out some of the aspects that should be developed in future work.

The main goal of this thesis was to study the distribution of load in an LTE network deployed over an urban scenario, taking into account different combinations of frequency bands, each with a different associated bandwidth. In order to accomplish this goal, a model was developed and implemented in the form of a simulator based on previous works, and several simulations were done for high and low user densities throughout the considered network. The city of Lisbon was chosen as a reference scenario so that one could have a better approximation to a real network, and to have a comparison made with measurements performed along the city. Simulations were done for different numbers of users randomly distributed along the network using either typical data download services or VoLTE.

The first chapter is intended to briefly describe mobile communications systems, followed by a superficial explanation of the growing data traffic demands and finally addressing the motivation of this thesis and its contents.

In Chapter 2, a theoretical background on LTE's network architecture is presented, describing its main constituting elements and how they are able to interact with each other. Aspects of the modulations schemes, frame structures and spectrum organisation are provided in the subsequent section, followed by the description of the main characteristics of the services and applications. Also, the description of some traffic models is presented in this chapter, to help define the different types of traffic considered in this work. Afterwards, one can find information on inter-frequency HOs in LTE, explaining the different messages that are exchanged between the user and the network and describing the different types of events that occur during all stages of an inter-frequency HO. Chapter 2 ends with a brief description of the state of the art on the thesis subject, presenting some of the previously developed works that approach load distribution techniques.

Chapter 3 starts by presenting the models that were developed in the scope of this thesis, showing the equations and considerations taken into account that allow the simulator to obtain results in the most realistic way possible. Users considered in the simulator can be in a LoS or NLoS condition and their association to a sector is based on the existing frequency bands and respective received power rather than only on distance, since the firsts have a more important role in the allocation of resources to a user. Besides, this behaviour is closer to the one observed in a real network, as users attempt to connect to the sector antenna that offers them a higher received power, although the implemented model focuses firstly on assigning the user to the highest detectable frequency band. In order to calculate the received power, one used the link budget described in Annex A, taking only the slow fading margin into account, with a fixed value. For the calculation of the path loss, the COST 231 Walfisch Ikegami model was considered, as it is described in Annex B. The type of traffic that was considered comprises typical data downloads (denominated as FTP) and VoLTE, prioritising the latter due to its requirements in terms of QoS. The spectrum allocation method used was a contiguous one, which is the Resource Allocation Type 2 of localised type, since this method allows the allocation of either a single RB to a given UE or the entire available bandwidth. The calculation of the throughput is made with the assistance of the model previously developed in [Alme13], which takes into account the experienced SINR and the modulation scheme being considered, as explained in Annex C. Moreover, Section 3.1 contains the description of the LTE channel models considered in this thesis and the

explanation on the modulation and coding schemes that LTE is able to support. The description of the implemented algorithm and its primary routines is also presented in Chapter 3, in order to clarify how the network reacts to new users and how the analysis of the network is done, based on a static and a dynamic load situation. The algorithm takes into consideration the deployment of multiple frequency bands over the same site and it prioritises the highest ones by always attempting to assign users to them before trying to allocate them to the remaining frequency bands. This decision is based on the previously mentioned calculation of the SINR experienced by the user upon attempting to establish its connection to the network and also on the available resources that the corresponding band still comprises. The third section of this chapter is dedicated to the description of the different elements that compose the simulator together with its workflow, followed by the explanation on how the obtained results are generated. The model is assessed in Section 3.4 in order to confirm that the obtained results are of relevance for this thesis. Up to 50 simulations were performed for each defined scenario and for both high and low load situations, although one was able to verify that 30 would be enough to ensure statistical relevance of the obtained results. The dynamic analysis of the network load was made for two hours of simulation time in order to guarantee that, in the last half of this time period, the network would surely be stabilised, in terms of load.

Chapter 4 starts by describing the scenarios considered in this thesis, as the first section defines some parameters required to correctly implement the developed model in the simulator, such as the transmitter's and UE's antennas height, parameters regarding the characterisation of the city and others required for the DL simulations. The three frequency bands that were considered are the ones used by the Portuguese mobile operators to provide coverage. Each of them has an associated bandwidth, and they are used to define three different scenarios, according to the combination of two of the available frequency bands: Scenario 1 combines the 2600 MHz band with the 1800 MHz one, Scenario 2 combines the 2600 MHz and the 800 MHz bands and Scenario 3 combines the 1800 MHz band with the 800 MHz one. Each of these scenarios enables different coverage areas and different available bandwidths, depending on the frequency bands being used. Then, the expected results of the throughput calculation methods obtained using the model described previously as the work developed in [Alme13] are presented, followed by the description of the walk-tests that were made in the city of Lisbon, explaining the methods and equipment used for obtaining the measurements. Furthermore, it is also clarified how these data was generated and the reasons for choosing the areas of Baixa and Moscavide as suitable for measurements are explained.

The high load analysis is then presented, followed by the low load analysis, concerning the study of the load distribution algorithm when 1300 and 200 users are generated in the simulator, respectively, in order to understand how the implemented algorithm takes action with high and low user densities. The analysis is made in terms of load distribution for each carrier and for each service in all defined scenarios of carrier combinations, as well as the number of active users per frequency band and per service, followed by the study of the received power and of the SINR in each service and also in each deployed frequency band. Also, FTP users throughput is analysed for each scenario and, finally, the number of RBs allocated to FTP users per carrier as well as for each sector per service. The final section of Chapter 4 is intended to present the results obtained from the walk-test performed over two

areas of city of Lisbon. Measurements regarding RSRP, SINR, number of allocated RBs and achieved throughput are presented, each one followed by the comparison with the scenario that most resembled the obtained measurement results, even though the differences between them and the simulated results are quite large.

Before one presents the main conclusions obtained from the presented work, it is important to refer that the developed model proved to be less efficient than expected, in terms of load balancing. The implemented model forces users to always try to connect to the frequency band that is probably able to deliver a better throughput, but since this may lead (in the worst case) to the allocation of all users to the same frequency band, that same frequency band becomes less effective because more users are sharing the existing resources. Moreover, in this same situation, the co-located frequency bands may be empty, while some users could have a better throughput by using the resources from this other frequency band. Therefore, a great effort was made to present most of the factors that should be considered in future works for obtaining a better performance out of the presented model, as explained further on this chapter.

Nevertheless, the implemented algorithm proved to be more efficient in the high load situation, since this is when the prioritisation of the services and of the frequency bands is more relevant. Scenario 1 shows that the network can serve 525 users, achieving throughputs up to almost 2.5 Mbps per user while correctly maintaining the load below 90%. One can then conclude that the model is more suitable for high user density areas with high data rate requirements, since a great portion of the users is able to connect to the network and still have a high enough throughput to perform its service. Also for the high load situation, Scenario 3 is able to comprise an average of 517 users and still maintain the network load stabilised below 90%. However, since the frequency bands implemented in this scenario comprehend the lowest number of available RBs, the achieved throughputs are also lower than the ones in other scenarios, only reaching values of 1.5 Mbps. Therefore, one can conclude that Scenario 3 is more suitable for areas where the user density is high but the data rate requirements are lower. The main conclusion drawn from the developed work is that the established model is more efficient if implemented in a specific situation of high user density and in which the considered users are constantly active, i.e., users may have high or low throughput requirements but they should be constantly requesting resources from the network.

Besides enabling one to gather results to compare with the ones obtained from the developed simulator, the measurements that were performed in the city of Lisbon also allowed to confirm that LTE traffic has significantly increased, since in areas where in the past year an LTE user was able to take advantage of all the available resources in a sector [Alme13], the same is not verified in the presented walk-test results, leading to a great reduction of the number of RBs being allocated to the UE. Although multi-carrier eNBs are deployed in the areas where the tests took place, measurements show that this implementation is already being fully exploited. One can then conclude that the number of users taking advantage of LTE networks has dramatically increased, proving that the deployment of multiple carrier frequencies is an implementation of great importance to attend to the requirements of nowadays (and future) users.

Since the developed model has proven to be less effective than predicted initially in terms of load balancing, one should be aware of the main processes that were taken into account and understand the reasons that originate the obtained results. With the assistance of Vodafone, one was able to recognise that the implemented model is somewhat similar to the ones used in legacy 3G networks. Furthermore, it is of one's interest to recognise changes that should be considered in order for the model to achieve a better balancing of the load and suggest some alterations and improvements that lead to a better performance of the algorithm.

Future works that approach the subject of this thesis should focus on more appropriate methods for load balancing for these types of networks. A suggestion is that the available resources should be better exploited by taking into account the capacity of the sector or of the frequency band, and further distribute users among the existing frequency bands so that the resources of one of the deployed frequency band do not reach saturation before using the resources of the other band. In order to do so, one should take into account the achievable throughput and the available resources in each band before deciding in which of them the user should be connected to. By establishing a threshold for the number of allocated RBs or for the total throughput that a given sector is providing to its users, it would be possible to define when to begin using one frequency band, or another, thus allowing the prioritisation of the different deployed carriers and leading to an optimised load distribution. The calculation of the received power and SINR would still be of much relevance given that these parameters help in defining the achieved throughput. Another possible improvement to be implemented is to take into consideration the movement of the users throughout the network, enabling a more proper study of inter-frequency HOs and how they can aid in achieving a better load distribution. This would enhancement also allow the study of cell-edge users, which is of great importance regarding coverage and load balancing issues, since these users suffer from low signal quality and, therefore, require more resources to satisfy their service demands and since one can take advantage of the deployment of multiple frequency bands to help in overcoming the presented situation by using the co-located bands as targets for HO.

In order to obtain more realistic results, it is suggested that the effects of inter-frequency measurements on the achieved user throughput are further studied. Before a user can be handed-over from a given frequency band to another, measurements must be executed in order to evaluate the received signal quality. In LTE networks, the user is responsible for executing these measurements and, to do so, a portion of its bandwidth must be used and, as proven in previous works on this topic, these measurements have repercussions in the experienced throughput, justifying the fact that this effect should be considered in future works.

Developments in terms of usage of different carrier frequencies in co-located sites should also be taken into account. The use of CA in scenarios such as those considered in this thesis should correspond to an enormous advantage in terms of achievable throughputs, since the use of this technique should provide a better user experience due to the deployment of multiple frequency bands in the same area of coverage, by using two or more of these bands to serve a given user and, therefore, enabling it to achieve higher throughputs. This study should require the development of

multiple carrier management methods so that it is possible to establish models that respect the network capacity and that also allow the load distribution to be balanced throughout the network. Nevertheless, the latter should be of relatively low difficulty, due to the fact that one is able to simply switch the PCC with one of the SCCs, or vice-versa, making it simpler to manipulate the usage of the different carriers and corresponding generated load. Another interesting suggestion that also regards the deployment of multiple frequency bands in the same eNB is to have a performance study made on scenarios that comprise more than two frequency bands. Besides, the usage of CA is favoured in such scenarios, since there are more frequency bands to which the user may be able to establish connection and, moreover, achieve higher throughput values.

In LTE, users can be in a connected or in an idle state. This factor is of great importance, since users in idle state do not represent any load to the network. It is suggested that one takes this issue into account for future works, since it allows an approach that is closer to a real network. Moreover, it allows a user to camp in a given cell and later be moved to the best cell in terms of signal quality and achieved throughput. Should the scenarios take into account the existence of multiple frequency bands in the same site, the previously mentioned issue enables a more thorough study on inter-frequency HO. Additionally, improvements in terms of VoLTE associated throughputs were recently published by 3GPP, by making use of new voice codecs that allow the enhancement of IP-based voice calls quality, as presented in [3GPP14a]. Another enhancement that is suggested is the performance study on both DL and UL connections. This analysis is of relevance in the sense that it enables a more realistic approach to the behaviour of a real network. It also allows one to take into account signalling and message swapping times between the UE and the network, furthermore enabling the study of the consequences of delays associated with these times and its effects on the performance of the network.

Finally, the variation of other parameters, together with their implications on the subject under study, should also be analysed in order to have a better assessment of the network capabilities. Different transmitter output powers and antenna heights should be considered so that one can better understand how these parameters can influence the generated load and how their variation can help in obtaining better results.

Annex A

Radio Link Budget

This annex presents the link budget calculation regarding propagation between the transmitter and receiver, through the calculation of the losses along the link.

The radio link budget is a tool that allows one to estimate the acceptable signal attenuation between the BS and the UE, making it necessary for coverage planning. The required SINR determines the maximum path loss admitted, considering a set of parameters related to gains and losses of the system as well as environment noise and interference. This procedure is in agreement with the radio link budget suggested in [Corr13].

The signal power received by the UE can be determined by:

$$P_{r[\text{dBm}]} = P_{EIRP[\text{dBm}]} + G_{r[\text{dBi}]} - L_{p,total[\text{dB}]} \quad (\text{A.1})$$

where:

- P_r : Power available at the receiving antenna;
- P_{EIRP} : Effective Isotropic Radiated Power (EIRP);
- G_r : Gain of the receiving antenna;
- $L_{p,total}$: Total path loss.

The EIRP depends on the link. In DL, it is defined according to:

$$P_{EIRP[\text{dBm}]} = P_{Tx[\text{dBm}]} - L_c[\text{dB}] + G_t[\text{dBi}] \quad (\text{A.2})$$

where:

- P_{Tx} : Transmitter output power;
- L_c : Losses in the cable between the transmitter and the antenna;
- G_t : Gain of the transmitting antenna.

In UL, the EIRP is defined by the following expression:

$$P_{EIRP[\text{dBm}]} = P_{Tx[\text{dBm}]} - L_u[\text{dB}] + G_t[\text{dBi}] \quad (\text{A.3})$$

where:

- L_u : Losses due to the user, which take a value between 0 and 3 dB for data.

The power at the receiver, in DL, is given by:

$$P_{Rx[\text{dBm}]} = P_r[\text{dBm}] - L_u[\text{dB}] \quad (\text{A.4})$$

where:

- P_{Rx} : Power at the input of the receiver.

The power at the receiver, in UL, is given by:

$$P_{Rx[\text{dBm}]} = P_r[\text{dBm}] - L_c[\text{dB}] \quad (\text{A.5})$$

The average noise power at the receiver can be calculated using the following expression:

$$N_{[\text{dBm}]} = -174 + 10 \times \log(N_{RB} \times B_{RB[\text{Hz}]}) + F_N[\text{dBm}] \quad (\text{A.6})$$

where:

- N_{RB} : Number of RBs;
- B_{RB} : Bandwidth of one RB, which is 180 kHz;
- F_N : Noise figure at the receiver;

The multiplication of N_{RB} with B_{RB} corresponds to the noise bandwidth.

The total path loss can be obtained by:

$$L_{p,total}[\text{dB}] = L_p[\text{dB}] + M_{SF}[\text{dB}] + M_{FF}[\text{dB}] \quad (\text{A.7})$$

where:

- L_p : Path loss from the COST 231 Walfisch-Ikegami model;
- M_{SF} : Slow fading margin;
- M_{FF} : Fast fading margin;

Annex B

COST 231 Walfisch-Ikegami Propagation Model

This annex describes the propagation model used for the calculation of the path loss between transmitter and receiver.

This model allows one to estimate the path loss between the signal emitted by the UE to an eNB as shown in Figure A.1 and Figure A.2. It is used when studying urban and suburban scenarios for distances shorter than 5 km, and its input parameters are the following [Corr13]:

- h_b : Height of the eNB antenna from ground;
- H_b : Buildings height;
- h_m : UE height;
- w_s : Street width;
- f : Frequency;
- d : Distance between eNB and UE;
- w_B : Building separation;
- α_B : Angle of incidence of the signal in the buildings;
- φ : Street orientation angle.

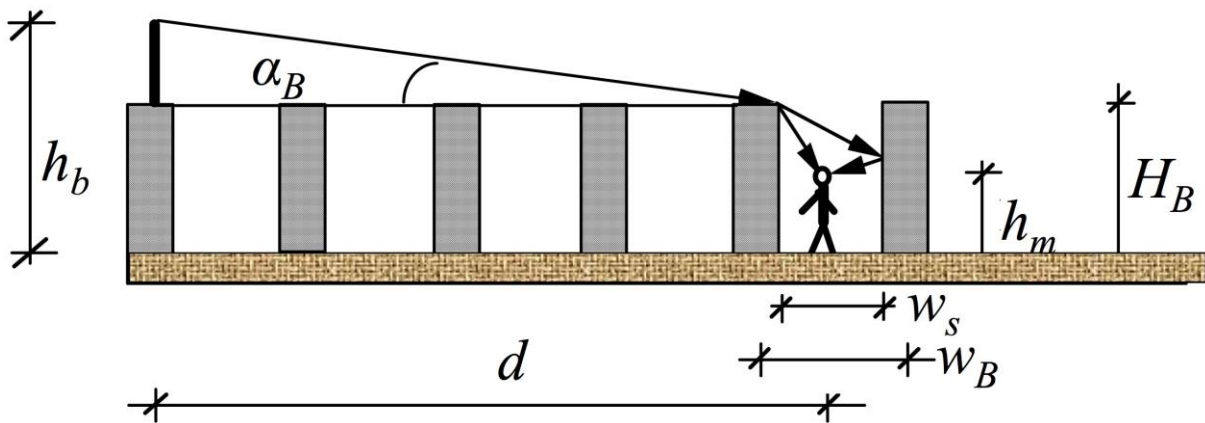


Figure B.1. COST 231 Walfisch-Ikegami Propagation Model, side view (extracted from [Corr13]).

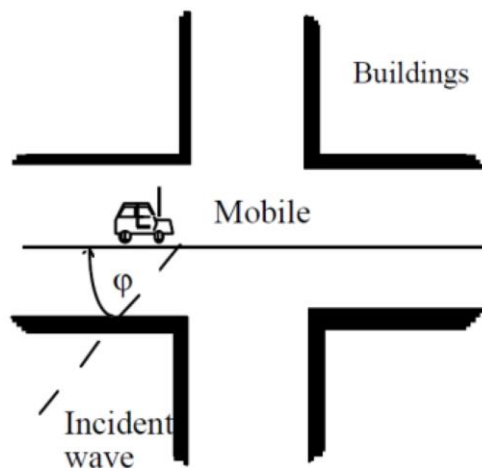


Figure B.2. COST 231 Walfisch-Ikegami Propagation Model, view from above (extracted from [Mart13]).

For LoS propagation in a street, and $d > 0.02$ km, path loss is given by:

$$L_{p[\text{dB}]} = 42.6 + 26 \times \log(d_{[\text{km}]}) + 20 \times \log(f_{[\text{MHz}]}) \quad (\text{B.1})$$

For all other cases, path loss is defined as:

$$L_p[\text{dB}] = \begin{cases} L_0[\text{dB}] + L_{rt}[\text{dB}] + L_{rm}[\text{dB}] & , L_{rt} + L_{rm} > 0 \\ L_0[\text{dB}] & , L_{rt} + L_{rm} \leq 0 \end{cases} \quad (\text{B.2})$$

where:

- L_0 : Free space propagation path loss;
- L_{rt} : Attenuation due to propagation from eNB to the last rooftop;
- L_{rm} : Attenuation due to diffraction from last rooftop to the UE.

Being the path loss experienced in free space propagation given by:

$$L_o[\text{dB}] = 32.44 + 20 \times \log(d_{[\text{km}]}) + 20 \times \log(f_{[\text{MHz}]}) \quad (\text{B.3})$$

The propagation from the eNB to the last rooftop experiences the following loss:

$$L_{rt}[\text{dB}] = L_{bsh}[\text{dB}] + k_a + k_d \times \log(d_{[\text{km}]}) + k_f \times \log(f_{[\text{MHz}]}) - 9 \times \log(w_{B[m]}) \quad (\text{B.4})$$

where:

- $L_{bsh}[\text{dB}] = \begin{cases} -18 \times \log(h_{b[m]} - H_{B[m]} + 1) & , h_b > H_B \\ 0 & , h_b \leq H_B \end{cases}$
- $k_a = \begin{cases} 54 & , h_b > H_B \\ 54 - 0.8 \times (h_{b[m]} - H_{B[m]}) & , h_b \leq H_B \wedge d \geq 0.5 \text{ km} \\ 54 - 1.6 \times (h_{b[m]} - H_{B[m]}) d_{[\text{km}]} & , h_b \leq H_B \wedge d < 0.5 \text{ km} \end{cases}$
- $k_d = \begin{cases} 18 & , h_b > H_B \\ 18 - 15 \times \frac{h_{b[m]} - H_{B[m]}}{H_{B[m]}} & , h_b \leq H_B \end{cases}$
- $k_f = \begin{cases} -4 + 0.7 \times \left(\frac{f_{[\text{MHz}]}}{925} - 1\right) & , \text{urban and suburban scenarios} \\ -4 + 1.5 \times \left(\frac{f_{[\text{MHz}]}}{925} - 1\right) & , \text{dense urban scenarios} \end{cases}$

Finally, the loss due to diffraction from the last rooftop to the UE is given by:

$$L_{rm}[\text{dB}] = -16.9 - 10 \times \log(w_{s[m]}) + 10 \times \log(f_{[\text{MHz}]}) - 20 \times \log(H_{B[m]} - h_{b[m]}) + L_{ori}[\text{dB}] \quad (\text{B.5})$$

with:

- $L_{ori}[\text{dB}] = \begin{cases} -10.0 + 0.354 \times \varphi_{[^\circ]} & , 0^\circ < \varphi < 35^\circ \\ 2.5 + 0.075 \times (\varphi_{[^\circ]} - 35) & , 35^\circ < \varphi < 55^\circ \\ 4.0 + 0.114 \times (\varphi_{[^\circ]} - 55) & , 55^\circ < \varphi < 90^\circ \end{cases}$

The validity range for some parameters of this model imposes that:

- $f \in [800; 2\,000]$ MHz
- $d \in [0.02; 5]$ km
- $h_b \in [4; 50]$ m
- $h_m \in [1; 3]$ m

The presented frequency range does not contain all the frequency bands studied in this thesis, therefore, one should consider higher relative errors than expected. The standard deviation of the model takes values in [4; 7] dB, and the error increases when h_b decreases relative to H_B .

In the absence of specific values, the following are recommended [Corr13]:

- $w_B \in [20; 50]$ m
- $w_s = w_B/2$
- $\varphi = 90^\circ$
- $H_B = 3 \times (\#floors) + H_{roof}$
- $H_{roof[m]} = \begin{cases} 3, & \text{pitched} \\ 0, & \text{flat} \end{cases}$

Annex C

SINR and Throughput

The LTE models used to determine the SINR and throughput for a given set of system configurations are provided in this annex.

Based on the models presented in [Alme13] one can obtain very good approximations for the DL throughput calculation using the experienced SINR. The expressions that represent this relationship are the logistic functions that provide the best-fit approach to a set of values collected by 3GPP based on throughput performance tests done by manufacturers, presented in [3GPP11]. In order to have a realistic approach of the behaviour of a real network, three modulation schemes are considered in the DL: QPSK, 16QAM and 64QAM. Also, each one is associated with the median value of the coding rates obtained according to the Channel Quality Indicator (CQI) reported by the UE, resulting in coding rates of 1/3 for QPSK, 1/2 for 16QAM and 3/4 for 64QAM. All users are considered to follow the EPA5 channel model.

For QPSK modulation, coding rate of 1/3 and considering MIMO 2x2, throughput per RB is given by:

$$R_{b[\text{bit/s}]} = \frac{2.34201 \times 10^6}{14.0051 + e^{-0.577897 \times \rho_{IN[\text{dB}]}}} \quad (\text{C.1})$$

For 16QAM modulation, coding rate of 1/2 and considering MIMO 2x2, throughput per RB is given by:

$$R_{b[\text{bit/s}]} = \frac{47613.1}{0.0926275 + e^{-0.295838 \times \rho_{IN[\text{dB}]}}} \quad (\text{C.2})$$

For 64QAM modulation, coding rate of 3/4 and considering MIMO 2x2, throughput per RB is given by:

$$R_{b[\text{bit/s}]} = \frac{26405.8}{0.0220186 + e^{-0.244491 \times \rho_{IN[\text{dB}]}}} \quad (\text{C.3})$$

For QPSK modulation, coding rate of 1/3 and considering MIMO 2x2, SINR in the DL is given by the following expression, taking into account (C.1):

$$\rho_{IN[\text{dB}]} = -\frac{1}{0.577897} \times \ln \left(\frac{2.34201 \times 10^6}{R_{b[\text{bit/s}]}} - 14.0051 \right) \quad (\text{C.4})$$

Annex D

User's Manual

A brief explanation on how to run a simulation in the developed simulator is provided in this annex.

When opening UMTS_Simul.mbx, MapInfo is executed and two consecutive windows appear, asking the user to select the following files:

- DADOS_Lisboa.tab, which contains information about the city of Lisbon, namely its districts;
- ZONAS_Lisboa.tab, which characterises the areas of Lisbon.

Afterwards, one should access the “System” tab on the upper bar of MapInfo and click on the available features of “LTE-DL”, one at a time. Each click on “Propagation Model”, “Traffic Properties”, “Network Settings” and “Services” invokes its corresponding window.

The “Propagation Model” window is presented in Figure D.1 and it provides suitable options to select the desired propagation model parameters, such as the height of the BS antennas, the height of the buildings, the street width, the distance between the centre of the buildings, the departing angle from the closest building, the mobile terminal height and the type of environment (urban or dense urban).

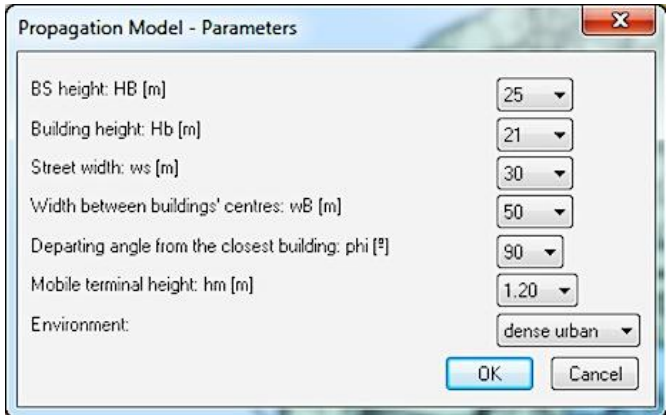


Figure D.1. Propagation model parameters.

Figure D.2 shows the “Traffic Properties” window, where the priority for each service can be chosen. Note that although six different services appear in the window, the simulations only take into account typical data usage and VoLTE services. In order to correctly simulate this situation, one should define the priority of “Streaming” as 4 and the priority “FTP” as being 7. This small adjustment is specific of this thesis, and the names of the services remain unchanged due to the fact that the simulator is based on previous developed works.



Figure D.2. Traffic properties.

In the “Network Settings” window one can insert many of the parameters that characterise the system, such as antenna parameters, resource allocation method, transmission power and other parameters required for the link budget. The bandwidth and frequency band can also be changed, even though no effect will take place since the simulator was developed to study different carrier frequencies with specific available bandwidths, as stated in Section 3.1. Figure D.3 depicts the described window.

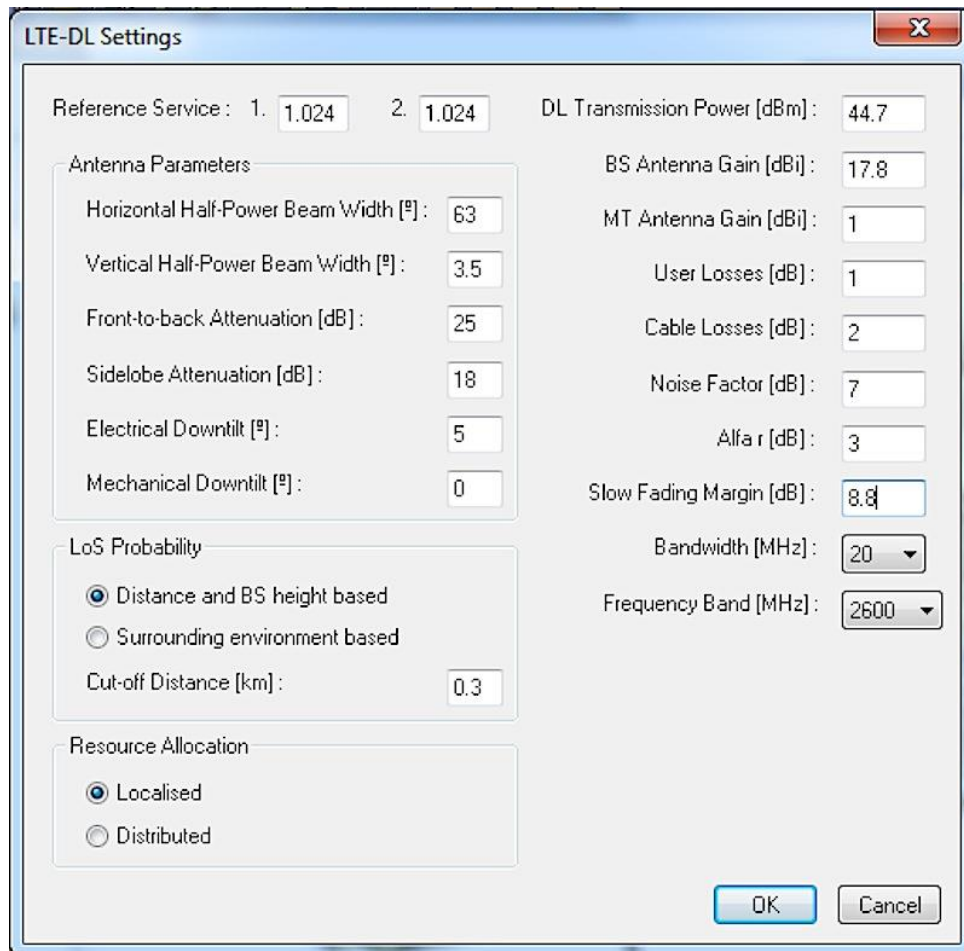


Figure D.3. Network settings.

The “Services” window simply allows selecting the colour assigned to each service, to be used in the simulations. After the data presented in Figure D.1, Figure D.2 and Figure D.3 is filled in, the “User Profile” window becomes available, although the definition of the throughputs is done afterwards, according to the specifications of the developed work, instead of being defined for each simulation. Afterwards, the “Insert Users” option becomes available and, when selected, it asks for a file containing the users positioning along the city of Lisbon, making the option “Deploy Network” available. This option allows one to select and load a file containing information about position and identification of the BSs. Then, the last option of “LTE-DL” also becomes selectable and, by pressing on “Run Simulation”, a simulation is performed.

References

- [3GPP11] 3GPP, Technical Specification Group – RAN WG4, *Summary of alignment and impairment results for eDL-MIMO demodulation requirements*, Report R4-112713, Barcelona, Spain, May 2011
- [3GPP12a] 3GPP, *LTE, Requirements for further advancements for Evolved Universal Terrestrial Radio Access (E-UTRA) (LTE-Advanced) (Release 11)*, ETSI TR, No. 36.913, Ver. 11.0.0, Nov. 2012 (<http://www.3gpp.org>).
- [3GPP12b] 3GPP, *Digital cellular telecommunications system (Phase 2+); Universal Mobile Telecommunications System (UMTS); LTE; Quality of Service (QoS) concept and architecture (Release 11)*, ETSI TS, No. 23.107, Ver. 11.0.0, Nov. 2012
- [3GPP12c] 3GPP, *Evolved Universal Terrestrial Radio Access (E-UTRA); LTE coverage enhancements (Release 11)*, ETSI TR, No. 36.824, Ver. 11.0.0, Jun. 2012 (<http://www.3gpp.org>).
- [3GPP13a] 3GPP, *LTE*, <http://www.3gpp.org/technologies/keywords-acronyms/98-lte>, Dec. 2013.
- [3GPP13b] 3GPP, *LTE; Evolved Universal Terrestrial Radio Access (E-UTRA); Physical channels and modulation (Release 11)*, ETSI TS, No. 36.211, Ver. 11.4.0, Oct. 2013 (<http://www.3gpp.org>).
- [3GPP13c] 3GPP, *Digital cellular telecommunications system (Phase 2+); Universal Mobile Telecommunications System (UMTS); LTE; Policy and charging control architecture (Release 11)*, ETSI TS, No. 23.203, Ver. 11.11.0, Sep. 2013 (<http://www.3gpp.org>).
- [3GPP13d] 3GPP, *LTE; Evolved Universal Terrestrial Radio Access (E-UTRA); User Equipment (UE) radio transmission and reception (Release 11)*, ETSI TS, No. 36.101, Ver. 11.6.0, Oct. 2013 (<http://www.3gpp.org>).
- [3GPP13e] 3GPP, *LTE; Evolved Universal Terrestrial Radio Access (E-UTRA); Requirements for support of radio resource management (Release 11)*, ETSI TS, No. 36.133, Ver. 11.6.0, Oct. 2013 (<http://www.3gpp.org>).
- [3GPP14a] 3GPP, *Enhanced Voice Services Codec for LTE*, http://www.3gpp.org/news-events/3gpp-news/1639-evs_news, Nov. 2014.
- [3GPP14b] 3GPP, *LTE; Evolved Universal Terrestrial Radio Access (E-UTRA) and Evolved Universal Terrestrial Radio Access Network (E-UTRAN); Overall description (Release 11)*, ETSI TS, No. 36.300, Ver. 11.8.0, Jan. 2014 (<http://www.3gpp.org>).

- [3GPP14c] 3GPP, *LTE; Evolved Universal Terrestrial Radio Access (E-UTRA); User Equipment (UE) procedures in idle mode (Release 11)*, ETSI TS, No. 36.304, Ver. 11.6.0, Jan. 2014 (<http://www.3gpp.org>).
- [3GPP14d] 3GPP, *LTE; Evolved Universal Terrestrial Radio Access (E-UTRA); Radio Resource Control (RRC); Protocol specification (Release 11)*, ETSI TS, No. 36.331, Ver. 11.6.0, Jan. 2014 (<http://www.3gpp.org>).
- [3GPP14e] 3GPP, *About 3GPP*, <http://www.3gpp.org/about-3gpp>, Nov. 2014.
- [Alme13] Almeida,D., *Inter-Cell Interference Impact on LTE Performance in Urban Scenarios*, M.Sc. Thesis, Instituto Superior Técnico, Lisbon, Portugal, Oct. 2013.
- [ANAC14] <http://www.anacom.pt/render.jsp?contentId=1105917>, Apr. 2014.
- [Asco15a] <http://www.ascom.com/nt/en/index-nt/tems-products-3/tems-discovery-11.htm>, Jan. 2015.
- [Asco15b] <http://www.ascom.com/nt/en/index-nt/tems-products-3/tems-investigation-5.htm>, Jan. 2015.
- [CCox12] Cox,C., *An Introduction to LTE – LTE, LTE-Advanced, SAE and 4G Mobile Communications*, Wiley, Chichester, United Kingdom, 2012.
- [ChJa89] Chiu,D., and Jain,R., "Analysis of the Increase/Decrease Algorithms for Congestion Avoidance in Computer Networks", *Journal of Computer Networks and ISDN*, Vol. 17, No. 1, Jun. 1989, pp. 1-14.
- [Cisc14] Cisco VNI Forecast, *Cisco Visual Networking Index: Global Mobile Data Traffic Forecast Update, 2013–2018*, Feb. 2014 (http://www.cisco.com/c/en/us/solutions/collateral/service-provider/visual-networking-index-vni/white_paper_c11-520862.pdf).
- [Corr13] Correia,L., *Mobile Communications Systems, Lecture Notes*, Instituto Superior Técnico, Lisbon, Portugal, 2013.
- [Eric14] Ericsson, *Ericsson Mobility Report*, Public Consultation, Stockholm, Sweden, Aug. 2014 (<http://www.ericsson.com/ericsson-mobility-report>).
- [Falc13] Falcão,J., *Inter-Cell Interferences in LTE Radio Networks*, M.Sc. Thesis, Instituto Superior Técnico, Lisbon, Portugal, Oct. 2013.
- [HoTo11] Holma,H., and Toskala,A., *LTE for UMTS: Evolution to LTE-Advanced*, Wiley, Chichester, United Kingdom, 2011.
- [Huaw15] <http://consumer.huawei.com/au/mobile-broadband/dongles/tech-specs/k5150-au.htm>, Jan. 2015.
- [KSMW09] Kazmi,M., Sjöbergh,O., Müller,W., Wiorek,J., and Lindoff,B., "Evaluation of Inter-Frequency Quality Handover Criteria in E-UTRAN", in *VTC Spring 2009 - 69th IEEE Vehicular Technology Conference*, Barcelona, Spain, Apr. 2009.

- [KuHK08] Kurjenniemi,J., Henttonen,T., and Kaikkonen,J., "Suitability of RSRQ Measurement for Quality Based Inter-Frequency Handover in LTE", in *ISWCS '08 - IEEE International Symposium on Wireless Communication Systems*, Reykjavik, Iceland, Oct. 2008.
- [LHPL11] Li,Z., Wang,H., Pan,Z., Liu,N., and You,X., "Joint optimization on load balancing and network load in 3GPP LTE multi-cell Networks", in *WCSP 2011 - International Conference on Wireless Communications and Signal Processing*, Nanjing, China, Nov. 2011.
- [LSJB10] Lobinger,A., Stefanski,S., Jansen,T., and Balan,I., "Load balancing in downlink LTE Self-Optimizing Networks", in *VTC Spring 2010 – 71st IEEE Vehicular Technology Conference*, Taipei, China, May 2010.
- [Mart13] Martins,J., *Impact of MIMO and Carrier Aggregation in LTE-Advanced*, M.Sc. Thesis, Instituto Superior Técnico, Lisbon, Portugal, Oct. 2013.
- [Pire12] Pires,R., *Coverage and Efficiency Performance Evaluation of LTE in Urban Scenarios*, M.Sc. Thesis, Instituto Superior Técnico, Lisbon, Portugal, Nov. 2012.
- [PHHK12] Poikselka,M., Holma,H., Hongisto,J., Kallio,J., and Toskala,A., *Voice over LTE (VoLTE)*, Wiley, Chichester, Feb. 2012.
- [SeTB11] Sesia,S., Toufik,I. and Baker,I., *LTE – The UMTS Long Term Evolution: From Theory to Practice (2nd Edition)*, John Wiley & Sons, Chichester, UK, Aug. 2011.
- [Voda13] Vodafone Portugal, *Internal communication*, 2013.
- [WPSM10] Wang,Y., Pedersen,K., Sørensen,T., and Mogensen,P., "Carrier load balancing and packet scheduling for multi-carrier systems", *IEEE Transactions on wireless communications*, Vol. 9, No. 5, May 2010, pp. 1780-1789.
- [XuXX11] Xuena,C., Xiao,D., and Xiu,C., "Handover performance of relaxing SCell measurement period in LTE-A with carrier aggregation", in *ICEICE 2011 - Electric Information and Control Engineering*, Wuhan, China, Apr. 2011.
- [YNII11] Yagyu,K., Nakamori,T., Ishii,H., Iwamura,H., Miki,N., Asai,T., and Hagiwara,J., "Investigation on Mobility Management for Carrier Aggregation in LTE-Advanced", in *VTC Fall 2011 – 73rd IEEE Vehicular Technology Conference*, California, USA, Sep. 2011.